JOURNAL OF APPLIED PHYSICS

APRIL
1940
Vol. 11 No. 4

New
Mass Spectrometer

JOURNAL OF APPLIED
PHYSICS

APRIL, 1940 Vol. 11, No. 4

In This Issue

Page

Magnetic Cooling; the Production and Measurement of Temperatures Below 1°K CHARLES F. SQUIRE 232

Stellar Temperatures G. P. KUIPER 241

Letters to the Editor

Correction C. H. BACHMAN 240

Piezoelectric vs. Spring Pressure Gauge R. H. KENT AND A. H. HODGE 240

Contributed Original Research

Some Relations Between Molecular Structure and Plasticizing Effect ARNOLD KIRKPATRICK 255

Diffusion of Hydrogen from Water Through Steel FRANCIS J. NORTON 262

Preferential and Initial Ionic Recombination in Gases N. E. BRADBURY 267

Tension and Birefringence in a Vinylite Plastic H. W. FARWELL 274

Analysis of Symmetrical Vibrating Systems LOUIS A. PIPES 279

Solution of Torsion Problems by Numerical Integration of Poisson's Equation R. WELLER, G. H. SHORTLEY AND B. FRIED 283

Polonium Alloy for Spark Plug Electrodes J. H. DILLON 291

Wave Propagation in Shearing Quartz Oscillators of High Frequency EDWARD W. SANDERS 299

In Every Issue

Contributors to This Issue 250

Here and There 251

Recent Booklets 253

Innovations in Instruments 254

Index to Advertisers X

BOARD OF EDITORS

ELMER HUTCHISSON, *Editor*

Associate Editors

F. BITTER
W. E. FORSYTHE
L. A. JONES
B. E. WARREN
J. B. WHITEHEAD

Publication of the American Institute of Physics

ADMINISTRATIVE STAFF

HENRY A. BARTON, *Director*

MADELINE M. MITCHELL, *Publications Manager*

JOHN T. TATE, *Adviser on Publications*

GOVERNING BOARD

PAUL E. KLOPSTEG, *Chairman*
GEORGE B. PEGRAM, *Secretary*
KARL T. COMPTON
WHEELER P. DAVEY
FLOYD A. FIRESTONE
HARVEY FLETCHER
R. C. GIBBS
ARTHUR C. HARDY
GEORGE R. HARRISON
A. STUART HUNTER
H. R. LILLIE
FREDERIC PALMER, JR.
GEORGE B. PEGRAM
W. B. RAYTON
JOHN T. TATE
WALLACE WATERFALL

THE JOURNAL OF APPLIED PHYSICS, published monthly at Prince and Lemon Sts., Lancaster, Pa., is devoted to physics in its role as the science basic to other natural sciences and to the arts and industries. Previous to 1937 this publication was known as PHYSICS. It aims to be of service not only in physical laboratories, but also in the laboratories of industrial, chemical, geological, geophysical, meteorological, radio, and similar concerns. THE JOURNAL OF APPLIED PHYSICS publishes editorials, news of physicists and reviews, as well as technical papers of applied physics.

SUBSCRIPTION PRICE

	U. S., POSS. AND CANADA	FOREIGN
To members of scientific societies	$5.00	$5.70
To all others	7.00	7.70

Manuscripts should be submitted to Elmer Hutchisson, Editor, University of Pittsburgh, Pittsburgh, Pennsylvania.

Changes of address and proofs should be addressed to the Publications Manager.

Subscriptions and orders for back numbers should be addressed to Prince and Lemon Streets, Lancaster, Pa. or to the American Institute of Physics, 175 Fifth Avenue, New York, N. Y.

Single copies are $.70 each and should be ordered from the American Institute of Physics, 175 Fifth Ave., New York, N. Y.

Advertising rates supplied on request. Orders, advertising copy and cuts should be sent to the American Institute of Physics.

Entered as second class matter at the Post Office at Lancaster, Pennsylvania, under the Act of March 3, 1897. Accepted for mailing at the special rate of postage provided for in the Act of February 28, 1925, authorized May 2, 1932.

Copyright 1940, by the American Institute of Physics.

Materials which liquefy or freeze at extremely low temperatures are studied with this Type G-2 Mueller Bridge equipment

THE MOST ACCURATE THERMOMETER WE MAKE

Decreasing the limit of temperature error in calorimetric and other relatively low temperature measurements, the Type G-2 Mueller Bridge, in combination with our recently developed 8163 Resistance Thermometer, is capable of greater accuracy, between −190 and +500 C, than any other means available.

With calibration data applied, resistance measurements can be made on this combination within a limit of error of a few hundred-thousandths of an ohm or a few parts per million, whichever is larger. A thermostatically controlled constant-temperature chamber for the most important measuring resistors helps make this accuracy possible. Ambient temperature corrections are unnecessary, and the Bridge operates with an entirely new degree of convenience.

By measuring temperature changes in calorimetry with an accuracy comparable to, or higher than, that of the weight measurements, Mueller Bridges increase the accuracy with which heats of combustion of coals, gases, oils and other fuels are determined. Other applications include the calibration of all kinds of thermometers and the measurement of specific heats. Mueller Bridges have also been used to measure boiling and freezing points of many chemicals and in various physical chemistry researches.

Write for Catalog E-33C(1)

LEEDS & NORTHRUP COMPANY, 4978 STENTON AVE., PHILA., PA.

LEEDS & NORTHRUP

MEASURING INSTRUMENTS · TELEMETERS · AUTOMATIC CONTROLS · HEAT-TREATING FURNACES

Jrl Ad E-33C(2)

NEW REINHOLD BOOKS

PROPERTIES OF ORDINARY WATER-SUBSTANCE IN ALL ITS PHASES: WATER-VAPOR, WATER AND ALL THE ICES

N. Ernest Dorsey
National Bureau of Standards, Washington, D. C.

A monumental compilation of physical data, this volume represents a life-time of effort on the part of the author, himself an eminent authority on the subject. In it he assembles, extends, and critically evaluates all the available information on water-substance, with special emphasis on that published in the International Critical Tables. His statements are copiously documented and are accompanied at every point by data gathered by hundreds of observers.

The scope of this monograph is so comprehensive that only a few of the more general topics can be mentioned. Among these are thermodynamic considerations involved in the synthesis and dissociation of water-substance; thermal energy of dilated water-vapor; molecular and pressure-volume-temperature data for all forms of water-substance; acoustic data; optical properties; the structure of water and ice as revealed by Raman spectra and x-rays; the reflectivity of ice and snow; electrical properties of water-substance; the color of water and of the sea, etc.

This exhaustive work will be of unique value to workers in many diverse fields. Of particular interest to aeronautical engineers is the material presented on such subjects as the mechanism of ice formation and the viscosity of fog; the data on icebergs and glaciers will be useful to geologists, oceanographers and hydrographers; and detailed information on rain, hail and snow will be indispensable for meteorologists. Hydraulic, steam and marine engineers, and physicists and physical chemists will also find a vast amount of vital information in this compilation.

710 Pages **289 Tables** **Illustrated** **Price $15.00**

A.C.S. Monograph No. 81

THE RAMAN EFFECT AND ITS CHEMICAL APPLICATIONS

James H. Hibben
Geophysical Laboratory, Washington, D. C.

Immediately after publication of this volume, Sir C. V. Raman, discoverer of the Raman Effect, cabled us as follows: "The publication of the monograph by Dr. Hibben is a notable scientific event. He surveys with insight and accuracy the entire literature of this new and fertile field of research, and makes its present status admirably clear. The theoretical introduction by Hibben and Teller is just what is required to give a clear conception of the subject with its achievements and its possibilities. The book is assured of a warm welcome and will prove itself an indispensable companion to the student and the investigator."

The importance of the Raman Effect in furnishing new means of studying the behavior and structure of molecules already rivals that of the x-ray. This volume is the first to describe in complete detail the great contribution of Raman spectra to our present understanding of matter. Its purpose is to bring about a fuller realization of the potentialities as well as the accomplishments of this valuable technique in current problems of industry and scientific research.

544 Pages **Illustrated** **Price $11.00**

A.C.S. Monograph No. 80

PHENOMENA AT THE TEMPERATURE OF LIQUID HELIUM

E. F. Burton
Director of McLennan Laboratory of Physics
University of Toronto

A.C.S. Monograph No. 83

Ready soon!

PROPERTIES OF GLASS

George W. Morey
Geophysical Laboratory
Washington, D. C.

"The premier text on glass in the English language."
—Frank Preston.

The researches of the last two decades have resulted in important advances in our understanding of the constitution and structure of glass. Dr. Morey's book, more than ten years in preparation, gives detailed and critical discussions of all phases of the physics and chemistry of glass, including viscosity, heat capacity, optical and elastic properties, strength, hardness, etc. The attempt has been made to include all measurements on glasses of known composition. The many tables contain a wealth of data.

561 Pages **Illustrated** **Price $12.50**

A.C.S. Monograph No. 77

THE TOOLS OF THE CHEMIST

Their Ancestry and American Evolution

Ernest Child
Foreword by C. A. Browne
U. S. Dept. of Agriculture

The history of the manufacture of laboratory apparatus and the part it has played in the development of American chemistry. In an entertaining and instructive way, the author describes the events and personalities that were responsible for the creation and growth of chemical laboratories in this country, with appropriate emphasis on the European background from which they sprang. He infuses his work with the spirit of Holmyard's remark, "Every piece of apparatus hides a romance." The history of many famous manufacturers of instruments and apparatus and dealers in chemical supplies is given in much detail; and many facts are presented that were heretofore unknown, thanks to the persistence with which the author has collected his material. He traces the history of such laboratory necessities as balances, glassware, filter paper, porcelain, heating apparatus, metal ware, Alundum, rubber ware, platinum ware and scientific optical instruments. The contributions of various cities and, sections of the country to this field are also discussed.

224 Pages **Illustrated** **$3.50**

ADD THESE BOOKS TO YOUR LIBRARY

REINHOLD PUBLISHING CORPORATION, 330 W. 42nd St., New York, N. Y.

New notes on research in a forward-looking laboratory—

KOVAR

"REGISTERED TRADE MARK NO. 337,962"

developed by Westinghouse

MODERN RESEARCH PROVIDES THIS IDEAL ALLOY FOR SEALING TO GLASS

Research is responsible for hundreds of scientific achievements that speed the progress of American industry. An example is KOVAR, the new alloy developed by scientists in Westinghouse laboratories.

Increased applications for sealed-off gaseous conduction devices; such as small rectifiers, grid-glow tubes and Ignitrons, made it essential to have a vacuum tight metal-to-glass joint for conducting power into a glass vessel or for insulating electrodes from metal walled vessels. The problem was to develop a metal which would incorporate the desirable qualities of a number of different metals and overcome their limitations.

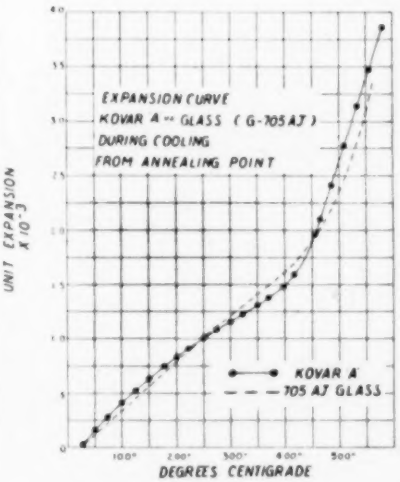

Graph illustrates how very closely KOVAR "A" matches the characteristics of "Clear Sealing Glass," from annealing point to room temperatures.

KOVAR "A"

After exhaustive tests the solution was found in a specially developed group of alloys, to which the trade name KOVAR has been applied. A specific form, KOVAR "A", is an iron-nickel-cobalt alloy which combines the following properties:

1. Readily seals into hard glass permitting high resistance to thermal shock.
2. Produces a permanently vacuum tight seal.
3. Resists mercury attack.
4. Easily machined and otherwise formed, permitting use on intricate shapes.
5. Relatively inexpensive, eliminating restraints on size and capacity of sealed-off gas conduction devices.
6. Uniform composition, permitting duplication of results.
7. Eliminates the need of a "feather edge" on tubular shapes.

FOR ADDITIONAL INFORMATION WRITE WESTINGHOUSE ELECTRIC & MFG. CO., FEEDER DIVISION, EAST PITTSBURGH, PA.

NEW WILEY BOOKS SPRING 1940

GENERAL PHYSICS FOR STUDENTS OF SCIENCE

By **ROBERT B. LINDSAY**, *Hazard Professor of Physics, Brown University.*

An elementary book introducing the fundamental concepts of physics in logically rigorous fashion for students who have had mathematics through elementary calculus. For students who have already had an elementary non-mathematical course, the book will provide an intermediate and more thorough treatment, and to a certain extent, an elementary introduction to theoretical physics.

534 pages; 6 by 9; 265 illustrations; $3.75

FUNDAMENTAL PROCESSES OF ELECTRICAL DISCHARGE IN GASES

By **LEONARD B. LOEB**, *Professor of Physics, University of California.*

A book on discharge through gases written from the viewpoint of the modern knowledge of atomic structure. A connecting and clarifying link between the classical books giving original data and theories on electricity in gases and the welter of current scientific papers dealing with single aspects of the question. A source book of recently coordinated information.

717 pages; 6 by 9; 297 figures; $7.00

PROCEEDINGS OF THE SEVENTH SUMMER CONFERENCE ON SPECTROSCOPY

Edited by **GEORGE R. HARRISON**, *Professor of Physics, Massachusetts Institute of Technology.*

The twenty-nine papers of the 1939 Conference presenting latest developments in the applications of the rapidly-growing science of spectroscopy. General background and methods, specific types of analysis, recently developed apparatus, absorption spectrophotometry are some of the subjects covered.

154 pages; 7½ by 10; 69 illustrations; $2.75

TELEVISION—THE ELECTRONICS OF IMAGE TRANSMISSION

By **V. K. ZWORYKIN** and **G. A. MORTON**, *R.C.A. Manufacturing Company.*

A detailed survey of this newest of practical means of communication. The book is written from an engineering standpoint and is devoted to the practical aspects of the subject. The authors are two of the foremost men in the field.

646 pages; 6 by 9; 494 illustrations; $6.00

JOHN WILEY & SONS, INC., NEW YORK, N. Y.

Please mention this journal when writing to advertisers

HARVARD COLLEGE
APR 6 1940
LIBRARY

Journal of Applied

Physics

Volume 11 April, 1940 Number 4

Congratulations to the A.S.M.

THE twentieth anniversary of the American Society of Metals was celebrated last month. During this time the society has built up a record of which they may well be proud. In the March issue of *Metal Progress* a short but impressive history of the society is given. Local metallurgical societies began to be formed about 1914 which, in 1920, combined to form the national group now known as the American Society of Metals. In the early days some projects which were started had to be abandoned for lack of funds. However the issuance of a *Metals Handbook* was a venture which after early difficulties became a great success. In 1939 a 2000-page handbook including survey of the most recent practices in both ferrous and nonferrous metallurgy was published.

Another important venture of the A.S.M. was the initiation in cooperation with other societies of the National Metal Congress. At this congress a large number of technical papers are presented showing new developments in research and in practice. An essential part of the congress is the huge exposition in which manufacturers of almost every conceivable device of interest to metallurgists show their wares.

Like most societies the A.S.M. has had its publication problem. Most of the papers and many of the lectures presented at the congresses were published in its *Transactions*. This publication grew so fast that in 1930 it was decided to limit it entirely to technical papers and to start a new publication called *Metal Progress* which presented authoritative material in a form which was attractive to the eye. *Metal Progress* was an instant success and is now read by 99 percent of the membership.

In the March Anniversary Issue of this publication is a collection of striking reports comparing metallurgical practices and products of 1915 with those of 1940. After reading a few of these progress reports, one realizes the great part which the American Society of Metals has had in this progress by directing special lines of inquiry, by promoting exchange of ideas and by the mutual stimulation of all its members. For all these things we say, "Congratulations!"

For May

Trends in Design of Fractionating Pumps, by KENNETH C. D. HICKMAN

The Development of Water-Cooled Quartz Mercury Lamps, by EDWARD B. NOEL

Pendulum Analysis in the Scale Industry, by G. R. CARLEY

Also contributed research papers on:

An X-Ray Method of Determining Rates of Diffusion in the Solid State, by JESSE DUMOND AND J. PAUL YOUTZ

A Recorder for Electrical Potentials: The Damping of Piezoelectric Systems, by FRANKLIN OFFNER

Computation of Some Physical Properties of Lubricating Oils at High Pressures. I. Density, by R. B. DOW AND C. E. FINK

For June

Special Temperature Issue. Originally the papers in this issue on magnetic cooling and stellar temperatures, which were given at the A.I.P. Temperature Symposium, were scheduled to go into the special temperature issue of the *Journal of Applied Physics*. However, because of space limitations, it was necessary to divide the series of papers, and two of them are printed here.

Magnetic Cooling; the Production and Measurement of Temperatures Below 1°K†

BY CHARLES F. SQUIRE

Department of Physics, University of Pennsylvania, Philadelphia, Pennsylvania

GIAUQUE,[1] and independently, Debye, suggested in 1926 that by use of a large magnetic field, one could cool certain paramagnetic salts below the temperature available with liquid helium. Giauque and MacDougall[8] at the Berkeley laboratory were the first to overcome the experimental difficulties and realize temperatures well below 1°K. Shortly thereafter, at Leiden by de Haas and Wiersma, and at Oxford by Kurti and Simon, similar results were reported. Temperatures of the magnitude 0.001°K have been produced by these laboratories; on the other hand, temperatures down to 0.01°K have been measured and identified with the thermodynamic temperature scale. It will be the purpose of this article to present a discussion of the experimental and theoretical research on the production and measurement of temperature in the region below 1°K. A list of references, grouped as to subject, will guide the reader in a more comprehensive study.*

A. Low Temperatures and the Creation of Order

We must begin an explanation of the magnetic cooling effect by examining the thermodynamic principles behind the production of low temperatures. The experimentalist wishes to lower the temperature of a system which is in some phase and composed of atoms, electrons, etc. There is a supply of energy (electrical or mechanical) with which he may operate on the given system. It is an everyday experience that the supply of energy could be allowed to dissipate itself into the system and so increase the temperature. This spontaneous natural process which gives the system extra energy also increases the entropy in accordance with the second law of thermodynamics. Entropy is an index of the degree of disorder of the system and for our discussion is as important as the role of energy. For example, our system might have been ice which the energy had transformed to water and then steam. The molecules locked into the crystalline pattern constitute order; in the vapor phase, disorder. We may, therefore, expect difficulty in attempting to lower the temperature of the system since this means, besides removal of energy, a creation of order in the system. However, entropy is a statistical quantity and is a function of parameters such as temperature, volume, and electromagnetic fields. Thus if the entropy may be influenced by one of these parameters (other than temperature of course) we may look for a thermodynamic process which will leave the system in a state of order and with a lower temperature.

B. Lowering Entropy of a Gas by Compression

Let us consider the process of liquefaction of a gas such as hydrogen so that these principles may be illustrated. The supply of energy available to the experimenter is used to compress the gas to about 100 atmospheres. This process is done isothermally (in practice of course it is precooled to liquid nitrogen temperatures) and then the gas is allowed to expand without thermal contact with its surroundings. The expansion causes a drop in temperature and by letting the cool gas pass out of the expansion chamber in such a way as to pre-cool the incoming gas, liquefaction soon begins.

The compressor has lowered the entropy because the system has been squeezed into a small volume without the change of temperature. For the physicist, trained in the concepts of statistical mechanics, it is more accurate to state that the distribution of the system in phase space (i.e. momentum-volume space) has been squeezed into a narrow region. Entropy is proportional to the width of the region the system occupies in phase space.

† Presented at the American Institute of Physics Temperature Symposium, New York, New York, November 2–4, 1939.

* The author is indebted to Professor Franz Simon of Oxford University, with whom he worked, for much of the material presented in this article. See references 2 and 3.

The thermodynamic definition of entropy change is

$$\Delta S = \Delta Q / T, \qquad (1)$$

where ΔQ is the heat change in the process (considered as a perfectly reversible process) and T is the absolute temperature. We shall presently consider this equation as the definition of temperature and make use of it to determine the temperature scale below 1°K. During the adiabatic expansion there is no thermal contact—i.e., $\Delta Q = 0$ and hence the absolute value of the entropy remains unchanged. The semblance of order which was given to the system by the volume parameter has now been taken over by the temperature.

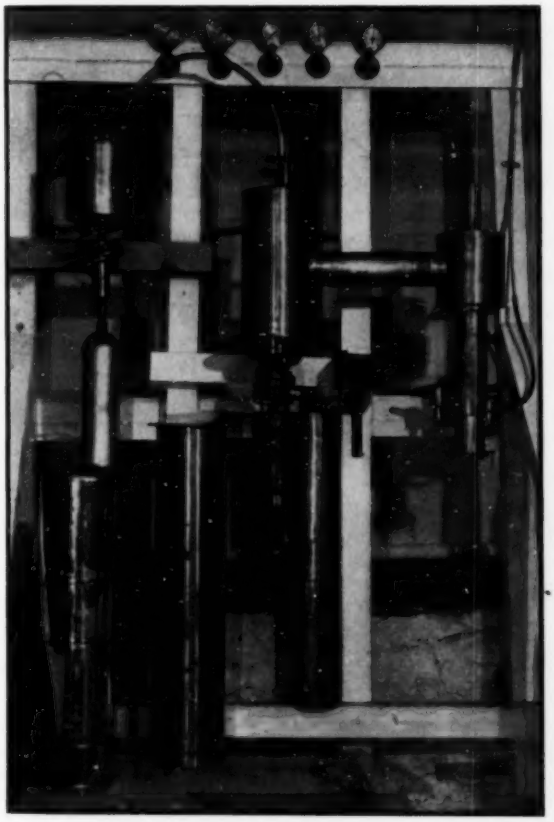

FIG. 1. Photograph of hydrogen liquefier; University of Pennsylvania.

C. *Lowering Entropy by a Magnetic Field*

By pumping the vapor phase away, the liquid hydrogen produced above can become a solid with a consequent lowering of temperature. But this is the limit for this system since the solid represents order. These remarks bring out the important features behind the production of temperatures below 1°K. For the new region, we must find a system which is still in a state of disorder at 1°K and a parameter (other than temperature) with which we may bring the disorder into a state of order. Such a system is

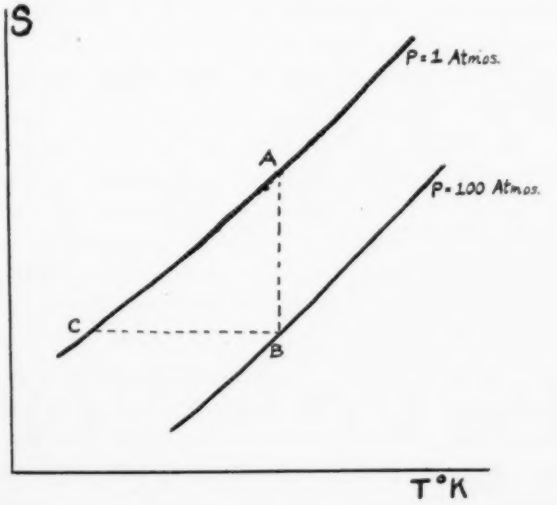

FIG. 2. Entropy temperature diagram for cooling a gas. Isothermal compression (A to B) is followed by adiabatic expansion (B to C).

to be found in those paramagnetic salts whose internal magnetic dipoles show a random spacial orientation even at 1°K. This arbitrariness of orientation on the part of the dipoles (or more properly the electron spin moment) constitutes a degree of disorder and it may be brought into a degree of order by means of a magnetic field. Thus a magnetic field is the parameter which squeezes the entropy to a lower value. The transfer of the newly created order in the system from the magnetic field parameter to the temperature parameter is entirely analogous to the $S-T$ diagram for gases in Fig. 2. An adiabatic demagnetization constitutes the transition B to C which was formerly an adiabatic expansion of the gas.

In Fig. 3 we see a photograph of the cryostat of Professor F. Simon as it appears between the pole pieces of the giant electromagnet of the Academy of Science, Paris, France. Capable of producing fields of as much as 60 kilo-gauss, this laboratory has produced temperatures below 0.01°K. In order to indicate the essential features

of the procedure, we show in Fig. 4 a sketch of the experimental chamber. Liquid helium at 1°K is in the double wall section, and the paramagnetic salt—$Fe(NH_4)(SO_4)_2 6H_2O$—is placed within the space so formed. A number of suitable salts have been used by experimenters; Professor Giauque first used the hydrate of gadolinium sulfate. The pole pieces are shown in the figure but the entire upper portion of the apparatus, the outer liquid hydrogen Dewar flask, etc., are omitted.

Three tubes lead into the cylindrical chamber from the upper portion of the apparatus. Two of these lead into the helium chamber and are for the purpose of: (1) condensing the helium into the chamber and, (2) measuring the vapor pressure of this helium in order to know the temperature of the bath. Keesom and coworkers at Leiden[17] have established this convenient vapor pressure-temperature relationship. The third tube (3) is to allow helium gas into the space about the salt so that it may serve as a heat exchanger while the powerful magnetic field is on. After the heat of magnetization has been removed—i.e., the quantity Q of Eq. (1), the "heat exchange gas" is pumped out and an adiabatic demagnetization is the result of turning off the magnetic field. The entire process of getting the heat of magnetization out of the salt, i.e., of getting both salt and bath back into a state of thermal equilibrium at 1°K, and of completing the demagnetization requires about 20 minutes. A flow meter on the evaporating gas from the helium bath indicates that the heat of magnetization has been removed when it returns to its normal reading. It is impossible to convey in a brief article an idea of the enormous amount of precision "plumbing" associated with cryostats of the above type. The months of preparation are followed by months of most strenuous experimentation—a single low temperature production and the measurements during the available period requires about 24 hours continuous operation.

D. How Low Will the Temperature Drop?

The general thermodynamic process of influencing the entropy by means of a magnetic field and so lowering the temperature of the paramagnetic salt should be clear from the above paragraphs. The question of how the field accomplishes this and of what the end temperature will be for any given salt next presents itself. Such a detailed question of the system requires a detailed description of the properties of the system.

In the case of iron ammonium sulfate, there are five electrons in the Fe ion which constitute the magnetic dipoles. At 1°K we may picture these dipoles as having a random spacial orientation. This disorder may be removed by the alignment of the dipoles with the direction of the external magnetic field. However, this creation of order by a magnetic field may be identified with the Zeeman effect. New energy states are created and the electrons move into these new states.*

In Fig. 5 we show on the entropy-temperature diagram the value at 1°K for the entropy of Fe-alum which arises from the disorder in the dipoles. The contribution to the entropy arising from the lattice vibrational energy is negligible at these temperatures. We may now make use of the Nernst law and say that at the absolute zero of temperature the entropy of the salt is zero. Thus on lowering the temperature, we may expect that the salt will, of itself, lower the entropy and so we may draw some seemingly arbitrary connecting curve as in Fig. 5. If the salt itself is to remove the degeneracy of the electron state, we must expect electric and magnetic forces within the crystal to become influential somewhere between 0°K and 1°K. In salts where these forces are strong, then their influence causes a drop in entropy at a temperature which is up towards 1°K.

* It is more accurate to think of the disorder as being connected with the fact that the five electrons exist in one energy state—i.e., a degenerate energy state. The degeneracy is removed by an external magnetic field, because the single state is split into several states. This is similar to the splitting of states observed in the Zeeman effect. In describing an energy state, we make use of so-called quantum numbers; among these is the magnetic quantum number which is made up of the spin and orbit momentum quantum numbers of the electrons in the state. In the case of Fe-alum, the 5 electrons will give rise to 6 magnetic quantum numbers: $m = \pm 5/2,\ \pm 3/2,\ \pm 1/2$ and the single degenerate energy state will split up into 6 energy states in the presence of a magnetic field. These new states will be in energy units greater and smaller than the original state as given by the expressions: $\epsilon = \pm 5\beta H,\ \pm 3\beta H,\ \pm \beta H$ where β is the Bohr magneton. The entropy per mole for this sixfold degeneracy is: $S = R \ln 6$.

The entropy-temperature curve in Fig. 5 is for zero external magnetic field. The adiabatic demagnetization process which has been discussed in the earlier paragraphs may be followed on this diagram. Starting at 1°K, a magnetic field is turned on such that the salt remains in thermal contact with the liquid helium at 1°K. The entropy is lowered by an amount proportional to the magnetic field intensity (see Appendix). An adiabatic demagnetization from this point means the entropy remains constant—thus the temperature falls to such a value as corresponds with the entropy-temperature curve in zero magnetic field. We have thus answered the question

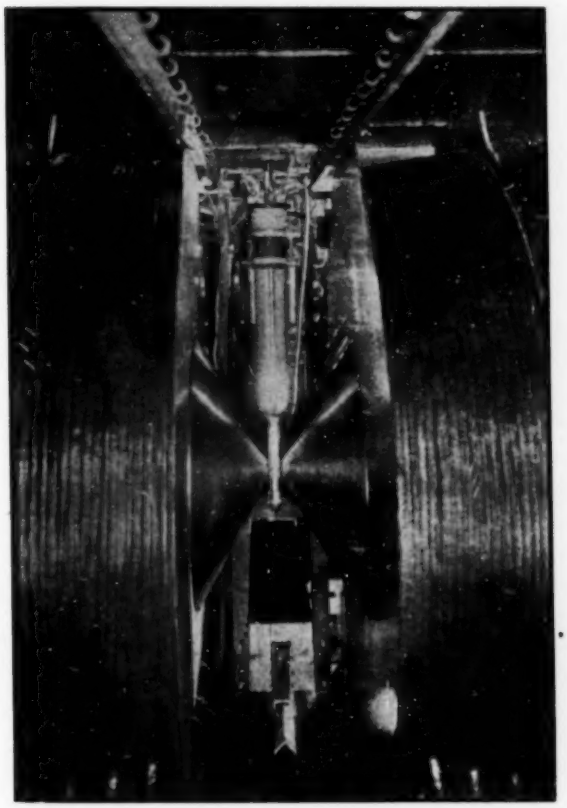

FIG. 3. Photograph of magnetic cooling cryostat; Academy of Science, France.

of how far the temperature will drop. It is clear that the magnitude of the interaction forces determines where on the temperature coordinate the entropy begins to diminish. Thus the lowest temperatures are to be obtained by those salts which are magnetically dilute i.e., the paramagnetic ions are far apart so that their interaction is indeed feeble. This is entirely analogous to the way that He gas liquefies at a lower temperature than H_2 gas because the interaction (van der Waals) forces are so feeble.

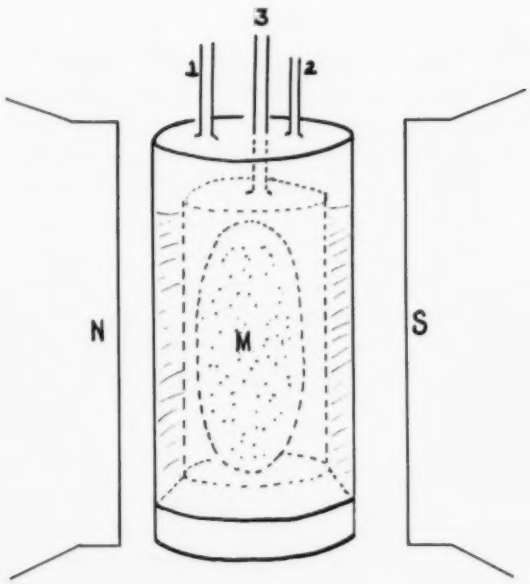

FIG. 4. Cryostat for magnetic cooling. The salt M is inside the double-walled container which is filled with liquid helium.

E. The Interaction Forces

A few words concerning the origin and nature of the above-mentioned "entropy squeezing" forces, will clarify what follows on the determination of temperature. Let us consider Fe-alum. The alum crystallizes in the cubic system; the Fe and (NH_4) ions form a "rocksalt" lattice and the 6 water molecules are placed octahedrally around the cell. The SO_4 ions are within the unit cell and thus compensate the total electrostatic charge to zero. The Fe^{+++} ions thus exist in a crystalline electric field and we may expect such a field to interact with the degenerate electron state of the Fe^{+++} ion, i.e., influence the order of the dipoles. Since each Fe ion constitutes a magnetic dipole, it will cast a magnetic field on its neighbors. A distant neighbor is another Fe ion and we may expect a feeble interaction between the magnetic dipoles.

The interaction forces arising from these two sources will serve to bring the entropy of the alum from a value $R \ln 6$ at 1°K to a value approaching zero as the temperature is lowered

to 0°K. The possibility of a further type of interaction, namely, an exchange force between the dipoles, can perhaps not be completely neglected. The magnitude of these interaction forces depends upon the particular characteristics of the paramagnetic salt. Thus also the temperature at which the forces are able to lock the system into a state of order is a particular characteristic of the salt. In Fig. 5 the drop in entropy occurs in two steps; (a) when the kT energy of the crystal becomes equal to the electric field, and (b) equal to the magnetic interaction energy.

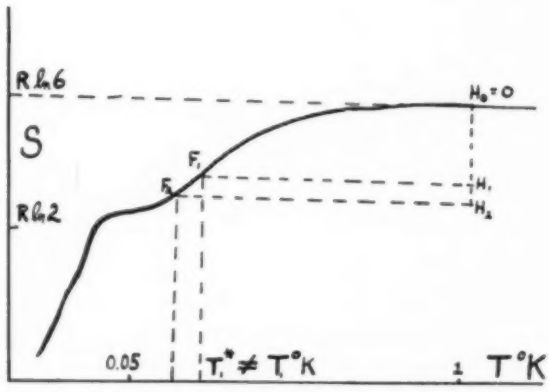

FIG. 5. Entropy temperature diagram for magnetic cooling. Isothermal magnetization (H_0 to H_1) is followed by adiabatic demagnetization (H_1 to F_1).

It is very instructive to have some idea as to the entropy changes brought about by the interaction forces. Starting from a value R ln 6, the crystalline electric field can only partially remove the degeneracy because there is left at least a twofold degeneracy corresponding to the parallel or antiparallel orientation of the dipoles to a possible external magnetic field.[26] Thus the entropy is lowered to R ln 2 by the electric field. The effect of the magnetic coupling is to lower the entropy even further. Before this action sets in one may consider the salt as composed of N independent paramagnetic ions. After the coupling action sets in, the crystal behaves like a giant molecule which has a single lowest energy state. This single lowest energy state may possibly be z-fold degenerate but in any case $z \ll N$ and so the entropy falls to the nearly zero value: $S = k \ln z$ where k is the Boltzmann constant.[23]

F. Magnetic Thermometer Below 1°K

The establishment of an absolute temperature scale in this new region has been one of the major problems for the experimentalists. The measurement of temperature in general is made possible through the regular (if not linear) behavior of some physical parameter with a change of temperature. Thus the change in pressure of the constant volume helium gas thermometer serves as a temperature indicator. But this thermometer becomes awkward at liquid helium temperatures because the gas no longer behaves sufficiently regularly. This is an important point: the failure of thermometers in temperature regions where interaction forces destroy ideal behavior. In the region below 1°K the only parameter which behaves regularly (and which can still be easily measured) is the magnetic susceptibility of the salt used in the new cooling process. However, at sufficiently low temperatures, even this thermometer departs from ideal behavior.

In Fig. 6 a simplified electrical circuit is shown for the measurement of the magnetic susceptibility of a salt (M) within the cryostat. The salt is both its own refrigerant and thermometer. The switch is closed to send a current through the primary P such that a magnetic field of several gauss is created. The two secondaries S_1 and S_2 are wound equal and opposite to one another. In the absence of a paramagnetic salt, the induced e.m.f. in the secondaries are equal and opposite so that the galvanometer (G) shows no deflection. However, when the paramagnetic salt (M) is placed within S_1 the induced e.m.f. of S_1 is increased such that the galvanometer receives a ballistic throw. The throw of the galvanometer for a given current in the primary is thus proportional to the susceptibility of the salt. The coils of Fig. 6 are kept in liquid hydrogen to lower their resistance and so make the measurements possible with an ordinary galvanometer. The salt (M) is, of course, deep nested within the cryostat as shown in Fig. 4. The current in the primary coil may be reversed in direction by a suitable switch for studying hysteresis effects in the salt. An external constant magnetic field may be superimposed on the induction system. Most workers have used alternating current in a modification of the circuit

shown here. Giauque has also maintained a small steady field and the change of induction with temperature was measured with a potentiometer across the leads of the secondary.

The magnetic susceptibility χ of the salt is the number of dipoles per unit volume per unit magnetic field exerted on the salt. The classical view was that in a solid one has a certain density of magnetic dipoles and all or part of these could be oriented by an external magnet. The experimental fact that the lower the temperature of the solid the easier for the external field to orient the dipoles led to the Weiss-Curie Law:

$$\chi = C/(T-\Theta), \qquad (2)$$

where C is Curie's constant (a characteristic constant for each salt studied) and T the absolute temperature. Θ is a temperature constant and is given by the intersection of $1/\chi$ with T axis. For salts used in magnetic cooling, Θ is approximately zero. It is not the damping of atomic vibration at low temperatures which allows the dipoles to orient so much as it is the diminution of the energy factor kT in the Boltzmann distribution expression. Starting at 4.2°K with boiling-point liquid helium we may measure χ on down to 1°K and in this way establish the curve of Eq. (2). The temperature measured from the susceptibility will be called the Curie temperature and denoted by T^*.

But one cannot rely on an extrapolation of such a scale to extremely low temperature. We have mentioned in earlier paragraphs the existence of forces within the salt which at low temperatures can influence the orientation of the dipoles. This can only mean that at this very low temperature the constant C of Eq. (2) will begin to change its value. This breakdown of the validity of the magnetic thermometer is similar to the limitation on the gas thermometer. In the latter the interaction forces cause the gas to condense. Thus the breakdown of the above magnetic method of temperature measurement occurs in just the very region we wish to measure. The difficulty cannot be removed by the choice of a salt whose interaction forces do not set in at these temperatures; indeed, it is only because the interaction forces set in at temperatures below 1°K that we are able to produce such temperatures. Further, the use of secondary thermometers involves experimental difficulties of temperature equilibrium. Giauque and MacDougall, using magnetically dilute gadolinium phospho-molybdate, have shown that at 0.15°K the Curie temperature differs by only 0.03°K. There is little to be gained by using one type of salt as a cooling agent to say 0.1°K and another, in thermal contact, whose interaction forces set in at 0.01°K as the thermometer. The intermediate temperature can be obtained with the thermometer salt and lower temperatures are available when needed.

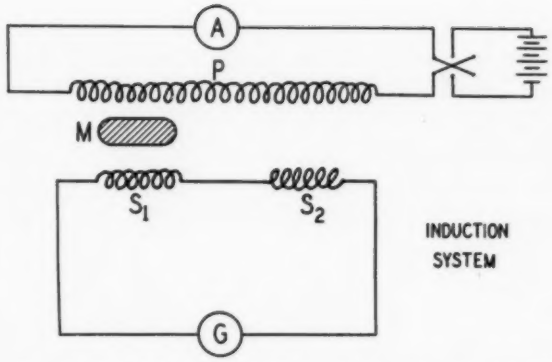

FIG. 6. Simplified electrical circuit for the measurement of magnetic susceptibility of a salt (M) within the cryostat.

G. The Thermodynamic Temperature Scale Below 1°K

Giauque and MacDougall, Keesom, Kurti and Simon, and de Haas and Wiersma have variously worked out the steps necessary for the establishment of an absolute temperature scale in the new region. The thermodynamic principles are in most cases the same, i.e., $T=\Delta Q/\Delta S$ and the quantities ΔQ and ΔS are experimentally determined. Let us consider the entropy-temperature curve of Fig. 5 to illustrate the required steps. Starting at 1°K a field H_1 lowers the entropy by a definite amount (see Appendix) whilst the temperature remains constant owing to the contact with the liquid helium. Adiabatic demagnetization proceeds to the point F_1 which has a much lower temperature T_1 measured on the Curie temperature scale. Letting the salt return to 1°K, we now begin with a field H_2 and proceed to the point F_2 which has a temperature T_2. The curve of S against T is thus established. Whilst the values of S are taken from theoretical relationships, the validity of the expression was

checked between 4.2°K and 1°K where specific heats and temperatures are determined by standard methods. By directly determining the quantity ΔQ released upon magnetization at 1°K the entropy drop can be further checked. This can be done by measuring the amount of extra liquid helium boiled away due to the heat ΔQ.

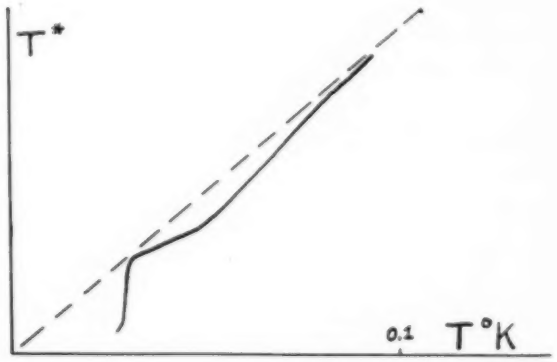

FIG. 7. Curie temperature T^* plotted against absolute temperature T°K.

The next step requires the measurement of Q against T. Having made a demagnetization to quite low temperatures the procedure calls for pouring in a known amount of heat ΔQ, whilst the Curie temperature is continuously determined. Giauque and MacDougall have accomplished this by means of an induction heater made of a gold-silver alloy which is not a super-conductor. The amount of heat introduced by such a furnace per second is determined to an unknown constant; this constant is experimentally measured in the region above 1°K where the Curie temperature and the absolute temperature are identical. A very serious objection to this technique is the fact that only the surface of the salt is heated by the furnace and thermal equilibrium throughout the salt is not established because of the salt's poor conductivity. Kurti, Laine and Simon have used another very clever technique; the heating was accomplished by bombarding the salt with γ-rays from a radium salt. Here again the unknown constant is determined by requiring the absolute temperature to be identical with the Curie temperature at 1°K. Thermal equilibrium is secured by placing the radium symmetrically about the salt.

Having measured Q and S as functions of T, the ratio of the slopes of the curves at any point determine the absolute or thermodynamic temperature:

$$T = \Delta Q/\Delta S = (\partial Q/\partial T^*)_{H=0}/(\partial S/\partial T^*)_{H=0}.$$

Magnetic fields must be held at zero because both S and Q are functions of the field. The striking results of such measurements are shown in Fig. 7 from the work of Kurti, Laine and Simon.

The first departure of T^* from T°K occurs when the crystalline electric field interaction sets in; the second when the magnetic interaction enters. Theoretical treatments by Van Vleck, Hebb and Purcell, and by Debye are in accord with the experimental results.[23–25]

One should mention the magnetic method of de Haas and Wiersma which tests the ideal behavior of the salt and sets the limit at which the magnetic thermometer may determine the thermodynamic temperature scale. The ideal behavior does not obtain for zero field, i.e., a field of 100 gauss is needed to make the energy in this field large as compared to the energy of the interactions for caesium titanic alum.

Kurti and Simon have introduced a combination of susceptibility measurements with and without external additional field which determines the absolute temperature. Heating with γ-rays is required and the ideal behavior of the substance is assumed at high temperatures for extrapolation purposes. It was verified that the act of magnetization was really reversible at these very low temperatures. This method, valid for the entire temperature region, promises to be most useful for future research.

There are of course many interesting features in connection with the physical properties of these salts, and of metals cooled by them, which we cannot discuss in this article. The temperature of a metal Tm may be quite different from the temperature of the electron spins Ts of the cooling salt because of poor equilibrium conditions.

H. Towards Absolute Zero

It has been pointed out by Kurti and Simon and by Gorter that still lower temperatures are possible by using substances with nuclear paramagnetism. The interaction energy between nuclear spin and electron spin (hyperfine struc-

ture) is so very small that the entropy drop caused by it must occur at extremely low temperatures, i.e., order of 1/10,000°K. Heitler and Teller have indicated that the interaction between crystal lattice and nuclear spin may be so feeble as to give long time effects before equilibrium is established. The experimental procedure will probably consist of a cascade of demagnetizations from an electron spin paramagnetic salt to a nuclear spin one. Thermal contact by liquid helium is possible. The problem of measuring these temperatures will be even more difficult, involving the disturbing of the system by the measuring device similar to the experiments illustrating the uncertainty principle.

I. Appendix:—Dependence of Entropy on a Magnetic Field[23]

At a temperature of 1°K the N independent paramagnetic ions have a Gibbs free energy, G, expressed by

$$G=U-TS-H\sigma \tag{3}$$

where σ is the magnetic moment of a single ion. The entropy is calculated from this by:

$$S=-(\partial G/\partial T)_H. \tag{4}$$

The free energy is calculated from the statistical expression:

$$G=kT\ln\sum_i g_i e^{-\epsilon_i/kT}. \tag{5}$$

We now calculated the above expression (5) for Fe-alum. Since kT is greater than the crystalline electric field energy, we have energy states in a magnetic field given by:

$$\epsilon_i=\pm 5\beta H,\ \pm 3\beta H;\ \pm\beta H,$$

where $\beta=eh/4\pi mc$ is the Bohr magneton.

Substituting, the free energy becomes:

$$G=-KT\ln 2[\cosh 5x+\cosh 3x+\cosh x], \tag{6}$$

where $x=\beta H/kT$.

We now get from (4)

$$S=K\ln\frac{\sinh 6x}{\sinh x}-Kx[6\coth 6x-\coth x]. \tag{7}$$

The same entropy dependence may be calculated from the Langevin-Brillouin expression for the magnetization of a paramagnetic salt. It is to be emphasized that these calculations involve a detailed knowledge of the particular salt used in the experiment.

$$\Delta S=\int_0^{H_1}\left(\frac{\partial M}{\partial T}\right)_H dH. \tag{8}$$

Where M is the magnetic moment calculated by the Brillouin function. See Van Vleck.[46]

Bibliography

References are grouped according to the subjects treated in the article.

A & B

1. W. F. Giauque, Ind. and Eng. Chem. **28**, 743 (1936).
2. F. Simon, *Handbook of the Science Museum*, Vol. III (1937).
3. F. Simon, Science Progress **133**, 31 (1939). For a more general background see M. and B. Ruhemann, *Low Temperature Physics* (Cambridge, 1937).

C

4. P. Debye, Ann. d. Physik **81**, 1154 (1926).
5. P. Debye, Physik. Zeits. **35**, 923 (1934).
6. W. F. Giauque, J. Am. Chem. Soc. **49**, 1864 (1927).
7. W. F. Giauque, J. Am. Chem. Soc. **49**, 1870 (1927).
8. W. F. Giauque and D. P. MacDougall, Phys. Rev. **43**, 768 (1933).
9. W. F. Giauque and D. P. MacDougall, J. Am. Chem. Soc. **57**, 1175 (1935).
10. F. Simon and N. Kurti, Physica **1**, 1107 (1934).
11. F. Simon and N. Kurti, Proc. Roy. Soc. **149**, 152 (1935).
12. F. Simon and N. Kurti, Proc. Roy. Soc. **151**, 610 (1935).
13. W. J. De Haas, Naturwiss. **21**, 723 (1933).
14. W. J. De Haas, Nature **132**, 372 (1933).
15. W. J. De Haas and E. Wiersma, Physics **2**, 335 (1935).
16. W. H. Keesom, Comm. Phys. Lab. Leiden **20**, (1932).
17. W. H. Keesom and G. Schmidt, Physica **4**, 963 and 971 (1937).

D

18. F. Simon and N. Kurti, Naturwiss. **21**, 178 (1933).
19. N. Kurti, Zeits. f. physik. Chemie **B20**, 316 (1933).
20. F. Simon, Nature **135**, 763 (1935).
21. W. J. de Haas, E. Wiersma and H. Kramers, Physica **1**, 1 (1933).

E

22. P. Debye, Ber. Sachs. Acad. Wiss. **36**, 105 (1934).
23. P. Debye, Ann. d. Physik **32**, 85 (1938).
24. J. H. Van Vleck, J. Chem. Phys. **5**, 321 (1937).
25. M. H. Hebb and E. M. Purcell, J. Chem. Phys. **5**, 338 (1937).
26. H. A. Kramers, Proc. Acad. Sci. Amst. **32**, 1189 (1929).
27. J. H. Van Vleck, J. Chem. Phys. **6**, 81 (1938).

F

28. F. Simon, N. Kurti and B. Rollin, Physica **3**, 266 (1936).
29. F. Simon, N. Kurti, P. Laine and B. Rollin, Comptes rendus **203**, (1936).
30. F. Simon, N. Kurti and P. Laine, Comptes rendus **204**, 675 (1937).
31. F. Simon, N. Kurti and P. Laine, Comptes rendus **204**, 754 (1937).
32. W. J. De Haas, H. Casimir and D. de Klerk, Physics **6**, 241, 255 (1939).
33. W. J. De Haas, H. Casimir and D. de Klerk, Physics **6**, 365 (1939).

G

34. W. F. Giauque and D. P. MacDougall, Phys. Rev. **47**, 885 (1935).
35. W. F. Giauque and D. P. MacDougall, J. Am. Chem. Soc. **58**, 1032 (1936).
36. W. F. Giauque and D. P. MacDougall, J. Am. Chem. Soc. **60**, 376 (1938).
37. W. F. Giauque, J. W. Stout and C. W. Clark, J. Am. Chem. Soc. **60**, 1053 (1938).
38. F. Simon, Nature **135**, 763 (1935).
39. F. Simon and N. Kurti, Phil. Mag. **26**, 840, 849 (1938).
40. W. J. de Haas and E. Wiersma, Physics **3**, 491 (1936).
41. W. J. de Haas, H. Casimir and G. J. van den Berg, Physica **5**, 225 (1938).
42. W. H. Keesom, Physica **2**, 805 (1935).
43. W. H. Keesom, J. de phys. et rad. **5**, 373 (1934).
44. A. H. Cooke and P. A. Hull, Proc. Roy. Soc. **162**, 404 (1937).

H

45. W. Heitler and E. Teller, Proc. Roy. Soc. **155**, 629 (1936).

I

46. J. H. Van Vleck, *Electric and Magnetic Susceptibilities* (Oxford University Press, 1932), p. 257.

Letters to the Editor

Correction

In connection with my paper on negative ions[1] Professor Dempster has called my attention to the fact that K. S. Woodcock[2] studied the phenomenon of negative ion formation due to positive ion bombardment at the Ryerson Laboratory and reported it several years earlier than the references quoted in my paper.[3–6] I overlooked the article and wish to call attention to its priority over the other references.

C. H. Bachman

Vacuum Tube Engineering Department,
General Electric Company,
1 River Road, Schenectady, New York,
February 21, 1940.

[1] C. H. Bachman, "Ring focusing of negative ions in a cathode-ray beam," J. App. Phys. **11**, 83–85 (1940).
[2] K. S. Woodcock, "The emission of negative ions under the bombardment of positive ions," Phys. Rev. **38**, 1696–1703 (1931).
[3] F. L. Arnot, "A new process of negative ion formation. II," Proc. Roy. Soc. **A158**, 137–156 (1937).
[4] F. L. Arnot and C. Beckett, "Formation of negative ions at surfaces," Nature **141**, 1011–1012 (1938).
[5] R. H. Sloane and R. Press, "Formation of negative ions at surfaces," Nature **141**, 872 (1938).
[6] R. A. Smith, "Formation of negative ions at metal surfaces," Proc. Roy. Soc. **A168**, 19–42 (1938).

Piezoelectric *vs.* Spring Pressure Gauge

In an article in the December number of this magazine, Webster[1] presents curves which indicate that the response of a spring pressure gauge was quicker than that of a piezoelectric gauge in firings at Aberdeen Proving Ground in June, 1922. Since these results, if unexplained, might lead to misconception, an explanation should be given.

During these firings the charge developed by the piezoelectric crystals was recorded by a ballistic galvanometer as proposed by Karcher.[2] Since the mirror of the galvanometer is elastically connected to the coil, as the coil rotates driven by the current produced by the crystals, the mirror tends to lag behind the coil producing the lag in the piezoelectric gauge record noted by Webster.

This ballistic galvanometer method of recording was abandoned in 1925 and an amplifier and electromagnetic oscillograph substituted for it. More recently a cathode-ray oscillograph was substituted for the electromagnetic oscillograph as described by us.[3] The type of apparatus now used has an over-all natural frequency much higher than can be practically obtained with a spring pressure gauge.

R. H. Kent
A. H. Hodge

Aberdeen Proving Ground,
Aberdeen, Maryland,
February 27, 1940.

[1] R. A. Webster, J. App. Phys. **10**, 890 (1939).
[2] J. C. Karcher, Nat. Bur. Stand. Sci. Pap. No. 445 (1922).
[3] Trans. A. S. M. E. **61**, 197 (1939).

Stellar Temperatures*

BY G. P. KUIPER
Yerkes Observatory, University of Chicago, Chicago, Illinois

1. Introduction

THE temperatures found in astronomical literature may be classed into two main groups, referring, respectively, to (1) the observable surfaces of the stars and planets, and (2) the interiors of these bodies. The first group depends directly on observations, although some well-established theoretical results are usually needed in the reductions; the second group depends entirely upon theoretical deductions, in connection with observed values for the boundary in order to make the problem defined. In addition we have temperature determinations of the highly diluted material filling the large spaces between the stars; they depend on observations interpreted with the aid of atomic physics.

The total range of temperatures thus covered runs from about 3° absolute to about 50,000,000°. The lower limit is well exceeded by that obtainable in the physical laboratory; but the upper limit remains reserved for the domain of astronomy, as are the upper limits of pressure and density found in astronomical bodies. The reason is that all three limits can only be reached or approached as a result of the action of gravity on large compressible masses.

Although the high pressures and densities found in the interiors of some of the stars can in no way be duplicated in the laboratory, some aspects of the high temperatures (the high kinetic energy of the particles) can now be covered by the fast particles produced in the study of nuclear processes. The energy generation in the stars, which is a result of the high temperatures and densities prevailing near the center, is therefore accessible to physical interpretation. The progress made in interpretating this process of energy generation may in turn be considered to provide a general confirmation of the temperatures computed for the interiors, on which the energy generation appears to depend in a very sensitive manner.

* Presented at the American Institute of Physics Temperature Symposium, New York, New York, November 2–4, 1939.

2. Surface Temperatures of the Stars

Obviously it is not possible to measure the surface temperatures of the stars by contact methods; but two other methods are applicable, depending, respectively, (1) on the laws of radiation, and (2) on the laws of ionization, in combination with those of atomic physics.

The observed spectral-energy curve, corrected for absorption in our atmosphere, provides the empirical data for both methods. The first method deals largely with the "continuous spectrum," i.e., the intensity distribution of the smoothly-varying background in the spectrum on which absorption and emission lines appear. The second method deals with the total intensities (or profiles, if high dispersion can be used) of these absorption and emission lines.

The empirical data are restricted to the wavelength interval of about 2900A to 140,000A, the absorption in our atmosphere being practically complete outside these limits. The lower absorption limit is caused by the ozone in our atmosphere. From about 3000A to 25,000A the atmosphere is comparatively transparent, although several heavy absorption bands due to water vapor and carbon dioxide occur in the near infra-red. These absorptions become even heavier between 25,000 and 80,000A (2.5 and 8 microns). Finally from 8 to 14 microns our atmosphere is comparatively transparent, at least if it is dry. The long-wave cut-off at 14 microns is due to carbon dioxide. The transmission curve of the atmosphere for the Mount Wilson Observatory, published in 1930 by Pettit and Nicholson,[1] is reproduced in Fig. 1. It was computed for 0.7 cm of precipitable water. Since that time many new details of the transmission curve, and their identifications, have been published by Adel.[2] As is well known, much of the earlier work on the transmission of the atmosphere is due to Langley, Abbot, and Fowle of the Smithsonian Institution; Fig. 1 is largely based on their work.

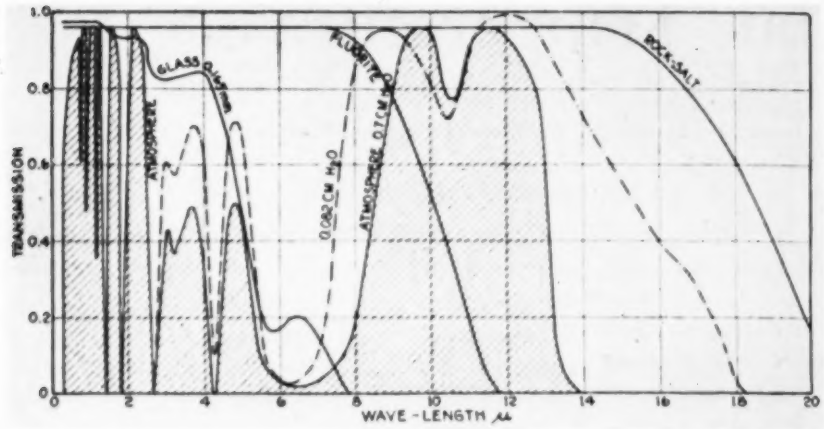

FIG. 1. Transmission curves of (*a*) the atmosphere above Mount Wilson (the shaded curve); (*b*) water vapor 0.082 cm precipitable water; (*c*) microscope coverglass, 0.165 mm thick; (*d*) fluorite 4 mm; and (*e*) rocksalt 2 mm.

3. *Stellar Temperatures Derived from the Continuous Spectrum*

The continuous spectrum has so far been the more important of the two sources of information on stellar temperatures. With the transmission curve of our atmosphere known (Fig. 1) it is possible to reduce the observed energy curves of the Sun and the brightest stars to true energy curves (as they would be observed outside our atmosphere). It now appears that these energy curves roughly, but not exactly, correspond to those due to "blackbodies," i.e., to Planck curves. We must distinguish now between two cases: (1) the diameter of the star is known (like for the Sun); (2) the diameter is not known. In the first case the ordinates of the energy curve may be reduced to absolute units (ergs emitted per cm² per sec.); but in the second case the ordinates are only relative. In the latter case, therefore, in fitting a Planck curve to the observed energy curve only the *shape* can be used; and if the wave-length interval is rather small, only the *slope*. Nevertheless we shall find only one value of the temperature giving the best fit, because the slope varies in a monotonic way with temperature. This temperature is called *color temperature*.[3] If the star should radiate like a blackbody this color temperature (T_c) would be the true temperature of the emitting layer. Actually deviations from a Planck curve always appear if the wave-length interval covered is large. This shows that T_c will depend on the wave-length used, and has no fundamental significance. Its significance is a purely practical one: T_c is easily determined empirically for a great number of stars. Because after it has once been determined for a few bright standard stars, further determinations can be made relative to these standards by making observations at the same zenith distance; then the atmospheric absorption is the same at corresponding wave-lengths for the stars compared, and is therefore eliminated in the ratio of the energies. If these spectrophotometric comparisons are made photographically, with large telescopes, color temperatures may thus be determined for stars 10,000 times fainter than the faintest stars visible with the naked eye. We shall later mention some cases where this technique is of special interest.

More progress can be made if the diameter of the star is known. We saw that then the ordinates of the energy curve may be expressed in ergs/cm² sec. We can still derive the color temperature, as before, but in addition the *total* amount of radiant energy leaving the star per cm² per sec. may be found, by integration over the energy curve. This total flux is obviously a fundamental quantity; we may express it in terms of temperature by means of Stefan's law. In astronomy this temperature is called the *effective temperature*,[4] abbreviated as T_e. It is a precisely defined quantity, of great importance for the equilibrium of the stellar atmosphere, and related to the total luminosity, L, by the relation:

$$L = 4\pi R^2 \cdot \sigma T_e^4 \qquad (1)$$

(R is the stellar radius, σ the radiation constant).

The aim of stellar temperature determinations is the evaluation of T_e for as many stars as possible. The color temperatures, T_c, are only

derived as an intermediary step, simply because they are more easily determined for a great number of stars, and are already a first approximation to effective temperatures. They may be reduced to effective temperatures once the relation between T_c and T_e is established by means of those stars where both can be determined empirically. There is well-founded hope, however, that in the near future this relation may be reliably determined from theoretical considerations, after the theory of the continuous absorption coefficient for the stellar atmosphere has been completed satisfactorily.

From Eq. (1) it follows that T_e may be found for those stars for which both L and R are known (or for which the emission per unit surface area, $L/4\pi R^2$ may be derived). Only for the Sun are these quantities accurately known; $T_e(\text{Sun}) = 5713°$ absolute. For three eclipsing binaries the data are still useful. Finally there are half a dozen stars for which the angular diameter could be measured interferometrically at Mount Wilson Observatory. They can be used also, since the apparent brightness gives L/D^2, if D is the unknown distance to the Sun, and the angular diameter gives R/D; hence L/R^2 is found independently of D.

These ten objects exhaust the list at present, and they would be entirely inadequate if the color temperatures were not already good approximations to the effective temperatures, so that only some adjustments remain necessary.

On the basis of the foregoing discussion it would seem natural to tabulate the T_e just derived against T_c. But there is an observational quantity even more easily determined with accuracy than T_c and closely related to it. It is the so-called *spectral type*. Originally the stars were ordered by their spectra according to the symbols A, B, $\cdots$ etc.; but later several symbols were dropped as superfluous, and the order of the remaining ones, if arranged according to decreasing surface temperature, is now O, B, A, F, G, K, M, if we omit a few rare types from consideration. These types are further subdivided into 10 smaller steps: $B0$, $B1$, $B2$, $\cdots B9$, $A0$, $A1$, $\cdots A9$, $F0$, etc. Most of the stars in a volume of space belong to the sequence O, B, $\cdots M$, in which the radii of the stars progressively decrease, and also the luminosities. But the latter

TABLE I. *The stellar temperature scale.*[1] *d = dwarf; g = giant. Temperatures in centigrade absolute.*

Sp.	T_e	Sp.	T_e
$A0$	10,700°	$gG0$	5200°
$A5$	8500	$gG5$	4620
$F0$	7500	$gK0$	4230
$F5$	6470	$gK5$	3580
$dG0$	6000	$gM0$	3400
$dG2$	5710	$gM2$	3200
$dG5$	5360	$gM4$	2930
$dK0$	4910	$gM6$	2750
$dK2$	4650	$gM8$	2590
$dK5$	3900		
$dM2$	3200		

[1] For the details of the derivation, see a paper by the author, Astrophys. J. **88**, 429 (1938). Table I of this paper corresponds to Table 13 of the paper quoted.

decrease very much faster than the former, because most of the decrease of the luminosities is due to the decrease in T_e (cf. Eq. (1)). These stars are said to belong to the *main sequence* (or the *dwarf* stars); the Sun is one of them. For this sequence there is practically a one to one correspondence between spectral type and T_e, and also between T_e and T_c. Hence the most practical procedure is to give T_e immediately as function of the spectral type. This is done in Table I.

In addition to the main sequence (or dwarfs) there are *giant* stars which are roughly 100 times larger in diameter than the dwarfs, and have somewhat larger masses. Since the value of the surface gravity is proportional to M/R^2 it follows that the surface gravities, and consequently the pressures and densities in the atmospheres, are roughly 10^2–10^4 times lower in giants than in dwarfs. In general the spectral type is based on the strength of the spectral lines, and is therefore a measure of the degree of ionization and excitation in the stellar atmosphere. With the greatly diminished densities in the giants lower temperatures than existing in the dwarfs are sufficient to produce the same degree of ionization (or the same spectral type). This difference in temperature between giants and dwarfs is considerable for types G and K, as is shown in Table I. Certain complications arise at the ends of the spectral sequence, connected with the significance of the criteria used in the classification.

We have indicated how L/D^2 is obtained from integration over the energy curve (L = luminosity, D = distance of star to Sun). In practice it appears to be sufficient to do this for a number

of standard stars of different spectral type, and then to determine which corrections should be applied to the apparent *visual* brightnesses in order to obtain the so-called apparent *bolometric* brightness, L/D^2. Such corrections are called bolometric corrections. The word bolometric refers in both cases to the nonselective recording of energy by the bolometer.

For the Sun the energy curve has been determined in considerable detail,[5] but for stars it is not possible to use high dispersion in the infra-red, where the sensitive photographic methods cannot be used. For cool stars ($T_e < 4000°$), which have a considerable infra-red intensity, the energy curve is most readily studied by means of a sensitive thermocouple placed in the focus of a large telescope; the different intervals of wave-length are then separated by means of filters.[6] If the known atmospheric absorption is allowed for the true energy curve is at once obtained. For stars of about the solar temperature (with the maximum of the energy curve near 5000A) either the photographic or the photoelectric method of recording energies in the spectrum are useful; but both methods need a calibration by means of a standard having a known energy distribution, before the true energy curve is found. For still higher temperatures the same two methods may be used, but for temperatures much higher than 10,000° the results become uncertain, since the maximum of the energy curve then falls below 3000A. Fortunately for these high temperatures additional information may be obtained by the method discussed in Section 5.

4. Applications

The previous discussion indicates how the energy curve, L/D^2, T_c, and T_e are determined. We have also mentioned the importance T_e has for the interpretation of the stellar spectrum, and the mechanism of the atmosphere. But the most urgent reason for making precise T_e determinations is a different one.

The three most fundamental empirical data about a star are its mass, M, its luminosity, L, and its radius, R. It is the object of theoretical astrophysics to use these data for as many stars as possible in a study of stellar structure, stellar energy generation, and stellar evolution, which are perhaps the most fundamental astronomical problems. The determination of masses is restricted to certain suitable groups of binaries. For one of these groups (visual binaries with well-known D), L may be found, but R has to be computed from Eq. (1), after T_e has been determined; whereas for the other group (eclipsing binaries) R is found in absolute units, but L can only be found by (1) from R and T_e, since D for these objects is too large for a determination from the parallax.[7]

Another application of T_e determinations is made in the study of *white-dwarf* stars. They are stars of low luminosity (dwarfish), rather high surface temperature (white), and hence, by Eq. (1), of very small radius. Since the masses of these stars are roughly equal to that of the Sun, the average densities (being proportional to M/R^3) are excessively high, 10^5–10^8 times water. The matter of these objects, except for an outer fringe which is gaseous, is in the degenerate state, obeying Fermi-Dirac Statistics. Here again we have conditions far outside the range obtainable in physical laboratories. Because the essential conclusions depend directly on the results of T_e determinations the writer's recent results on eight of these objects are given in Table II. They are the first measures of temperature made on white dwarfs (most of which are very faint), and are only approximate and somewhat provisional except for the second star, which is well determined. There is no doubt, however, that the order of magnitude is correct for all stars included.

It is necessary to point out that for white dwarfs the relation between the observed T_c and the desired T_e cannot be established empirically. Fortunately the theory of the continuous absorption coefficient is sufficiently well advanced to be useful here; it appears that with exception of a certain range of temperatures, the relation of T_c to T_e is the same as for the main sequence, where this relation is known empirically.

In Table II we have expressed L and R in terms of the Sun; they are fairly well established. The mean densities, depending on M/R^3, are less well known, first, because errors in R are increased more than threefold in these values, and second, because M is known empirically only for the first three stars. For the remaining stars M has been computed from R by means of Chandrasekhar's theoretical relation between

these two parameters. This relation involves, however, the mean molecular weight per electron, which may vary between 1 and 2 depending on the amount of hydrogen present. We have given the minimum values of the mean density, based on the extreme case in which no hydrogen is present. The other extreme, valid for pure-hydrogen stars, would give values about 4 times higher; the actual value is probably closer to the lower limit than to the upper limit.

The foregoing discussions will suffice as illustrations of the importance of the temperature problem in astronomy. In the next section we mention briefly how surface temperatures ranging from 10,000° to 100,000° are determined.

5. *Stellar Temperatures Derived from Spectral Lines*

The strength of an absorption line in a stellar spectrum depends on a great number of factors, of which the temperature is only one: it depends on the ratio of the absorption coefficient inside the line (taken for each wave-length separately) to that just outside the line, in the continuous spectrum. This means that a theoretical prediction of the strength of a line requires the knowledge of the mechanism responsible for the continuous spectrum as well as of the concentration of atoms in the level from which the absorption takes place, the atomic transition probability, and the various effects which broaden the line (radiation damping; Doppler effect of the atoms, due to temperature motion as well as to convection currents of the gases; and pressure effects). The concentration of atoms in the level under consideration depends on the abundance of the element, the degree of ionization (which depends on temperature and surface gravity), the excitation potential of the level, and again the temperature. Since, however, in a stellar atmosphere no strict thermodynamic equilibrium obtains (since otherwise no lines would be visible!) the populations of atoms in different levels is not strictly governed by the Boltzmann law. The precise allowance for this deviation from thermodynamic equilibrium is very difficult. Hence it is in general not practicable to obtain temperatures from absolute intensities of absorption lines, even apart from the difficulty caused by the uncertainty of the abundance of the element.

TABLE II. *Surface temperatures of white dwarfs, and results derived therefrom.*

NAME	T_e	L	R	MEAN DENSITY
Sirius B	9500°	0.0030	0.020	170,000
40 Eridani B	13,500	.0080	.016	160,000
van Maanen 2	8200	.00016	.0062	12,000,000
AC 70°8247	35,000±	.021	.0039	>30,000,000
Ross 627	15,000±	.0010	.0046	>19,000,000
Wolf 489	5070	.00007	.0105	> 1,000,000
Wolf 457	10,000±	.00011	.0034	>50,000,000
Wolf 219	15,000±	.00052	.0033	>50,000,000

Several of these difficulties are avoided if the behavior of a line or a series of lines originating from the same level (as the Balmer series of hydrogen) is studied along the main sequence (*O*, *B*, *A*, etc.). Assume for a moment that the continuous absorption coefficient were constant along this sequence. Then the *variation* in the strength of the line (or the series) would indicate the variation of the number of atoms in the appropriate level. Now consider as an example the Balmer series, which does not originate from the ground level of hydrogen, but from the second level. For low temperatures nearly all of the atoms are in the ground state, and very few in the second state. For very high temperatures nearly all of the atoms are ionized, and again very few atoms will be in the second state. In either case the Balmer lines will be weak. But there will be an intermediate temperature at which the ionization is not yet too far advanced, but which is yet high enough to raise many of the neutral atoms to the second quantum level. Obviously this interplay of two opposing tendencies will lead to a maximum of intensity of the Balmer series at medium-high temperatures. Actually the position of the maximum will be somewhat affected if we now take into account the known variation with temperature of the continuous absorption. But the assumption of the constant abundance along the main sequence remains unavoidable. Fortunately we have evidence that most of the stars of the main sequence have roughly the same composition; furthermore, the position of the maximum is not based on one star, but on many stars, so that individual variations of abundance are mostly eliminated in the mean result. Finally we have not one, but several elements which are suitable for this analysis: H, He, N, Si, C, and O, some of them in

TABLE III. *The stellar temperature scale. Temperatures in centigrade absolute.*

SPEC.	LOG T_c	T_c	SPEC.	LOG T_c	T_c
O5	4.9	80,000°	*B2*	4.31	20,000°
O6	4.8	63,000	*B3*	4.27	18,500
O7	4.7	50,000	*B4*	4.23	17,000
O8	4.60	40,000	*B5*	4.19	15,500
O9	4.50	32,000	*B6*	4.16	14,500
B0	4.40	25,000	*B8*	4.09	12,300
B1	4.36	23,000	*A0*	4.03	10,700

various stages of ionization. These different elements give independent results, in which the small variations in abundance remaining in the determination of the intensity maxima enter as accidental errors. From the remarkable accord between the temperature determinations as a function of spectral type, obtained from the different elements, we conclude that the effect of variations in abundance on the temperature scale may be considered to be negligible.[8]

The resulting temperature scale is found in Table III; it has been taken from a paper by the writer,[9] and is largely based on computations by Pannekoek (cf. reference 8).

6. *Planetary Temperatures*

For stars we have no *a priori* knowledge of the surface temperatures. But for the planets and the Moon we are able to predict the surface temperatures with fair accuracy if we assume that the planetary heat is due entirely to absorbed solar radiation, and not partly to internal sources.

Suppose the planet absorbed and emitted as a blackbody. Then, if L is the known luminosity of the Sun, the energy received by the planet per unit area at a point where the Sun is in the zenith, is $L/4\pi D^2$, if D is the known distance of the planet from the Sun. Since by hypothesis all this energy is absorbed and re-radiated, the surface temperature T is given by

$$\frac{L}{4\pi D^2}=\sigma T^4, \text{ or } T=\left(\frac{L}{4\pi\sigma}\right)^{\frac{1}{4}}\cdot\frac{1}{D^{\frac{1}{2}}}=\frac{390°K}{D^{\frac{1}{2}}}, \quad (2)$$

if the numerical values of L and σ are substituted, and if D is expressed in astronomical units (distance Sun − Earth = 1).

Actually the planets and the Moon are not black; but their reflectivity can be determined from the measured brightness and the known distances of the planet from the Sun and the Earth, together with the known brightness of the Sun. These reflectivities vary from about 0.07 for the Moon and Mercury, to about 0.59 for Venus. The light that is not reflected is absorbed, and its amount is therefore also known. We may call the absorbing power A. The emissivity for planetary radiation, E, can only be estimated. Eq. (2) now becomes

$$\frac{AL}{4\pi D^2}=\sigma E T^4, \quad \text{or} \quad T=\frac{390°\text{K}}{D^{\frac{1}{2}}}\cdot\left(\frac{\text{A}}{E}\right)^{\frac{1}{4}}\cdots. \quad (3)$$

This relation holds for a nonrotating planet, for the so-called subsolar point (the point that has the Sun in the zenith). If we take a point where the zenith distance of the Sun is Z the amount of heat received and emitted per unit area will obviously contain the additional factor $\cos Z$, and the temperature $(\cos Z)^{\frac{1}{4}}$. If the planet rotates fast (so that the daily temperature variation is small) an additional factor $1/\pi$ is introduced in the amount of heat received, and $\pi^{-\frac{1}{4}}$ in the temperature. If the planet rotates slowly the temperature fluctuations around this "average" will be greater, depending on the properties of the planetary atmosphere, and the speed of rotation.

The principle of determining planetary temperatures empirically is the same as that described in Section 3 for stars. Although at first sight the case might seem more complicated because the radiation received from the planet does not only consist of the heat radiated by the planetary surface but also of reflected sun light, yet this complication disappears in practice since the two kinds of radiation are practically entirely separated in wave-length, so that a filter may be used to distinguish between the two. This separation is a result of the difference in temperature between the two sources, about 6000° and 300°K, so that the wave-lengths of the maxima fall at about 5000A and 100,000A (0.5 and 10 microns), respectively. Fortunately our atmosphere is fairly transparent between 8 and 14 microns if it is sufficiently dry (Fig. 1), so that the surface temperatures of most of the planets, and the Moon, may be measured. Only for the planets beyond Saturn the distance to the Sun becomes so large ($D>10$) that the temperatures drop below 100°K; for these planets the radiation of

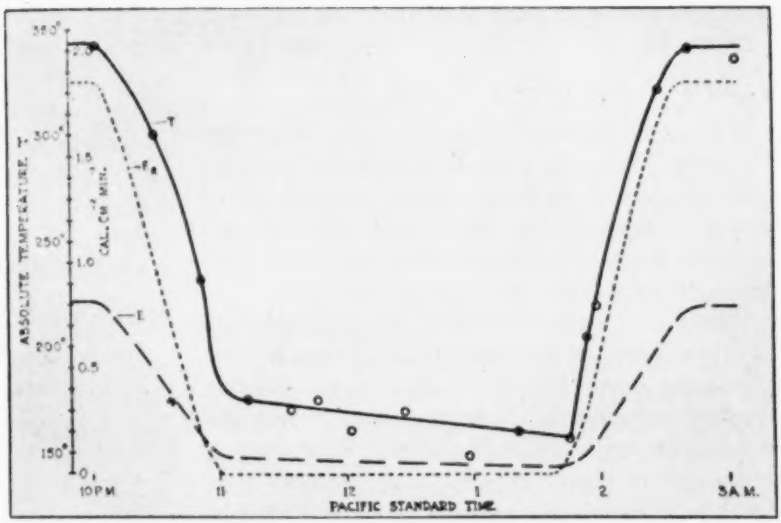

FIG. 2. March of absolute temperature, T, of energy received from the sun by the moon, E_R, and of energy radiated, E, during the total lunar eclipse of June 14, 1927.

wave-length shorter than 14 microns is too weak to be measured.

For the planets Mercury, Venus, Mars, Jupiter, and Saturn, and for the Moon, temperatures have been determined empirically, chiefly at the Mount Wilson and Lowell observatories.

For Mercury (which has no atmosphere) Pettit and Nicholson[10] found about 330°C for the subsolar point when the planet has its mean distance from the Sun. This value is only about 10°–15° lower than computed theoretically for a nonrotating planet (as indicated above). Part of the difference may be due to conduction.

For Venus Coblentz and Lampland,[11] and Menzel[12] found about 50°C at noon. Pettit and Nicholson[13] found lower values, but at both observatories the day and night temperatures on the planet were found to be rather similar, indicating that the planet is rotating slowly. (A fast rotation is excluded on the basis of measured Doppler shifts.) The temperature found for Venus may well refer to some average layer in the atmosphere, since this atmosphere is quite opaque to visual, and even infra-red, light.

On Mars the temperature at the subsolar point is near 0°C, probably somewhat higher in certain dark areas. The polar caps are about −70°C. The night at Mars is probably very cold, perhaps −60°C. The dew point at Mars is probably about as low as this latter value, in view of the extremely small water-vapor content of the atmosphere. The existence of liquid water on the planet (for which there is no direct observational evidence either) can therefore probably be excluded.

Jupiter appears to have a temperature of about −135°C, Saturn −150°C, and Uranus less than −185°C. These temperatures refer to an atmospheric layer in each case. For none of the planets is there definite evidence that the measured temperatures are higher than those to be expected theoretically; hence there is no evidence of internal heat raising these temperatures.

For the Moon, Pettit and Nicholson[14] found for the subsolar point +134°C when viewed from above, and only +85°C if viewed horizontally. The difference is explained by the rough surface of the Moon which allows more heat to escape vertically than horizontally. Taking into account the solar radiation lost by reflection the theoretical temperature at the subsolar point comes out to be 101°C. The dark side of the Moon was found to be about −150°C, a value difficult to determine with precision because of its extreme lowness.

A series of very interesting observations was made by Pettit and Nicholson during a lunar eclipse. A point near the edge of the Moon was kept under observation for about 5 hours, during which it was first illuminated by the Sun, then passed into the shadow of the Earth, and finally emerged again. The diagram showing the temperature variation is reproduced in Fig. 2. It shows the extremely rapid cooling of the surface (from about 70°C to −115°C) which must be the result of a small conductivity, comparable to that of pumice or volcanic ash which, on the basis of measures of the polarization of the reflected light,

had already been assumed to cover the surface of the Moon.[15]

7. *Interstellar Temperatures*

Although interstellar space is a far better "vacuum" than the best obtainable in the physical laboratory, it is by no means devoid of matter. The dark obscuring clouds in the Milky Way, as well as the "interstellar" absorption and emission lines prove this conclusively.

These two lines of evidence point at once at the two kinds of matter occupying space. The obscuring clouds are composed of dust particles of which a good fraction have diameters between 0.1 and 1 micron; this follows from the scattering properties of these particles, and estimates that may be made of the mass of absorbing clouds. The interstellar absorption and emission lines prove the existence of gases in the atomic state. Hydrogen is by far the most abundant interstellar element, as was recently shown by Struve. Calcium, sodium, titanium, and potassium have been found from their absorption lines; oxygen and nitrogen are present in emission. Some interstellar lines are still unidentified.

The temperatures to be ascribed to the interstellar particles need some explanation. There is no more difficulty in assigning a definite temperature to a dust particle than to a planet, and it may be computed by an equation similar to (2) or (3). A particle far away from any one star would be exposed, on the average, as we are on a clear night by the starry skies except, of course, that no atmosphere would absorb the ultraviolet light, and that the stars would cover a sphere, not a hemisphere. Eddington has shown[16] that such a particle would assume a temperature of about 3°K.

But the radiation in interstellar space is very far from being blackbody radiation corresponding to 3°K. It contains much ultraviolet light due to the *O* and *B* stars in the sky. Hence ionization and excitation of atoms will take place in spite of the low energy density. Since the density of matter is also very low, recombinations will occur at a very slow pace. Without computations it is seen, therefore, that a fair proportion of the atoms may well be ionized. The ionizations will in turn lead to considerable velocities of the ions and electrons. Since collisions between particles are still sufficiently frequent the velocities of the particles forming the interstellar gas will approximate a Maxwellian distribution corresponding to a high temperature, roughly 10,000°, and in the proximity of hot stars even higher. Obviously there is no universal temperature of the interstellar gas; it depends on the position with respect to the stars, as the planetary temperatures depend on the distance from the Sun.[17]

8. *Internal Temperatures of Stars*

It can be easily shown[18] that if a star as a whole is in hydrostatic equilibrium (which is probably true for normal, constant, stars), and if the perfect-gas law holds throughout (this assumption can be verified afterwards, and found to be justified), it is possible without any further assumptions about the internal structure of a star to obtain a *minimum* value for the average internal temperature, $\bar{T}$:

$$\bar{T} > 3{,}840{,}000(\mu\beta)M/R, \tag{4}$$

in which M is the mass of the star, R its radius, both expressed in terms of the Sun, μ its mean molecular weight, and β the ratio of the gas pressure to the total pressure (gas+radiation). For stars with $M<10$ we have $\beta \leqq 1$. Since the matter in a star is mostly ionized, and since the atomic weight is roughly double the atomic number except for hydrogen, we have $\mu \leqq 2$ if no hydrogen is present, and $\mu = \frac{1}{2}$ if the matter is all hydrogen.

If the additional assumption is made that the stars are built on the same pattern (except for factors of scale) then the relation

$$T = C \cdot (\mu\beta)M/R \tag{5}$$

holds for corresponding points in these stars, C depending on the point selected, and on the pattern common to the stars considered.

We derive some interesting conclusions from (5). For stars on the main sequence in the neighborhood of the Sun (types *A*, *F*, *G*, and *K*), having the same hydrogen content (μ = constant), the internal temperatures will vary only slowly, because $\beta \leqq 1$, as mentioned before, and M and R change in the same direction. But since M changes faster than R, the internal temperatures will increase if M increases. It is this slow increase in internal temperature which is sufficient, in connection with the high sensitivity of the energy generation on $T(\sim T^{15})$ to cause a very

TABLE IV. *Central temperatures.*

STAR	TYPE	T (CENTRAL)
Sirius	*dA*1	24,500,000°
Mizar	*dA*2	22,000,000
Procyon	*dF*3	18,000,000
Sun	*dG*2	19,500,000
70 Oph. A	*dK*1	17,500,000
Capella A	*gG*4	5,100,000

considerable increase of L with M (empirically $L = M^{4}$) for the range of masses considered).

The numerical values of the internal temperatures depend on numerical integrations which cannot be discussed here.[19] We quote the values for a few stars in Table IV.

It follows from (5) that the giants (with large radii) will have low internal temperatures. This gives rise to difficulties with the explanation of the energy generation which have not yet been solved completely. On the other extreme are the massive *O* stars having comparatively small radius. If they were built on the same model as the less massive stars their internal temperatures would exceed 100,000,000°C, and the energy generation would be too large by a considerable factor. Chandrasekhar has recently removed this difficulty by proposing a shell-source model for these stars, which leads to a more homogeneous density distribution than that of ordinary stars, and requires much lower temperatures for the hydrostatic equilibrium, temperatures not much higher than the minimum values required by (4), about 40,000,000°.

Perhaps the highest internal temperatures occur in sub-dwarfs, stars roughly $\frac{1}{2}$ to $\frac{1}{4}$ of the diameter of the Sun, having a small hydrogen content ($\mu \leqq 2$). The internal temperatures of some of these stars may well exceed 50,000,000°; their small hydrogen content would not lead to difficulties with the energy generation.

White dwarfs have still smaller radii, but Eq. (5) is not applicable to them, because the matter is degenerate. The internal temperatures are still somewhat uncertain, but are probably at most about 20,000,000°.

Bibliography

1. E. Pettit and S. B. Nicholson, Astrophys. J. **71**, 104 (1930).
2. A. Adel, Several papers in the *Astrophysical Journal*, 1938–1939.
3. The astronomical usage agrees here with that recommended in the glossary of the Temperature Symposium.
4. It corresponds to the *radiation* temperature of the glossary. The astronomical usage dates back several decades.
5. Cf. A. Unsöld, *Physik der Sternatmosphären* (1938), pp. 27–40.
6. Reference is made to the extensive series of measures by E. Pettit and S. B. Nicholson with the 100-inch telescope at Mount Wilson, Astrophys. J. **68**, 279 (1928), and **78**, 320 (1933). The instruments used in astronomical measurements of radiation, and their complete theory, are described by B. Strömgren, *Handbuch der Experimentalphysik* **26**, 795 (1937).
7. The reader will find the details of the derivation of M, L, and R for many stars in a paper by the author, Astrophys, J. **88**, 472 (1938). A theoretical discussion of the empirical data is found in Chandrasekhar's recent monograph, *Stellar Structure* (University of Chicago Press, 1939).
8. Space does not permit us to indicate more than some of the principles involved. For a more technical account, cf. A. Pannekoek, Astrophys. J. **84**, 481 (1936). (Pannekoek's results for temperatures lower than 8000° have to be modified in view of more recent work; but those for higher temperatures, in which we are chiefly interested, still stand.) For a general account on the interpretation of absorption lines, cf. O. Struve, Popular Astronomy **46**, 431–451, 497–509 (1938). Also: D. H. Menzel, *ibid.* **47**, 6–22, 66–79, 124–140 (1939).
9. G. P. Kuiper, Astrophys. J. **88**, 429 (1938).
10. E Pettit and S. B. Nicholson, Astrophys. J. **83**, 84 (1936).
11. W. W. Coblentz and C. O. Lampland, Popular Astronomy **30**, 551 (1922).
12. D. H. Menzel, Astrophys. J. **58**, 65 (1923).
13. E. Pettit and S. B. Nicholson, Popular Astronomy **32**, 614 (1924).
14. E. Pettit and S. B. Nicholson, Astrophys. J. **71**, 102 (1930).
15. For further information about planetary temperatures the reader is referred to the papers already quoted, and to: Menzel, Coblentz and Lampland, Astrophys. J. **63**, 177 (1926). H. N. Russell, *The Solar System and Its Origin* (Macmillan, 1935). T. Dunham, Publ. Astr. Soc. of the Pacific **51**, 253 (1939).
16. A. S. Eddington, *The Internal Constitution of the Stars* (Cambridge University Press, 1926), Chapter 13.
17. For an analysis of the physical conditions of the interstellar gas, particularly of hydrogen, cf. B. Strömgren, Astrophys. J. **89**, 526 (1939).
18. Cf. B. Strömgren, Ergeb. d. exakt. Naturwiss. **16**, 467–470 (1937). Chandrasekhar, reference 7.
19. Chandrasekhar, reference 7.

Contributors to This Issue

B. Fried

Bernard Fried is research physicist on the staff of the Engineering Experiment Station, Ohio State University. He holds a B.S. degree in engineering physics from the University of Illinois, and a Ph.D. degree in physics from Ohio State University, from which he was graduated in 1939.

N. E. Bradbury

Norris E. Bradbury, who received his Ph.D. degree from the University of California in 1932, is now Associate Professor of Physics at Stanford University. From 1932 to 1934 he held a National Research Fellowship at Massachusetts Institute of Technology.

C. F. Squire

Royal Weller, Ph.D. Ohio State, is now a member of the Department of Mechanical Engineering of Washington State College. Dr. Weller taught mechanical engineering at Rochester Mechanics Institute (1928–36) and physics at Ohio State (1938–39), and was employed as photoelasticity expert by the N.A.C.A. at Langley Field (summer, 1939). Dr. Weller's photograph appeared on p. 325, Vol. 9, No. 5, 1938.

F. J. Norton

Charles F. Squire is an Instructor of Physics at the University of Pennsylvania. He received his Ph.D. degree in 1937 from Johns Hopkins University where he was a Patrick Garvin Fellow. In 1938 he was a fellow at the French Academy of Science, Paris. While at the Academy he did magnetic cooling experiments.

A. Kirkpatrick

Francis J. Norton is a member of the Research Laboratory staff of the General Electric Company at Schenectady, New York. In 1924 he was graduated from Yale University with a degree of Ph.D. in the field of physical chemistry, and worked for the next six years with the Solvay Process Company at Syracuse, New York.

E. W. Sanders

Edward W. Sanders is an inspector in the Engineering Department, Field Section, Federal Communications Commission. He has studied at Villanova College and Temple University. From 1933 to 1938 Mr. Sanders was in the Crystal Laboratory of the RCA Manufacturing Company.

Arnold Kirkpatrick is in charge of plasticizers and resins in the Technical Service Department of the Monsanto Chemical Company, St. Louis, Missouri. Mr. Kirkpatrick received the B.S. degree from Hamline University, and has been associated with the Roessler and Hasslacher Chemical Company and Tubize Chatillon Corporation.

G. P. Kuiper

Gerard P. Kuiper received his Ph.D. degree in astronomy at the University of Leiden, Holland, in 1933. He was a member of the Dutch Eclipse Expedition to Sumatra in 1929. Since 1936 he has held a professorship in astronomy at the University of Chicago, dividing his time between the Yerkes Observatory in Wisconsin and the McDonald Observatory in Texas.

J. H. Dillon has been employed since 1931 in the Physics Research Division of the Firestone Tire and Rubber Company, Akron, Ohio, and has been head of that division since 1937. He received his B.A. degree from Ripon College in 1927, and his Ph.D. from the University of Wisconsin in 1931.

The following contributors have appeared before in the *Journal of Applied Physics*, and mention of them and their work has been included in earlier issues:

H. W. Farwell, p. 106, Vol. 10, No. 2, 1939.
Louis A. Pipes, p. 187, Vol. 10, No. 3, 1939.
George H. Shortley, p. 325, Vol. 9, No. 5, 1938.

Here and There

Cover Photograph

The illustration shows the mass spectrometer recently constructed at the Westinghouse Research Laboratories at East Pittsburgh. The chief feature of this device is the large spherical coil for obtaining a uniform magnetic field. Square copper tubing is wound on two brass hemispheres of 20" diameter, and the density of turns varies as the sine of the angle with respect to the axis—the spacing being obtained with maple wedges. A field of 19 oersteds per ampere is obtained, and by circulating water through the coil a field of 2500 oersteds can be maintained continuously with a moderate rise in temperature. The hemispheres are movable to permit convenient access to the vacuum tube, which is mounted on a fixed support. The satisfactory operation of the mass spectrometer attests to the uniformity of the magnetic field, which, by actual measurement, was found to be uniform throughout the enclosed sphere to at least 0.5 percent.

★

Applied Physics in the South

The sixth annual meeting of the Southeastern Section of the American Physical Society was held March 22 and 23, 1940, at the Citadel, Charleston, South Carolina. A portion of the program was devoted to the subject, "Applied Physics in the South." Dr. Paul D. Foote, Executive Vice President of the Gulf Research and Development Company, addressed the meeting on the topic, "Gasoline, from the point of view of the physicist."

★

Consulting Editor Appointed

The appointment of Dr. Lee A. DuBridge as Consulting Editor of the International Series in Physics was recently announced by the McGraw-Hill Book Company, Inc. Dr. DuBridge is Harris Professor of Physics and Dean of the Faculty of Arts and Science at the University of Rochester. As Consulting Editor of the International Series in Physics, he succeeds the late Dr. F. K. Richtmyer. This series was established in 1930 with the publication of Ruark and Urey's *Atoms, Molecules and Quanta*. It now comprises twenty-eight volumes, and the twenty-ninth volume, to be issued this spring, will be *The Modern Theory of Solids*, by Dr. Frederick Seitz of the University of Pennsylvania.

Research Fellowships Awarded

Eight college graduates have been granted Charles A. Coffin Fellowships, totaling $5000, for use in carrying on advanced scientific research during the next school year, it was announced recently by W. W. Trench, Secretary of the Charles A. Coffin Foundation. These Fellowships were established by the General Electric Company in 1922 to honor its retiring president and founder.

The students will carry on their work in five different educational institutions; two at Stanford University, and one each at Johns Hopkins, Michigan, Wisconsin, Rochester, California and Harvard Universities.

The eight men who have been awarded fellowships are: Marritt L. Kronberg, Baltimore, Maryland; Melvin L. Renquist, San Jose, California; Henry M. Foley, Birmingham, Michigan; Ernest C. Barkofsky, Madison, Wisconsin; LeRoy W. Apker, Rochester, New York; William H. Fenn, Berkeley, California; William J. Barclay, Palo Alto, California; and Robert J. Dwyer, Norwood, Ohio. Kronberg and Dwyer also received fellowships last year.

★

Mathematical Tables Being Computed

A project for the computation of mathematical tables sponsored by Dr. Lyman J. Briggs, Director of the National Bureau of Standards, Washington, D. C., is being conducted by the Federal Works Agency, Work Projects Administration for the City of New York. The aim of this project is to compute mathematical tables of fundamental importance in mathematics, physics, engineering and related sciences. The project has been in operation since January 1, 1938, under the technical supervision of Dr. Arnold N. Lowan. A table of the first ten powers of the integers from 1 to 1000 and a comprehensive table of exponential functions have already been published. Comprehensive tables of circular and hyperbolic functions, trigonometric and exponential integrals and certain physical tables have been completed and are now in process of reproduction. Tables of probability functions and Bessel functions for complex arguments are now in progress. Doctors A. N. Lowan and G. Blanch published, in the February issue of the *Journal of the Optical Society of America*, a paper entitled "Tables of Planck's radiation and photon functions." Requests for copies of the National Bureau of Standards tables should be sent to Dr. Lyman J. Briggs, Washington.

Radioactive Standards*

A series of radioactive standards are being prepared under the direction of the Committee on Standards of Radioactivity of the National Research Council. These standards will be deposited at the National Bureau of Standards in Washington, D. C., to be issued as working standards to investigators who may desire them. The standards under preparation at present are:

(1) *Radium standards.*—(a) 100-cc solutions sealed in 200-cc Pyrex flasks containing 10^{-9} and 10^{-11} gram of radium to be used as emanation standards either directly or by subdilution; (b) 5-cc solutions sealed in Pyrex ampoules containing 0.1, 0.2, 0.5, 1.0, 2.0, 5.0, 10, 20, 50 and 100 micrograms of radium to be used as gamma-ray standards. If desired, these may be obtained in sets of 13 with two each of the 0.2, 2, and 20-microgram standards.

(2) *Thorium standards.*—Sealed ampoules containing sublimed $ThCl_4$. These may be used in preparing standard thorium solutions. Directions for use will be furnished with the standards.

(3) *Standard rock samples.*—The following rocks, ground to pass 40-mesh screen and be retained on 100-mesh screen are available in 100-gram samples. Quartzite (Virginia), Triassic diabase (Virginia), Milford granite (Massachusetts), Chelmsford granite (Massachusetts), Gabbro-diorite (Massachusetts), Columbia River basalt (Idaho), Berea sandstone (Ohio), Dunite (North Carolina), Carthage granite (Missouri), Carthage limestone (Missouri), Deccan trap (India), Kimberlite (South Africa).

These samples of rock will be analyzed for radium and thorium content and are intended for use as working standards to check methods used in extraction of radon and thoron from rock samples. They may be used for direct fusion in the electric furnace or for carbonate fusion.

All of the above samples will be analyzed at a number of laboratories equipped to make such measurements and ultimately certificates will be issued by the National Bureau of Standards. This work is in progress but will require considerable time for its completion so that final figures are available only for a part of the samples at the present time.

Accurate knowledge of the radioactive content of the materials of the earth's crust is of primary importance in many phases of geology, geophysics and cosmology. Reliable radioactive standards are also essential in studies of radium and thorium poisoning and in biological and medical investigations using the technique of radioactive indicators, or internal artificial radioactivity therapy. For the latter purposes calibrated standard sources of β-rays will be made available.

It is hoped that the standards which have been prepared by the Committee will provide all workers in these fields with a common basis for comparison of measurements and also improve the accuracy of all measurements of this type. It is likely that they will have other applications and the Committee would appreciate hearing from interested persons who may desire similar standards for their work. The Committee is also glad to cooperate as far as possible in aiding investigators to use these standards to the best advantage and welcomes specific inquiries regarding their use. It is urged that any suggestions regarding other desirable radioactive standards, not at present available, be submitted promptly to the Committee. In particular, it will facilitate the work of the Committee if those laboratories and individuals which can make use of these standards advise the Committee of their probable requirements.

Communications may be addressed to the Chairman, Professor Robley D. Evans, Department of Physics, Massachusetts Institute of Technology, Cambridge, Massachusetts.

L. F. Curtiss
Clark Goodman
Alois F. Kovarik
S. C. Lind
C. S. Piggot
Robley D. Evans

* This work is being supported in part by a generous grant from the American Philosophical Society to the Massachusetts Institute of Technology.

★

Tension Test Symposium Planned

The American Society for Testing Materials announces that a special committee has been formed to organize technical discussions covering the subject "Significance of mechanical properties of metals." Dr. J. M. Lessells, Associate Professor of Mechanical Engineering, Massachusetts Institute of Technology, is chairman of the committee. The first of these discussions will take the form of a symposium on the tension test proposed as a part of the annual meeting of the Society in Atlantic City, June 24–28. The following program has been arranged for the symposium:

The Tension Test.—C. W. MacGregor, *Associate Professor, Massachusetts Institute of Technology*

The Strength Features of the Tension Test.—F. B. Seely, *Professor and Head, Department of Theoretical and Applied Mechanics, University of Illinois*

The Ductility Features of the Tension Test.—H. W. Gillett, *Metallurgist, Battelle Memorial Institute.*

★

Cited for Radio Development Work

The Gold Medal of the American Institute of the City of New York was presented to Dr. Frank Conrad, pioneer in radio broadcasting, on February 1, 1940; the presentation was made at a dinner at the Hotel Pierre, New York, attended by 200 leaders in various fields of science. The citation was for "his pioneering work in short wave and frequency modulation and for his guiding genius in developing the world's first radio broadcasting system." Dr. Conrad is Assistant Chief Engineer of Westinghouse Electric and Manufacturing Company.

In accepting the honor signified by the medal, Dr. Conrad recounted the beginnings of short wave radio and demonstrated the short wave set used by him and Mr. David Sarnoff, now President of the Radio Corporation of America, in London nearly 20 years ago when systems were being discussed for radio intercommunication between far-flung sections of the British empire.

Network Television

Network television was demonstrated to Federal Communications Commission members in Schenectady, February 1 by General Electric engineers. This was the first demonstration of its kind in which a program transmitted from New York was clearly received in Schenectady homes, 142 air-line miles away. It was made possible by the use of a new relay station working in conjunction with its main transmitter atop the Helderberg Mountains. Although telecast programs had been received at the Helderberg relay station before in tests, it was the first time that such programs were rebroadcast for the entertainment of persons in the area served by the local station. Both image and voice were considered excellent by members of the commission, equally as good as programs originating in the Schenectady studio, thus proving to the commission that network television is possible.

★

Dinner Honoring Dr. Miller

A dinner honoring Dr. and Mrs. Dayton C. Miller in recognition of Dr. Miller's 50 years of service to Case School of Applied Science, was held at Wade Park Manor on March 14. Dr. Philip M. Morse, Dr. J. J. Nassau and Dr. W. R. Veazey paid personal tributes to Dr. Miller. After the dinner a Founder's Day Convocation was held at which an oil portrait of Dr. Miller was presented to the college. Dr. W. F. G. Swann, Director of the Bartoi Research Foundation of the Franklin Institute, spoke at the convocation on "Science and Human Happiness."

★

Honorary Degree Awarded

Dr. Philip M. Morse, Professor of Physics at Massachusetts Institute of Technology, was awarded an honorary degree of Doctor of Science at the Founder's Day Convocation of Case School of Applied Science on March 14.

★

Nobel Prize Awarded

Dr. Ernest Orlando Lawrence received his Nobel prize award February 29 from the hand of Mr. C. E. Wallerstedt, the Swedish consul-general at San Francisco. The ceremonies were conducted by Dr. R. G. Sproul, President of the University of California, who stated that Dr. Lawrence was the first active faculty member of a state university to win a Nobel prize. Professor Raymond T. Birge, Chairman of the University's Department of Physics, reviewed Dr. Lawrence's career and emphasized the very practical applications of radioactivity in medicine and other fields. In accepting the award, Dr. Lawrence paid tribute to the important part which his colleagues have played in the development of the Radiation Laboratory at the University of California.

★

New Appointment

Dewey Deforest Knowles, inventor of the grid-glow tube and numerous other electronic devices, has joined the research engineering staff of the Westinghouse Special Products Department, Bloomfield, New Jersey, it was announced recently by H. J. Hoffman, manager of the Special Products Department. He will undertake special research and engineering studies on the Sterilamp.

Mr. Knowles was a member of the research staff of the Westinghouse Research Laboratories in East Pittsburgh, Pennsylvania, from 1923 to 1937, in which year he accepted the position of director of research and development for the Raytheon Production Corporation, Newton, Massachusetts.

★

Recent Booklets

The *General Radio Experimenter* for February, 1940, carries the following articles: "Routine frequency measurements to 0.005%," "Special megohm bridges," and "Modernization of broadcast frequency monitors." The *Experimenter* is published by the General Radio Company, 30 State Street, Cambridge A, Massachusetts.

Cenco News Chats, February, 1940, describes in one of its articles the life and work of Michael Faraday who also furnishes the theme for the magazine's cover. The February issue also includes an invitation for applications from senior college students with physics majors, and with minors in chemistry and mathematics or both, for the Cenco Industrial Fellowships. Chemistry majors with physics and mathematics as minors are also eligible for the fellowships, each of which carries a stipend of $1200 for a period of one year's work under the supervision of the Director of Research and Development of the Central Scientific Company. Application blanks may be secured on request from Dr. M. N. States, Central Scientific Company, 1700 Irving Park Boulevard, Chicago, Illinois.

★

Calendar of Meetings

April

7–13	American Ceramic Society, Toronto, Canada
8–12	American Chemical Society, Cincinnati, Ohio
9–11	Society of Exploration Geophysicists
17–19	American Society of Civil Engineers, Kansas City, Missouri
22–25	Society of Motion Picture Engineers, Atlantic City, New Jersey
24–27	American Geophysical Union, Washington, D. C.*
25–27	American Physical Society, Washington, D. C.
29–30	Acoustical Society of America, Washington, D. C.

May

1–3	American Society of Mechanical Engineers, Worcester, Massachusetts
6–10	American Foundrymen's Association, Chicago, Illinois
13–15	American Institute of Chemical Engineers, Buffalo, New York

June

6–8	National Colloid Symposium, Ann Arbor, Michigan
9–14	Society of Automotive Engineers, White Sulphur Springs, West Virginia
10–14	American Medical Association, New York, New York
17–19	American Society of Heating and Ventilating Engineers, Washington, D. C.
17–21	American Society of Mechanical Engineers, Milwaukee, Wisconsin
19–21	American Physical Society, Seattle, Washington
24–28	American Society for Testing Materials, Atlantic City, New Jersey
24–28	American Institute of Electrical Engineers, Swampscott, Massachusetts
27–29	Institute of Radio Engineers, Boston, Massachusetts

July

24–26	American Society of Civil Engineers, Denver, Colorado

August

27–30	American Institute of Electrical Engineers, Los Angeles, California

* It has been called to our attention that the dates for the A.G.U. were incorrectly given in the March issue.

Innovations in Instruments

Signal Generator

The RCA "Signalyst," a low priced signal generator designed for increased efficiency in radio and television receiver alignment work, has been announced by L. W. Teegarden, RCA Tubes and Equipment Sales Manager. The new service instrument is a companion to the Rider Chanalyst and the Rider VoltOhmst recently acquired by RCA. The instrument (designated as Stock No. 161) has a fundamental frequency range of 100 kilocycles to 120 megacycles on 10 bands, greater than is available on any service test oscillator. The Signalyst is accurate and stable to within plus or minus 1 percent scale calibration, according to the manufacturer, and heterodyne detection is provided for calibration purposes. Operating on 110–120-volt, 50–60-cycle power supply, the Signalyst has a maximum output voltage of 0.05 volt at low range and 1.3 volts at high range. It is useful for $R-F$ and $I-F$ alignment of radio broadcast receivers and special receivers operating in the ultra-high frequency bands, for television over-all tests when modulated by square waves or composite picture signals, and for direct calibration of television receiver local oscillator when used in conjunction with the Piezo Electric Calibrator.

Corrosion Resistant Needle Valve

A new Hoke corrosion resistant needle valve has recently been marketed by Hoke, Incorporated, 122 Fifth Avenue, New York City. This valve makes use of a full-floating spindle inasmuch as the axis of the valve spindle is not rigidly fixed in relation to the valve body, but rather is fixed in relation to the spindle thread gland. Another special feature insures that the relation of the valve seat to the spindle point, and consequently the rate of flow, will remain essentially unchanged when the packing nut is turned to tighten the packing. Valves are furnished with either V-point or blunt-point spindles, the V-point being the low flow type, while the blunt-point is suitable for larger flows or for on and off service.

Sterilamps Used in Air Conditioning

A "new dimension in air conditioning"—the use of ultraviolet rays to kill air-borne bacteria—was announced by Dr. H. C. Rentschler, Director of Research for the Westinghouse Lamp Division at Bloomfield, New Jersey, and Dr. Rudolph Nagy, of his research staff, to members of the American Society of Heating and Ventilating Engineers on January 24 during its 46th annual meeting in Cleveland, Ohio.

As a result of hundreds of tests made on an actual installation of Westinghouse "Sterilamps" in an air duct delivering 5800 cubic feet per minute in an auditorium at the Lamp Division, 40 lamps killed 99.5 percent of all bacteria passing through the duct; 32 lamps killed 98.2 percent.

Flowmeters

Two new low-cost instruments for measuring the rate of flow of gases and for vacuum work have been recently announced by the Laboratory and Pharmaceutical Division of Corning Glass Works, Corning, New York. The first is a new improved type flowmeter. Fabricated from Pyrex brand balanced glass, it is said to be of simpler, improved construction. It is completely self-contained and requires no extra parts. Four orifices approximately $\frac{1}{4}$, $\frac{1}{2}$, 1 and 2 mm are provided in a hollow stopper. Selection is made by turning the stopper to the desired orifice. Direction of flow is also indicated.

The new "Pyrex" manometer is claimed to be the most inexpensive so far introduced. It has heavy walls and a scale ranging from 0 to 160 mm which is acid etched and red pigment filled. The manometer is available in two types —straight side arm and "T" arm. Filling is fast and easy.

Fluorescent Lacquer-Enamels

A new series of fluorescent lacquer-enamels in twelve shades has been put on the market by the Continental Lithograph Corporation, 952 East 72nd Street, Cleveland, Ohio. These "Conti-Glo" lacquer enamels may be applied over any non-oily surface adapted to receive ordinary paint coatings. They emit brilliant colored light when held within range of the radiations from a black-light (near ultraviolet) lamp in a darkened room. The fluorescent enamels are said to be equivalent in permanency to the average indoor colored paints, and the "invisible green" shade is sufficiently resistant to sunlight for successful use in exposed window displays and temporary outdoor exhibits. These paints are designed for use for entertainment purposes, indoor displays, and decoration in theaters, hotels, clubs, restaurants, auditoriums, and homes. Additional information and sample cards showing the Conti-Glo lacquer-enamels may be obtained from the manufacturer.

Contributed Original Research

Some Relations Between Molecular Structure and Plasticizing Effect*

ARNOLD KIRKPATRICK
Monsanto Chemical Company, St. Louis, Missouri
(Received July 12, 1939)

The inter-relation between the chemical constitution and structure of plasticizers and plastics is discussed. The results obtained with sulfonamide, phthalate and phosphate plasticizers in cellulose acetate compositions are used as examples and the author speculates on the possibility of formulating general rules from such data.

INVESTIGATORS in the field of plastics have done much excellent work on the mechanics of condensation and polymerization and on the probable structure of synthetic resins. In the practical application of the various plastics, however, it is frequently necessary to add other materials designated as plasticizers in order to obtain properties not resident in the base plastic. In spite of the large number of compounds which have been proposed as plasticizers, there seems to have been no extensive effort made to correlate the plasticizers with the plastics and the properties resulting from their combinations.

Should it prove possible to formulate definite rules for plasticizing the various classes of plastics, including the cellulosic derivatives, much routine testing might be eliminated and the synthesis of plasticizers much simplified. Moreover, the study should throw additional light on the structure of the plastics themselves.

The problem presents several difficulties:

(1) The structures of the plastic molecules are still subject to some question.

(2) Exact comparable data regarding the properties imparted by plasticizers are not readily available.

(3) Interpretation of the results and speculation on the rules governing such interactions may require some departure from the more orthodox chemical ideas.

(4) Final proof of the truth or falsity of any theories formulated may require some rather complex and difficult physical measurements.

The purpose of this paper is more in the direction of indicating the type of data which may be of importance than in presenting a mass of data on the subject or in support of some one theory. The data offered touch only a few types of plasticizers and plastics. In this particular problem it seems that speculation and theorizing should be indulged in at this stage in order to stimulate the presentation of corroborating or conflicting data.

The literature reveals a number of references that have a bearing, although rather indirectly, upon the subject. Discussions of chemical constitution, x-ray patterns, structure of compounds of high molecular weight, chemical affinity, functional groups and spatial configuration provide data and theories which may become of importance in establishing the final answers. Discussions of the permeability of films to gases, vapors and liquids and the ways of decreasing such permeability bear more directly upon one phase of the problem. Theories regarding gel structures and the constitution and behavior of extensible compounds such as rubber may be found to apply to other phases. All of this emphasizes the scope of the problem and the probable value of the results once correlation is established between the various phases. Because of the practical industrial aspects involved, it is unlikely that any two investigators will long follow exactly the same line of attack.

A primary factor in the study of plasticizers is *retentivity*—that is, the amount of plasticizer which can be incorporated into a plastic without showing evidence of separation. Separation may

* Presented before the Society of Rheology at the Tenth Annual Meeting, Mellon Institute, Pittsburgh, Pennsylvania, December 28–29, 1938.

be evident by several things—crystals within the mass, minute crystals on the surface, droplets on the surface, or a reduction of transparency varying from a mere haze to complete opacity. It may show up immediately or after a long period of time and it may in some cases appear only after the plastic is bent or stretched.

Table I shows the retentivity of several compounds in one type of cellulose acetate. The compounds are grouped according to similarity in chemical structure. The retentivity values are expressed in percent based on the weight of cellulose acetate, i.e., in parts per 100 parts of cellulose acetate.

Three rather obvious facts can be garnered from this sort of data: (1) certain groups, such as oxygen attached to sulfur, phosphorus, or carbon, and the sulfur nitrogen group, tend to give compatibility; (2) the degree of compatibility (retentivity) is affected by the groups surrounding the active centers; (3) it is possible to increase the compatibility of a long chain grouping by inserting active centers at points along the chain.

Retentivity data are apt to be somewhat misleading, however, and should not be interpreted too exactly. It is agreed that all of our plastics, whether they be cellulose derivatives or synthetic resins are mixtures of compounds of quite similar constitution. Although the physical constants of the aggregate may imply identical chemical structure as regards two lots of plastic, there may actually be some variation. Moreover, the other added components, such as volatile solvents, may have an effect, as well as the method and conditions of incorporation, and the conditions of temperature, time and humidity when the test samples are made. For example, the re-

TABLE I. *Retentivity of several plasticizers in cellulose acetate.*

COMPOUND	STRUCTURAL FORMULA	RETENTIVITY IN *Ac/C*
Orthotoluene sulfonamide	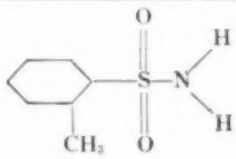	35
Paratoluene sulfonamide	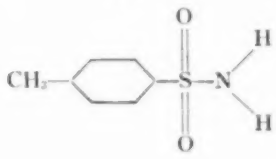	30
Mixed *o-p*-toluene sulfonamide		40
Ethyl *o-p*-toluene sulfonamide	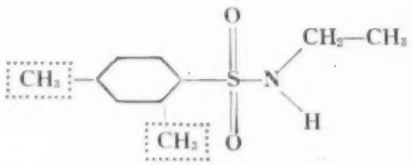	100
Cyclohexyl *p*-toluene sulfonamide	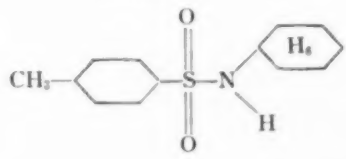	75
Dimethyl phthalate	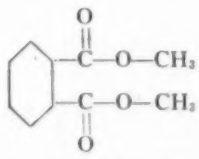	100+(Solvent)

TABLE I.—*Continued*

COMPOUND	STRUCTURAL FORMULA	RETENTIVITY IN *Ac/C*
Dibutyl phthalate	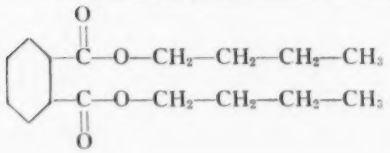	10
Diphenyl phthalate	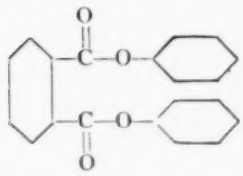	50
Triphenyl phosphate	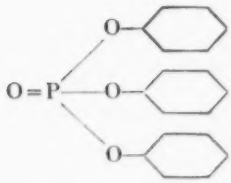	80
Tricresyl phosphate	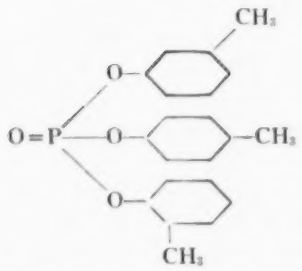	15

tentivity of triphenyl phosphate is that indicated in Table I only when films are cast from solution in volatile solvents. When colloided with a minimum amount of solvent, the retentivity is only about half that given in the table. Again, although dimethyl phthalate is one of the best solvents of all the plasticizers for cellulose acetate, its use is no guarantee that one will not get a large amount of so-called "cotton blush" unless the conditions under which the films are made are carefully controlled.

Some plasticizers make certain plastics very soft and of greatly reduced tensile strength. Others, especially when the retentivity limit is exceeded, make some plastics very brittle. Still others, even when separation takes place, do not make the plastics brittle or greatly reduce the tensile strength. This raises the question as to how a plasticizer functions. It seems pretty well established that plasticization can result in three ways: (1) by solvent action; (2) by simple lubrication of the plastic micellae; (3) by a combination of these two actions.

The first type tends toward soft and weakened plastics. The second produces less change in the physical characteristics of the plastic but is apt to develop separation. The third type is a compromise between the other two; one might consider every plasticizer to function as the third type—that is, some portion of the plasticizer molecule is attached, more or less strongly to some portion of the plastic molecule, thereby tending toward solvent action, and the unattached portions act as lubricants between the plastic molecules.

We are greatly restricted in our visualization of such action because of our incomplete knowledge of the actual arrangement in space of the various

parts of molecules. It may be, however, that we are nearer to the answer than we realize. A comparison of the most commonly accepted structural formulae of camphor and cellulose and a consideration of the unique action of camphor in nitrocellulose at least gives food for thought. Table II shows the structural formulae for the cellulose unit and camphor and, for comparison, polyvinyl acetate, polyvinyl acetal and the units of the three vinyl compounds, vinyl acetate, methyl methacrylate and styrene. If the camphor diagram is superimposed on the cellulose one and rotated, noting the points of greatest probable attraction and repulsion, one begins to get a picture of why camphor has a unique place among nitrocellulose plasticizers. The comparison also suggests a possible reason why camphor does not have a similar effect in other plastics.

One question which immediately arises is: What is the importance of the actual distance between the so-called active groups of the plasticizer in relation to corresponding groups in the plastic?

Another factor of interest in this problem is the effect of plasticizers on moisture resistance of a plastic. Figures 1, 2 and 3 show curves indicating the amounts of moisture penetration through cellulose acetate films containing 12.5 percent, 25.0 percent, 50.0 percent and 100.0 percent of several plasticizers. The films, 2.5 mils thick, were cast from solutions in acetone, aged a week, then tested by fastening over the mouths of bottles containing anhydrous calcium chloride and exposed in a humid atmosphere for twenty-

TABLE II. *Comparison of structure of cellulose unit, camphor, and vinyl compounds.*

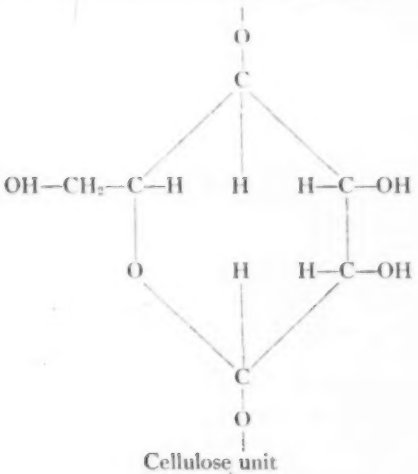

Cellulose unit

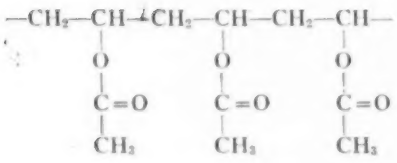

Vinyl acetate polymer

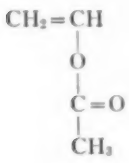

Vinyl acetate

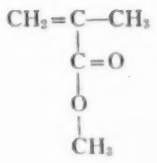

Methyl methacrylate

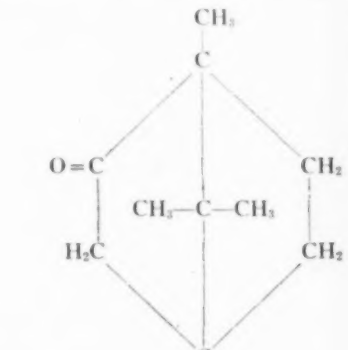

Camphor

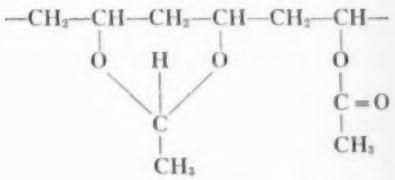

Vinyl acetal polymer

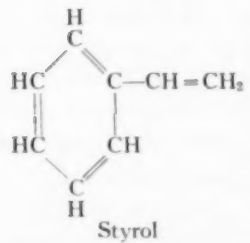

Styrol

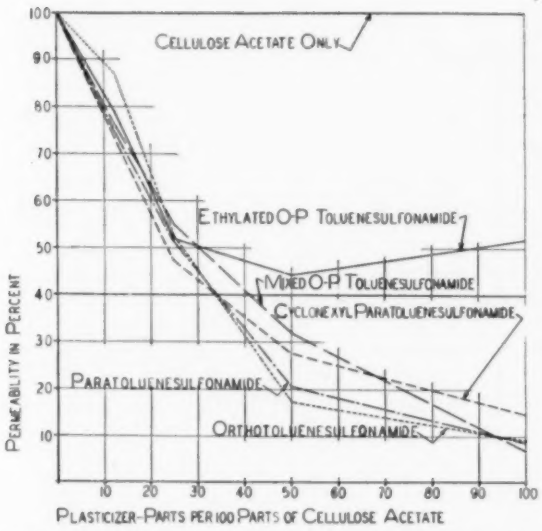

FIG. 1. Cellulose acetate with ethylated *o-p*-toluene sulfonamides, mixed *o-p*-toluene sulfonamides, cyclohexyl paratoluene sulfonamide, paratoluene sulfonamide and orthotoluene sulfonamide. (In the figure cyclohexyl is misspelled.)

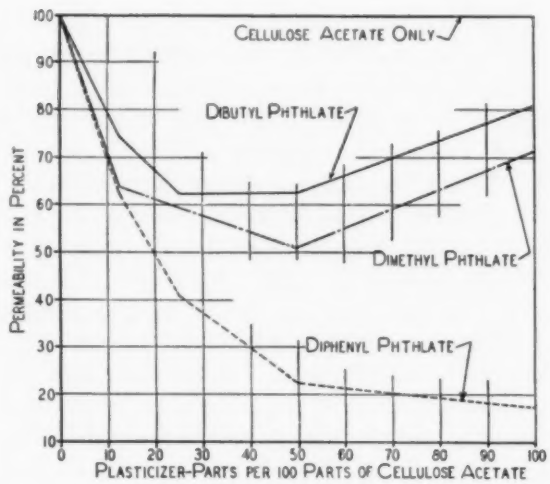

FIG. 2. Cellulose acetate with dibutyl, dimethyl and diphenyl phthlates.

four hours. The percentages of moisture penetration were calculated by taking the amount passing through an unplasticized film as 100 percent. The results are comparable with each other but the values are by no means to be taken as absolute values. Fig. 1 shows some sulfonamide derivatives (ortho, para, mixed ortho and para, mono ethyl mixed and cyclohexyl para, toluene sulfonamides). Fig. 2 shows dimethyl, dibutyl and diphenyl phthalates. Fig. 3 shows triphenyl and tricresyl phosphates.

The significant thing about these curves is that actual insolubility of the plasticizer in water appears to have little effect. Taking two of the phthalates which are liquids, we see that dimethyl phthalate, which is about four hundred times as soluble as dibutyl phthalate, actually allowed less moisture penetration. In the same way, comparing two solids, the mixed *o-p*-toluene sulfonamide gives values of about the same order as the cyclohexyl *p*-toluene sulfonamide, although its water solubility is about 2200 times as great (1 percent against 0.00045 percent). The solids do better than the liquids and the difference between triphenyl and tricresyl phosphates is interesting. The tricresyl curve is regular although separation begins at a relatively low concentration. The triphenyl curve follows the same regular trend until it begins to separate and then falls off sharply. Had an intermediate point been observed, say around 65 percent, it would probably have shown an almost flat extension from the 50-percent point and the entire fall would have come between there and the 100-percent point. This statement is based on other observations that with triphenyl phosphate in cellulose acetate, the break in the moisture penetration curve comes near the point where separation of the plasticizer becomes evident.

It will be observed that in several cases the curves actually rise after a certain concentration of plasticizer has been reached. This is not unusual and instances could be cited where in relatively large amounts the plasticizers actually increased the amount of moisture penetration over that of an unplasticized film. Again we come to the question—why?

The triphenyl phosphate curve would seem to indicate that retentivity has a great deal to do with the matter but the tricresyl phosphate and the diphenyl phthalate curves cancel that idea. Perhaps the answer lies in the structure of the plastic and can be tied in with our previous theorizing regarding the mechanics of plasticization. Again taking cellulose acetate as an example, we can consider a sheet of it to be in the form of a loosely woven fabric. The cellulose units are joined together in chains to form the filaments. The filaments are bundled together to form the threads and these woven into a definite pattern which is the fabric. The weave is

so loose that moisture passes through. The addition of a compound which distributes itself between the filaments tends to spread these, thereby increasing the diameter of the thread and decreasing the space between the threads. This results in lessened moisture penetration. The addition of practically any compound that is not highly water soluble will have that effect. When the amount of added material reaches the point that the attraction of the plastic units of the filaments no longer hold it in place, the plasticizer tends to gather on the threads and may show evidence of separation. From that point, the effect on moisture permeability will depend upon the physical character of a very thin film of the added material.

It should be pointed out that the same effect can be obtained in certain plastic materials by chemically producing cross linkages between portions of the molecule. A comparison of the formulae for vinyl acetate polymer and vinyl acetal polymer given in Table II indicates how this is done. Increasing the size of the aldehyde molecule used in bringing about this internal linkage tends to increase this effect, although it is possible that an aldehyde of too great chain length would bring about the opposite effect. This appears to be a purely physical interpretation. The water resistance of camphor can be explained by the complete coverage of the cellulose units and by formation of a continuous structure due to linkages of the camphor with parallel cellulosic chains or, as we have called them, filaments. The broad structure of the camphor molecule gives results which are not duplicated by compounds that have a narrow chain structure, even though the chain may tend to give numerous bonds between parallel filaments. On that basis one would not expect the same results from branched chain aliphatic compounds as from the corresponding normal compounds. This is borne out by observed differences in the moisture resisting qualities imparted by iso-butyl- and normal butyl-phthalate.

The assumptions already made may be extended to explain why any particular plasticizer gives dissimilar results with different plastics. If the retentivity depends upon mutual attraction between portions of the plastic and the plasticizer,

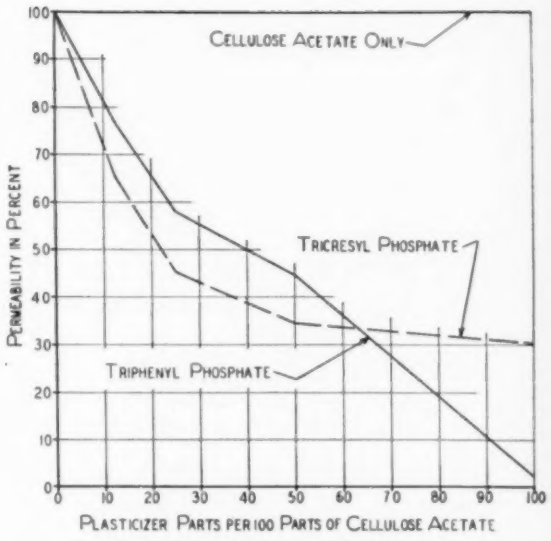

FIG. 3. Cellulose acetate with tricresyl and triphenyl phosphates.

then different results must be expected because in the several plastics the groups that serve as points of attachment will differ in composition, structure and the limiting effect of other portions of the molecule. Further, this attraction-repulsion principle may explain why the relative volatilities of compounds when alone do not necessarily indicate their volatilities when incorporated in plastics. Everyone is familiar with the speed at which some very nonvolatile plasticizers are lost from a plastic while some relatively volatile materials are held tenaciously. The evaporation rate of diethyl phthalate from cellulose acetate and the retentivity of low boiling esters in polyvinyl acetate resins are illustrations of this point.

The effect of a plasticizer upon the actual flow of a plastic in which it is incorporated is not easy to evaluate because of the many variables involved and the difficulty of devising tests which will cover more than a narrow range of conditions. The following method was used to obtain some comparative figures for thin films of cellulose acetate containing various amounts of several plasticizers: Strips 1 centimeter wide and approximately 6 centimeters long were cut from the prepared films which were two and a half mils thick. Spring clips were attached to each end of the strips so as to leave exactly 5 centimeters between the edges of the jaws of the two clips. One clip was then fastened to a glass rod and to

the other was added sufficient weight to make a total load of 5 grams on the film. These were placed in an electrically heated oven and the temperature slowly raised until the films began to stretch under the load. The highest temperature used was 150°C because this approached the point at which the cellulose acetate itself would begin to soften.

Using the same series of plasticizers as employed for the moisture penetration tests, that is, sulfonamides, phthalates and phosphates, in 25 percent, 50 percent and 100 percent concentrations, the results are interesting but not exactly what one would expect. The ethyl *o-p*-toluene sulfonamide was the only compound which showed flow in 25 percent concentration. This compound was also the only one whose effect was regularly dependent upon the amount present; the temperatures at which flow was evident for the three concentrations of 25 percent, 50 percent and 100 percent were, respectively, 135°, 96° and 45°C. The melting point of the plasticizer appears of little consequence. In 50 percent concentration the mixed *o-p*-toluene sulfonamide which has a melting point of about 105°C began to flow at 83°C, the cyclohexyl *p*-toluene sulfonamide with a melting point of 87°C began at 114°C, and the ethylated compound, which is a liquid, began at 96°C. The two nonsolvent liquids, dibutyl phthalate and tricresyl phosphate gave no flow, even in 100 percent concentrations. Diphenyl phthalate which we have considered a nonsolvent and which is a solid melting at 69°C did, however, show a very definite effect at 145°–150°C even in 50 percent concentration. One rather unexpected phenomenon is the fact that with the exception of the ethylated mixture of ortho- and paratoluene sulfonamide and the cyclohexyl paratoluene sulfonamide, all of the compounds showed a negligible effect on the flow at 25 percent concentration but apparently reached a maximum effect at about 50 percent concentration. Of the two exceptions one is a liquid and a solvent for the plastic base while the other is a solid and ordinarily considered a nonsolvent.

It is not only the temperature of flow but the character of the plastic combination at that temperature that is of great interest and this point shows up best in the highest concentration. With the *o-*, *p-* and mixed sulfonamides, the films softened suddenly and completely, or, as we might describe it, simply melted down over a few degrees temperature range. None of the others, including the ethyl and cyclohexyl sulfonamides, exhibited this phenomenon but instead showed a slow steady elongation over a rather wide temperature range. This is somewhat at variance with what we usually consider to be the effect of adding a solvent plasticizer to a material such as a cellulose ester.

The data obtained by this method are of use in evaluating plasticizers for some particular purpose where flexibility or flow over a definite temperature range is desired. Our present interest, however, lies in any possible light the data may shed on the relation between chemical constitution or structure and plasticizing effect. The information is as yet too meager to point to positive evidence but there are certain indications that should be considered. We refer to the difference in action between diphenyl phthalate and dibutyl phthalate, between triphenyl phosphate and tricresyl phosphate, and between the ethyl and cyclohexyl substituted sulfonamides as against the unsubstituted amides, these to be considered in the light of what we have said previously regarding points of attraction and repulsion and distance between those points in both plasticizer and plastic.

Summary

It should be possible to correlate the effects produced by plasticizers on various plastics by a study of their accepted structural formulae. We have tried to indicate the significance of a few results and interpret these in general terms applicable to classes of compounds. Absolute proof must rest on the compilation of a tremendous amount of comparative data obtained by many workers and evaluated by many minds. In the light of our present knowledge we suggest the following factors as being of importance: (1) Presence in both plasticizer and plastic of groups that afford points of mutual attraction. (2) Proper location of these groups in relation to each other so as to permit the attractive forces to function. (3) Proper shape of the plasticizing molecules so as to give the physical characteristics necessary to produce the exact results desired.

Diffusion of Hydrogen from Water Through Steel

FRANCIS J. NORTON*
Research Laboratory, General Electric Company, Schenectady, New York
(Received July 27, 1939)

Using a metal radio tube having a steel shell as an ionization gage, the diffusion of hydrogen through the steel into the interior was measured. This results from the fundamental corrosion reaction on the exterior, when it is dipped into water:

$$Fe+H_2O=FeO+H_2.$$

The protective paint on the tube prevents this, but a bare sandblasted iron surface admits hydrogen at 0.13 micron per hour with the shell in water at 25°C. Hydrogen does not diffuse into the tube when water vapor alone surrounds it. Rates of diffusion were measured through plain and composite metal shells, varying surface treatment and temperature.

THE reaction of water with iron to produce hydrogen and iron oxide is the fundamental corrosion reaction:

$$Fe+H_2O=FeO+H_2.$$

This type of reaction may occur in high pressure steam boilers operating in the temperature region of 300°C, giving black scale on the tubes and liberating hydrogen. The gas which forms inside enclosed hot water heating circuits is often hydrogen.

Whenever iron is put into water, this reaction occurs, even at room temperature. The hydrogen formed is not generally susceptible of observation. Some of it which has plated out on the surface may be evolved, and some is oxidized as a surface reaction by dissolved oxygen in the water. A third portion of this hydrogen dissolves in the steel and diffuses into it. It is the diffusion of this hydrogen through steel which forms the subject of this paper.

The phenomenon was originally observed by Cailletet[1] for the case of iron in dilute sulfuric acid. It has been measured by T. S. Fuller[2] and by Dällenbach[3] for the case of steel and water. Schikorr[4] found there was hydrogen evolution when rusted iron turnings were left in contact with air free water in a closed system. Other aspects are discussed by Smithells.[5]

The metal vacuum tube 6C5 makes an excellent means for observing the hydrogen flow. It is a small evacuated volume with thin steel walls (25 mils), and having in its interior a means of observing the pressure. The elements which cause it to function as a radio tube—plate, grid and filament—may be used as an ionization gage to measure gas pressure if appropriate calibration is made.

The circuit of the 6C5 tube used as an ionization gage is shown in Fig. 1. It was run under the following conditions:

Plate voltage	150 volts
Grid bias	−3 volts
Heater current	0.300 ampere
Plate current	5 to 10 milliamperes
Grid current	Proportional to gas pressure. Measured in microamperes.

It will be noted that the grid is at the most negative potential in the tube. Hence no electrons will reach it, but positive ions will flow to it, constituting the grid current. Since the number of positive ions is proportional to gas pressure, the grid current is a measure of gas pressure.

It should be understood that the metal tube shell alone is entirely vacuum tight under all normal operating conditions, where the tube functions in radio sets. Paint or enamel is put on in manufacture to protect against atmospheric corrosion and to add to the appearance.

For the purpose of these experiments the protective paint on the outside of the tube was sandblasted off. This formed the standard surface for most of the tests. The tube was then dipped into water at 25°C so the outside of the steel shell, but not the base, was covered. After various

* This paper was presented at a meeting of the American Chemical Society at Chapel Hill.

[1] Cailletet, Comptes rendus **56**, 847 (1863).
[2] T. S. Fuller, Gen. Elec. Rev. **23**, 702 (1920).
[3] W. Dällenbach, Elek. Tech. Zeits. **55**, 85 (1934).
[4] Schikorr, Zeits. f. Elektrochem. **35**, 62–70 (1929).
[5] C. J. Smithells, *Gases and Metals* (Chapman and Hall, Ltd., 1937), pp. 127–136.

periods in water it was taken out and the grid current measured. This grid current is proportional to gas pressure in the tube, and hence the amount of hydrogen diffusing through the steel into the tube was found.

The grid current shows a variation with time. The filament was turned on and the grid current measured. It was found (Fig. 2) that the longer the tube was left in water, the higher the second peak.

The cause of two peaks is not definitely known but represents the warming up of the tube to a condition where a certain balance is attained at about 2 minutes. After that the well-known effect of "clean up" of hydrogen in the tube takes place along the latter portion of the curve.

The fact that this second peak measures the amount of gas in the tube was checked by sealing one of the tubes to a vacuum system. A definite amount of gaseous hydrogen, at a definite pressure as measured on a McLeod gage, could then be admitted. This same type of curve for grid current *vs.* time was obtained when the sealed-off volume was kept small.

The plate current was about 10 milliamperes. It varied from tube to tube, depending on the degree of activation of the hot cathode. Hence all grid currents were corrected to a constant plate current of 10 ma. A convenient unit was taken:

$$Ig \text{ in } \mu a / Ig \text{ in ma} \times 10$$

and by means of a tube sealed to a separate system, as mentioned above, the following calibration was made for hydrogen and nitrogen.

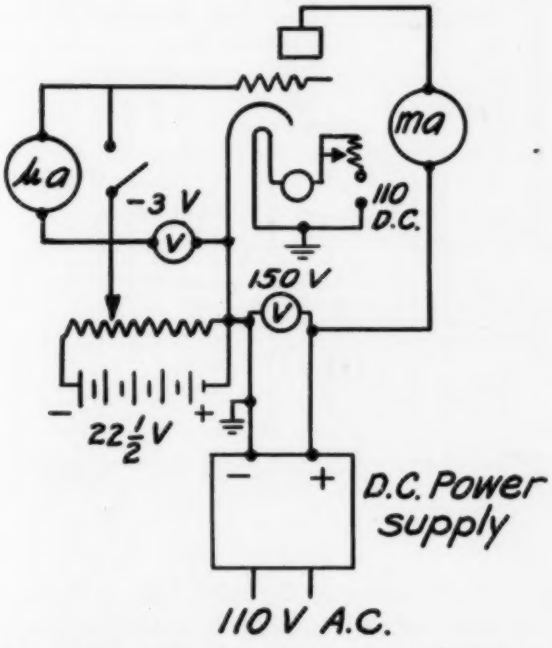

FIG. 1. Circuit using 6C5 vacuum tube as ionization gage.

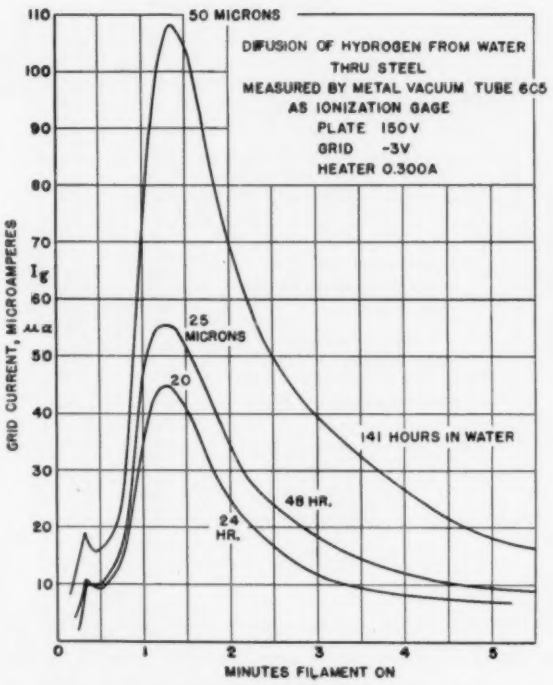

FIG. 2. Measurement of grid current.

Analysis of the gas which diffused from water through steel was made by the apparatus described by Norton and Marshall.[6] It was found to be hydrogen, and other work has shown that hydrogen diffused through iron is extremely pure. It contains so little oxygen that it enables the reduction of chromium oxide to chromium to be made.

The calibration of the vacuum tube acting as an ionization gage was carried further to find out the effect of gas pressures above 10 or 20 microns (1 micron $= 1\mu = 10^{-3}$ mm Hg pressure). It was found that at higher pressures the electron emission of the cathode was so lowered that the plate current approached zero, as Fig. 3 shows. On pumping the gas out, the emission and plate current returned to their normal value. This was true at 25°C and also at 200°C.

[6] F. J. Norton and A. L. Marshall, Trans. Am. Inst. Min. Met. Eng. **104**, 136 (1933). Paper presented New York Meeting, February, 1932.

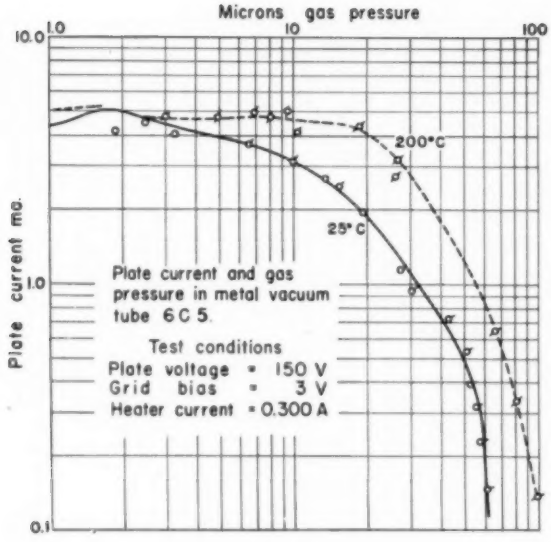

FIG. 3.

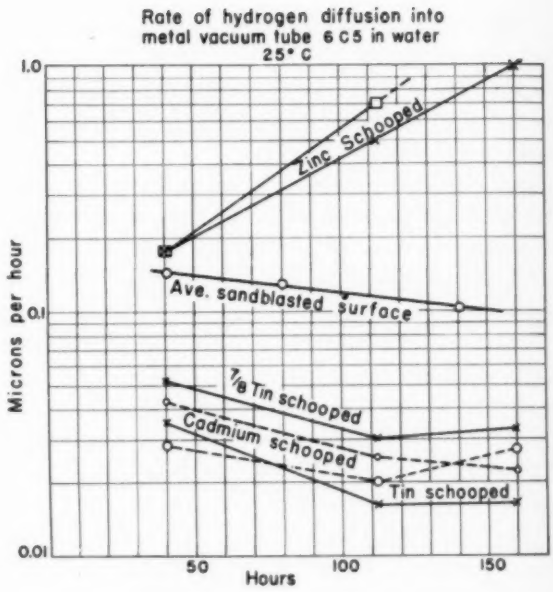

FIG. 4.

After the calibration curves for gas pressure and grid current were established, experiments were made on sealed-off tubes subjected to various conditions. Tubes with sandblasted surfaces were placed in water at 25°C, and gave rates of gas diffusion averaging 0.13 micron/hr.

The dimensions of the 6C5 tube are:

Thickness of steel shell	0.0635 cm
Area exposed to water	30.7 cm²
Free volume inside tube	15.0 cm³

Next, experiments were made with 0.1 percent sodium chromate in the water. This is known to inhibit corrosion and was found to stop the penetration of hydrogen through the steel. The limits of measurement showed the rate from 0.1 percent chromate solution was less than 0.001 micron/hr. This confirms T. S. Fuller's observations,[2] where another means of measuring hydrogen pressure was used.

Various coatings were put on the tube, and the rate of hydrogen diffusion measured upon immersion in water. The regular paint was found to be the best protection and various coatings yielded some protection, as shown in Table II and Fig. 4.

One coating gave an increased rate; zinc raised the rate from normal of 0.13 to 0.35 micron/hr.

Experiments were then made upon the effect of a salt spray at 25°C. This is a corrosion test and gives liquid droplets of a 20 percent NaCl solution, which deposit on the tube. This gave rates lower than tubes immersed in water. A porous copper plating here, however, was worse than the

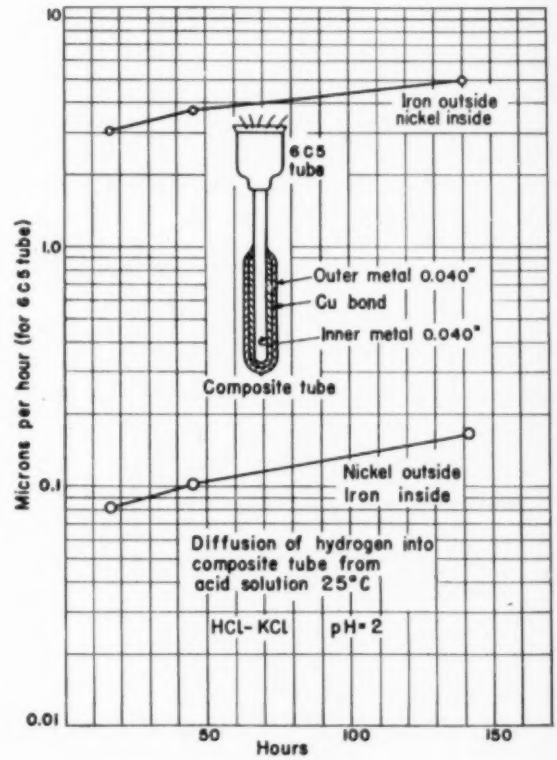

FIG. 5.

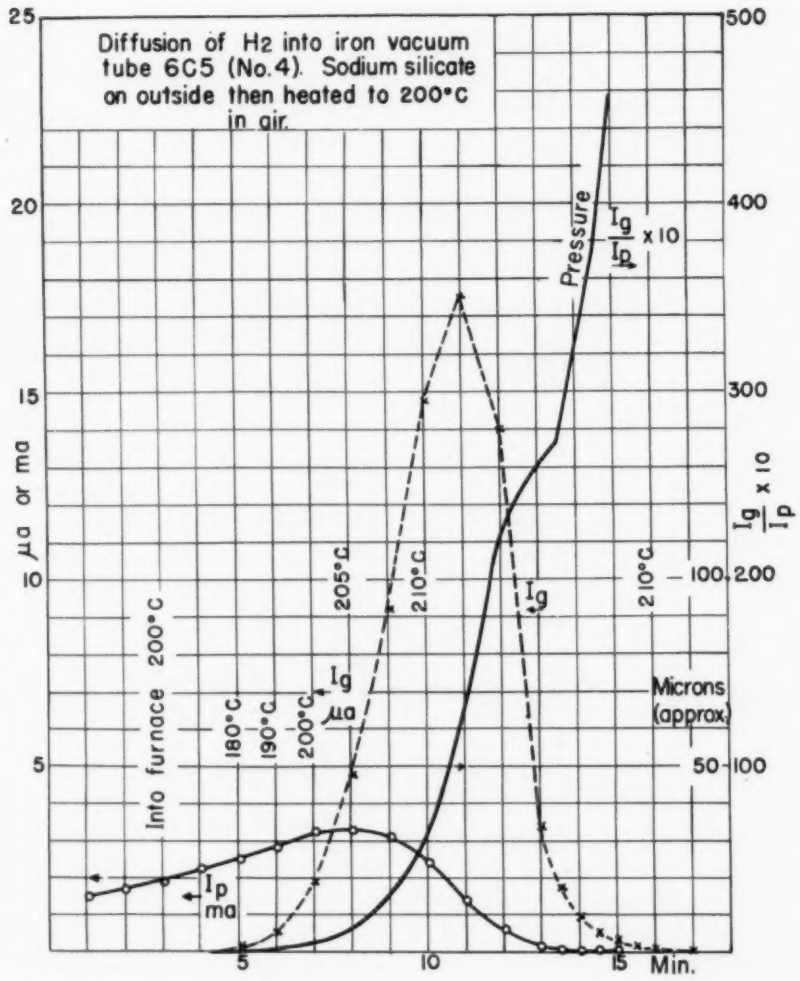

FIG. 6.

bare sandblasted surface. Table III gives these results.

Other tests were made in atmospheres of varying humidity up to nearly 100 percent, just short of actual condensation of liquid water. No diffusion of hydrogen was measurable from water *vapor* surrounding the tube.

The effect of temperature on the diffusion rate is evident from the following measurements made upon tubes with the standard sandblasted surface immersed in water:

25°C	0.13 micron/hr.
100°C	0.80 micron/hr.

All of these experiments point toward the fact that the reactions at the iron-liquid water

TABLE I. *Calibration of metal vacuum tube 6C5. Plate voltage = 150 v. Grid bias = −3 v. Heater current = 0.300 amp.*

$\frac{Ig \text{ IN } \mu A}{Ip \text{ IN MA}} \times 10$	MICRONS H_2	MICRONS N_2
0.5	0.25	0.16
1.0	0.5	0.3
5.0	2.4	1.2
10.0	4.7	2.2
50.0	23.0	9.0
100.0	45.0	16.0

TABLE II. *Diffusion of H_2 into metal vacuum tube 6C5 immersed in water 25°C.*

	H_2 MICRONS PER HR.
Regular painted tube	0.008
Sandblasted and nickel plated	0.009
Sandblasted and tin schooped	0.022
Sandblasted and $\frac{1}{8}$ of area covered by tin schooping	0.038
Sandblasted and cadmium schooped	0.028
Copper schooped	0.12
Plain sandblasted*	0.13
Zinc schooped	0.35

* Standard initial surface.

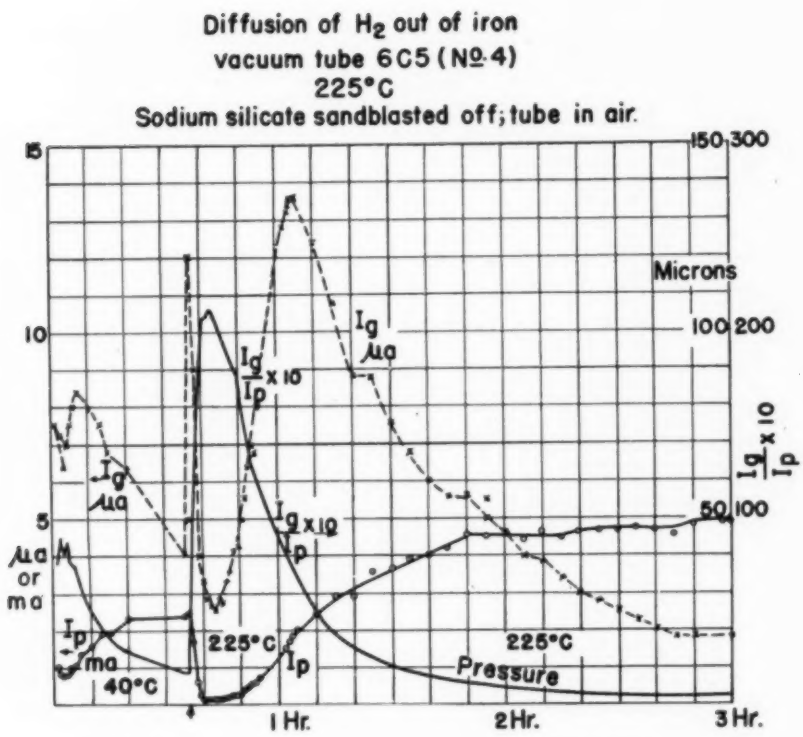

FIG. 7.

interface are what determine the rate of hydrogen diffusion through the steel into the interior of the tube. This is illustrated by two other sets of experiments.

A metal vacuum tube was constructed using stainless steel as the outer shell instead of the usual mild stamping steel. This gave an initial rate half the rate of steel and then the rate steadily dropped to an immeasurably low value.

Two other tubes were made, having composite walls: (1) iron outside, copper bond, nickel inside, and (2) nickel outside, copper bond, iron inside. These were placed in a KCl−HCl solution of pH = 2, at 25° and 100°C. The rates of hydrogen diffusion in microns per hour were:

	100°C	25°C
(1) Iron outside	50	4.0
(2) Nickel outside	1	0.12

In each case the total metal thickness was the same (80 mils), and the difference is due to the reaction at the exterior surface. The construction and rates at 25°C over a period of time are shown in Fig. 5.

One other set of experiments illustrates how very rapid this hydrogen diffusion through the steel can be.

A tube with a sandblasted iron surface was painted with sodium silicate, which was then air dried. The tube was put into a furnace at 200°C, and the grid and plate currents were followed. Within 5 minutes the grid current, Ig, started upward and at 10 minutes there were 30 microns of hydrogen on the interior of the tube. This continued to accumulate, as shown in Fig. 6, and after 15 minutes over 200 microns had accumulated, so much that emission was killed and grid and plate currents both fell nearly to zero.

The sodium silicate had retained some water even at 200°C, and the reaction with iron at the outer surface produced hydrogen, some of which diffused into the interior.

The tube was taken out of the furnace, the sodium silicate sandblasted off, and the tube put back into the furnace. Now there was no hydrogen being generated at the exterior surface, and the driving force for hydrogen was outward from the interior where several hundred microns were present, toward the outer air where none existed. Fig. 7 shows the course of outward diffusion of hydrogen until the grid current was low and the plate current nearly to its normal value.

This decrease in grid current is distinguished

from clean-up by the fact that alternate heating and cooling did not restore any of the gas pressure. Where clean-up has occurred, heating will release some of the gas.

The rate of gas release in various tubes with and without ordinary paint on the surface was studied at 200°C. It was found to be entirely negligible compared to the high rate observed when sodium silicate was on the exterior surface.

These results indicate that whenever iron is in contact with liquid water and particularly when corrosion occurs, hydrogen diffuses into the iron and comes out wherever the effective partial pressure of hydrogen is low, such as a vacuum or air.[7] This is of great practical importance for water-cooled vacuum tubes, rectifiers or other apparatus where water is on one side of an iron wall and a vacuum on the other. The phenomenon may also play a role in the embrittlement of steel in boilers.

[7] F. J. Metzger (Ind. Eng. Chem. **27**, 112 (1935)) states that if hydrogen is present in normal atmosphere it is not more than one part per million.

TABLE III. *Diffusion of* H_2 *into metal vacuum tube 6C5 in salt spray (25°C–20 percent* NaCl *solution).*

	H_2 MICRONS PER HR.
Regular painted tube	0.01
Tin dipped	0.03
Cu plate—tin dipped	0.03
Tin rub	0.05
Plain sandblasted*	0.05
Copper plated	0.14

* Standard initial surface.

For assistance in making the many experiments upon which this paper is based, I should like to express my appreciation to G. W. Dunlap, S. I. Pearson, G. Schaad and J. D. Seaver.

Preferential and Initial Ionic Recombination in Gases

N. E. BRADBURY
Stanford University, Stanford University, California
(Received December 14, 1939)

In an attempt to determine the fraction of ions lost by recombination in an x-ray ionization chamber, a theory has been developed for the processes involved in preferential and initial ionic and electronic recombination. The theory considers the change of the energy distribution of the electrons as they diffuse away from the parent atom. From this, together with a knowledge of the electron capture process, the space distribution of negative ions formed may be obtained. The probability of the initial electron recombining preferentially with the parent positive ion is considered as well as the preferential process for the negative ion. Knowing the initial spacing of the ions, it is possible to calculate the recombination occurring during the diffusion process until random distribution is reached. The final volume recombination may then be calculated in the usual manner. The theory may be employed in both electronegative and free electron gases and to ions formed in the presence or absence of an electric field.

AS suggested by Loeb,[1] the recombination of ions in an ionized gas may be discussed in three separate regimes. These are, briefly, *preferential recombination* in which recombination takes place between the parent positive ion and the ejected electron (which may, by capture, have become a negative ion); *initial recombination* in which recombination occurs between ions nonrandomly distributed in the gas (as, for example, along a beta-ray track); and finally, *volume recombination* in which the recombination process occurs between ions which have diffused to a uniform distribution throughout the gas. *Columnar recombination*, referring to the special case of nonrandom ionization occurring with alpha-particle ionization has been thoroughly treated by Jaffé.[2] It is the purpose of the present paper to examine the processes of initial and preferential recombination in the light of present knowledge of electron capture cross sections and the behavior of slow electrons in gases. Of particular interest in this connection is the magnitude of the lack of saturation in an x-ray ionization chamber

[1] L. B. Loeb, *Fundamental Processes in Electrical Discharge in Gases* (Wiley, New York, 1939), Chapter II, p. 86; also p. 144 ff.

[2] G. Jaffé, Ann. d. Physik **42**, 303 (1913).

when operated under limited voltage. For this reason the considerations of this paper will be limited to ordinary x-ray ionization and to the pressures usually employed in ionization chambers, i.e., between 0.1 and 10 atmospheres. This, however, is not necessary in principle.

(1)

The bulk of the ionization produced by x-rays in a gas is due to ejected photoelectrons and to Compton recoil electrons, the latter predominating with increasing hardness of the rays. The subsequent ionization produced by these particles will be initially distributed along tracks whose length is determined by the range of the ionizing electron. The average density of ions along the track (neglecting the extreme end) may be determined by the average energy necessary to form a pair of ions, i.e., about 33 volts. We consider first the history of an individual electron ejected from a neutral atom or molecule in such an ionizing act.

While no single function will describe the distribution in energy over all energies with which such an electron leaves the parent particle, nevertheless it is possible in a rough way to describe the probability $P_0(\epsilon)d\epsilon$ of emission in a given energy range.[3] $P_0(\epsilon)$ is zero for zero energy of the ejected electron, rises to a maximum at about one-half of the ionization energy of the parent atom, then decreases rapidly within a range comparable to the ionization energy, with, however, a slight tailing off to higher energies.

If ϵ is the energy in volts of an individual ejected electron at infinity, then, in the absence of an external electric field, as it diffuses away from the parent particle its energy as a function of distance $\epsilon(r)$ will be given by

$$\epsilon(r) = 300e/r + \epsilon(1-f)^n. \qquad (1)$$

In this expression n is the number of collisions made by an electron in diffusing a distance r and is related to r by the expression $r = n^{\frac{1}{2}}\lambda$ in which λ is the mean free path. The quantity f is the fraction of energy lost by an electron at a collision with a neutral particle and is classically $2m/M$. However, various measurements of electron mobilities in gases have shown that the collision of electrons with molecules is only elastic in the inert gases when the energy of the electron is below the critical potential. In the case of the molecular gases the average fraction of energy lost may be many times the elastic value. From the deviation between the computed value of the electron mobility taking into account proper Ramsauer cross sections and the experimentally measured values it is possible to get an average value for f as a function of X/p, and hence as a function of electron energy.[4]

The first term represents, obviously, the Coulomb attraction. Since this term contributes only about 0.1 volt at a distance of the order of the first mean free path at 10 atmospheres, we may neglect it in considerations of the energy. The rate of diffusion, however, in a field-free gas under these circumstances may be considerably altered inasmuch as the electric field at a distance comparable to the first mean free path is ~ 100 volts/cm. The exact effect of such fields on the diffusion of the particle is very difficult to calculate, although an approximate solution to the similar problem for ions has been given by Sommerfeld and Loeb,[5] and also by Harper.[6] For the present purposes it will suffice to assume that the effect of the charges upon the diffusion of the electron will essentially be determined by the ratio of the loss of momentum during a free path to the total momentum of the electron. The expression for the distance diffused after n collisions may then be rewritten as

$$r = n^{\frac{1}{2}}\lambda(1+\Delta p/P)^{-1}$$
$$= n^{\frac{1}{2}}\lambda[1+e^2/2n\lambda\epsilon(1-nf)^{\frac{1}{2}}]^{-1}. \qquad (2)$$

Under ordinary circumstances, this correction will be small owing to the relatively high velocity of the electron and may be neglected. Moreover, in practical applications an electric field of the order 10–100 volts/cm will be externally applied to the gas. Obviously, after the first few mean free paths this field will predominate over that due to the parent ion, and we will consider its effect presently in determining the terminal energy of the electron.

[3] N. E. Mott and H. S. W. Massey, *Theory of Atomic Collisions* (Oxford University Press, 1933), p. 170.

[4] N. E. Bradbury and R. A. Nielsen, Phys. Rev. **49**, 388 (1936); R. A. Nielsen, Phys. Rev. **50**, 950 (1936).

[5] L. B. Loeb, reference 1, pp. 108, 111.

[6] W. R. Harper, Proc. Camb. Phil. Soc. **28**, (II), 219 (1932).

It is apparent that the process involved after ejection of the electrons from their parent positive ions is essentially one which changes the initial energy distribution $P_0(\epsilon)$ to another distribution $P(\epsilon,r)$ which has a different average energy, different character, and is furthermore a function of r, the distance away from the parent ion. In the absence of an external field, the ultimate distribution will be a Maxwellian one with an average energy corresponding to the temperature of the gas. In the presence of a field, a distribution of the $v^2e^{-av^4}$ type suggested by Druyvesteyn and by Morse, Allis, and Lamar,[7] and others will be reached. The distance diffused by the electron in reaching the steady-state distribution may be readily determined from the number of collisions required to bring the electron to its terminal energy. This number is, to a first approximation, independent of the energy of the electron and is given by[8]

$$\frac{1}{2f}\log\frac{1}{1-\theta^2}, \tag{3}$$

in which f, as before, is the fractional energy loss per collision, and θ is the fraction of the terminal energy $\bar{\epsilon}_x$ reached after this number of collisions. Since the change of distribution function will go approximately as the number of collisions, we may form an approximate general distribution function which will have the form

$$P(\epsilon,r)=\left[\left(1-\frac{r^2}{r_\infty{}^2}\right)P_0(\epsilon)+\frac{r^2}{r_\infty{}^2}\pi(\epsilon)\right]$$
$$=[(1-x^2)P(\epsilon)+x^2\pi(\epsilon)]. \tag{4}$$

In this expression, r_∞ is the distance which an electron diffuses before attaining its terminal energy. It may be determined from (3) above subject to the correction imposed by (2) which will be in general, small. $\pi(\epsilon)$ is the steady state energy distribution, which, lacking experimental evidence, may be taken as of the Druyvesteyn type. It may be noted that the value of r_∞ should, in principle, be modified to take account of the distance diffused in the direction of the externally applied field during the time taken by the electron to attain its terminal energy. For fields and pressures which are usually employed in ionization chambers this correction is small, particularly for molecular gases. It may be shown that the distance diffused is ~ 10 times the distance moved in the direction of the field.

Neglecting for the moment the question of negative ion formation, it is necessary to consider the probability of preferential capture of the electron by the parent ion. This, of course, can occur only by some fortuitous return towards the positive ion after the first or subsequent collision. Kenty[9] has measured the capture cross section of 0.4-volt electrons in argon and found it to be 5×10^{-18} cm^2. The cross section varies inversely with electron energy and is probably not greatly different in magnitude for other gases. To obtain an estimate of the probability of the preferential capture process, the ratio of the capture cross section to the total area available for scattering for a collision occurring at a distance x from the parent ion is integrated over all distances. This gives the probability of preferential capture following the first collision. The process for subsequent collisions may be treated in a similar manner taking for the distance at which the collision occurs $n^{\frac{1}{2}}\lambda$. The order of magnitude is determined by the probability at the first collision which is

$$\frac{\epsilon\sigma_\epsilon}{1200\pi\lambda e}\ln\frac{r_0}{r_0+300e/\epsilon}. \tag{5}$$

In this expression, σ_ϵ is the capture cross section for electrons of energy ϵ in volts, and r_0 is the lower limit of integration (essentially the atomic radius). This probability is of the order of 10^{-8} at atmospheric pressure and the probability of return at any subsequent collision will be closely $e^{-\sqrt{n}\sigma_\epsilon}/4\pi n\lambda^2$. It is apparent that at ordinary pressures the probability of preferential electron recombination may be neglected.

Returning to the question of the behavior of Eq. (4) in a gas in which negative ions are formed by electron capture, it is seen at once that

$$\int_0^\infty P(\epsilon,r)d\epsilon,$$

initially unity, must decrease with increasing r as

[7] Morse, Allis and Lamar, Phys. Rev. **48**, 412 (1935).
[8] L. B. Loeb, reference 1, p. 185.
[9] C. Kenty, Phys. Rev. **32**, 624 (1928).

electrons are captured. If the capture cross section were known as a function of electron energy, it would not be difficult to put in the factor expressing the rate at which electrons of each energy were captured to form negative ions. The problem is not as simple as this, however, for Bloch and Bradbury[10] have shown that, in many types of capturing processes, only electrons of a specific energy can be captured. The ultimately complete capture of a group of electrons moving through a gas is thus due to the velocity distribution which continually throws electrons into the energy range from which they may be captured.

Fortunately, however, there does exist, at least for O_2, a measure of the effective capture cross section as a function of average electron energy for electrons moving in a gas with their normal velocity distribution.[11] If $\sigma_c(\bar{\epsilon})$ denotes this experimentally measured capture cross section function, then the change in P will be given by

$$dP]_{\text{capture}} = \frac{-2PN\sigma_c(\bar{\epsilon})rdr}{\lambda}. \tag{6}$$

This expression, combined with the rate at which the average energy changes with distance from the parent atom,

$$\bar{\epsilon} = \left(1 - \frac{r^2}{r_\infty^2}\right)\bar{\epsilon}_0 + \frac{r^2}{r_\infty^2}\bar{\epsilon}_\infty, \tag{7}$$

may then be integrated for a specific case to find the ultimate form of P for an attaching gas. This expression, when integrated over all electron energies, may be used to find the expression of final interest; namely, that which describes the formation of negative ions with distance. If N_0 be the initial number of ejected electrons, then the number of ions formed up to the distance r from each parent atom will be given by

$$N_0\Phi(r) = N_0\left[1 - \int_0^\infty P(\epsilon, r)d\epsilon\right] \tag{8}$$

and the space rate of formation by the derivative of $N_0\Phi(r)$. From the maximum of this quantity, the most probable or the average distance of ion formation may be at once obtained.

It must be noted that Eq. (8) may be used for $0 < r < r_\infty$. Beyond this point the electrons have attained their terminal energy and the capture process will proceed in the normal way. If $N_0P]_{r=r_\infty} = N_1$ be the number of electrons which remain free at r_∞, then the rate of change of N_1 with subsequent distance, r_1, will be, as usual,

$$\frac{dN_1}{N_1} = \frac{-2N\sigma_c r_1}{\lambda}dr, \tag{9}$$

and the remainder of the ion distribution found as above. From (9) the maximum rate of ion formation is found to occur at $r_1 = (\lambda/2N\sigma_c)^{\frac{1}{2}}$. If the rate of capture is slow, it may be necessary to correct for the distance moved in the direction of the field during the time preceding capture. This may be done approximately by computing r, the average distance from the parent ion as $(r^2_{\text{drift}} + r^2_{\text{field}})^{\frac{1}{2}}$ in which r_{field} is $kXn\lambda/v$, k and v being the electron mobility and random velocity, respectively, and X the applied field strength. Under most circumstances this is a small correction.

(2)

From the above it is possible to calculate the distribution of negative ions about their parent positives. In the case of a gas in which electrons do not attach to form negative ions, this distribution is, of course, meaningless, and the electrons merely diffuse until random distribution is attained. The recombination which occurs under this circumstance may be treated identically with the initial and volume recombination of ions save for the value of the recombination coefficient employed. Accordingly, the treatment of the present section will be limited to the case of gases which form negative ions. It may be assumed that, after formation, the ions have essentially a Maxwellian distribution of energies corresponding to the temperature of the gas which may be denoted $f(E)$, and that they are distributed about the parent ions with distances given by the function $\Theta(r)$ as obtained by the methods of Section (1).

Following the treatment of J. J. Thomson,[12]

[10] F. Bloch and N. E. Bradbury, Phys. Rev. **48**, 689 (1935).
[11] N. E. Bradbury, Phys. Rev. **44**, 883 (1933).
[12] J. J. Thomson, Phil. Mag. **47**, 337 (1924).

it may be assumed that an ion with an energy E will, in general, diffuse away from a neighboring ion of the opposite sign at a distance r providing $e^2/r<E$. For recombination to occur with the parent ion, therefore, the negative ion must be formed at such a distance and with such an energy that its Coulomb potential energy is greater than its thermal kinetic energy, and furthermore, presumably, the ion must execute and survive an orbit about the positive ion without a collision. This last condition must be modified somewhat, for if r is small and consequently E large, then a collision will, on the average, reduce the energy and make recombination even more probable. The energy distribution may accordingly be divided into two parts having more and less than the average energy, respectively. This leads to the result that out of N ions the following number will recombine preferentially with the parent ion:

$$N\Big[\int_0^{e^2/(\frac{3}{2}kT)}\int_{\frac{3}{2}kT}^{e^2/r} f(E)\Theta(r)dEdr + \int_0^{e^2/(\frac{3}{2}kT)} e^{-2\pi r/\lambda}\int_0^{\frac{3}{2}kT} f(E)\Theta(r)dEdr + \int_{e^2/(\frac{3}{2}kT)}^{\infty} e^{-2\pi r/\lambda}\int_0^{e^2/r} f(E)\Theta(r)dEdr\Big]. \quad (10)$$

Although the completion of an orbit about the ion for capture may be too stringent a requirement for the completion of electron transfer, nevertheless it is probably true in order of magnitude. A more accurate assumption must await the solution of the detailed problem of the recombination of two ions.

The above discussion neglects the effect of an external field upon preferential recombination. For the range of pressures and field strengths usually encountered in ionization chambers this seems to be permissible for the following reasons: The field at the critical distance due to the parent ion is ~10,000 volts/cm for an ion of average energy. Since this field is at least 10 times greater than any external field likely to be employed, the effect of such fields would seem to be negligible. Secondly, even should the external and ion fields be comparable for ions of very low energy, nevertheless with random directions of separation, as many ions will be pulled together as will be separated. Thus it seems possible to neglect this effect under ordinary circumstances.

Knowing the character of preferential recombination from (10) it is possible to find the final form of Θ after those ions which recombine in this manner have been removed from the distribution. The factors by which Θ will be changed are

$$e^{-2\pi r/\lambda}\int_0^{e^2/r} f(E)dE \qquad \infty > r > \frac{e^2}{\frac{3}{2}kT}, \quad (11)$$

$$\Big[\int_{\frac{3}{2}kT}^{e^2/r} f(E)dE + e^{-2\pi r/\lambda}\int_0^{\frac{3}{2}k} f(E)dE \qquad 0<r<\frac{e^2}{\frac{3}{2}kT}. \quad (12)$$

It is here assumed that $f(E)$ has been so normalized that its integral over all energies is unity. After taking the preferential recombination into account in this manner, there remains now only the initial, nonrandom distribution of ions whose characteristics may be determined from (8), (9), (11) and (12). These ions now tend to diffuse apart but in doing so, the resulting recombination is determined by this diffusion and no ion is specially favored over any other as a partner in this process.

(3)

To calculate the amount of initial recombination, it may be assumed that this type of recombination follows the ordinary recombination equation, save that the actual volume density of ionization in the region of the tracks must be employed, rather than the macroscopic density. Thus if ν is the ion density and α the recombination coefficient as determined by experiment for wholly random ion distribution, then

$$d\nu/dt = -\alpha\nu^2. \quad (13)$$

Letting L be the average length of a beta-ray track, μ the number of ion pairs per centimeter track, γ the number of tracks per cm^3, and $\bar{r}$ the average distance between the ions of a pair as determined from Θ, then the actual volume involved per cm^3 will be $\sim L\gamma\pi\bar{r}^2$. Furthermore, this volume will change with time as diffusion and an external field, if applied, exert their effects.

The actual density of ions in the track will then be, as a function of time.

$$\nu=\mu/\pi[\bar{r}+4kXt/3+(\bar{c}\lambda t)^{\frac{1}{2}}]^2. \qquad (14)$$

The numerical factor which appears in the second term in the denominator is only approximate and arises from the fact that both ions move in response to the applied field X, but that with random distribution all directions of motion do not change the volume of the track as calculated in this manner. The final term in the denominator accounts for diffusion of the ions and $\bar{c}$ is their average velocity of agitation with a mean free path λ. The lack of knowledge of this latter quantity with any exactness for ions of this age precludes the use of a more exact factor than one for this term.

If ν_0 denotes the actual number of ions per cm^3, then the time rate of change of this quantity due to recombination will be given by

$$\frac{d\nu_0}{dt}=-\frac{\alpha\mu^2\nu L}{\pi[\bar{r}+4kXt/3+(\bar{c}\lambda t)^{\frac{1}{2}}]^2}. \qquad (15)$$

This expression must now be integrated over a certain length of time to get the total loss of ions per cm^3 during the period of initial recombination. This time may be determined from (14) by finding the value of t necessary to give the measured macroscopic density. If this latter quantity be denoted ν_{00} = total number of ions/total volume, then t may be determined such that $\nu=8\nu_{00}$. The factor arises out of the fact that all tracks are diffusing, and each need go but half the distance to random separation. The loss of ions during the period of initial recombination may thus be determined.

The ions have now achieved random separation, and subsequent recombination will follow the ordinary volume recombination law as expressed in (13). If the ions are drawn to separate electrodes by an appropriate field, it is easy to calculate the amount of recombination which occurs during the time portions of the two ion clouds are intermixed. This will of course depend upon the beam and ionization chamber geometry as well as upon the ion mobilities.

(4)

In the preceding sections, the recombination problem has been considered as one which follows a flash of x-rays of infinitesimally short duration. In practice, the recombination occurring with prolonged x-ray exposure will be more frequently encountered. Two cases may be distinguished in this event: (1) The x-rays ionize the gas in the absence of a field for a finite time, the beam is then shut off, and, after the lapse of a greater or less interval of time, the ions are collected by applying a field; (2) The x-rays ionize the gas with a steady field applied which then draws a steady ionization current from the gas. The first type of practice is that generally employed in recombination measurements, while the second occurs most frequently in x-ray intensity measurements. In both cases it may be of interest to know the number of ions lost by recombination.

It is apparent from Sections (1) and (2) that preferential recombination is a process which is independent of the ionization density, but which has a probability which may be determined for each ion pair formed if the character of the gas, hardness of the x-rays, and other required quantities are known. Since, under the restrictions of this investigation, this probability is generally small, it may be applied directly as a further correction to the measured number of ions after the amount of initial recombination is taken into account.

The initial recombination, however, depends directly on the density of ionization, since this determines the time over which (15) must be integrated. Considering the case in which an external field is absent with a time of x-ray exposure τ and in which the macroscopic density of ionization follows a function $\nu_{00}(t)$, the total number of ions lost per cm^3 by initial recombination during the time of exposure will be

$$\int_0^\tau dt\int_0^{t'(t)} d\nu_0', \qquad (16)$$

where ν_0' is now the number of ions formed per cm^3 per second. The limit of integration, t', must be determined from (14) and $\nu_{00}(t)$. To this must be added the amount of volume recombination occurring after the period of initial recombination. This will be

$$\nu_0'\tau-\nu_{00}(\tau),$$

in which $\nu_{00}(\tau)$ is given from the integration over the time of the x-ray exposure of

$$d\nu_{00}/dt = \nu_0' - \int_0^{t'} d\nu_0' - \alpha\nu_{00}^2. \qquad (17)$$

Equation (17) is merely a statement of the familiar recombination law taking into account the initial recombination. Subsequent recombination after the x-rays are removed may be calculated in the elementary manner.

If a field is present during the time of x-ray exposure, the problem of determining the approximate ion density ν_{00} as a function of space and time is more complicated. Since, under ordinary circumstances, only the steady-state current will be of interest, this case only will be considered. In the steady state, a certain spatial distribution of both positive and negative ions will be set up which may be determined to a first approximation by the equation

$$\frac{\partial n_+}{\partial t} = 0 = \nu_0' - \alpha n_+ n_- - k_+ X \frac{\partial n_+}{\partial x},$$

in which α is the ordinary coefficient of recombination, and n_+ and n_- are approximate ion densities, and ν_0' is the number of ions formed per cm^3 per second after preferential recombination has occurred. Since initial recombination will in general be completed in times short compared to that required for the ions to traverse the ionized space, the initial recombination may be treated as a subtractive quantity from ν_0'. This initial recombination current expressed as ions lost per cc per second will be given by the integration as in (16) of

$$\int_0^{t'} d\nu_0',$$

where t' is to be determined from the length of time required for random distribution to be reached as determined from Eq. (14). Since the ion density will be different for ions of different sign, that employed at random distribution must be the density of the preponderant ion. Thus t' will be a function of x measured in the direction of the field, and hence the subtractive correction to ν_0' will be a function of x. If ν_0'' denotes the resultant number of ions available per cc per second after initial and preferential recombination have been taken into account, then only the volume recombination remains to be considered and that will lead to an ion density determined by the equation

$$\frac{\partial \nu_{00+}}{\partial t} = 0 = \nu_0'' - \alpha\nu_{00+}\nu_{00-} - k_+ X \frac{\partial \nu_{00+}}{\partial x},$$

where ν_{00+} and ν_{00-} represent the macroscopic densities of the different ion signs. There will be a similar equation for the negative ions, and their simultaneous solution with proper boundary conditions will lead to ν_{00-} and ν_{00+} as functions of space. From the evaluation of ν_{00+} and ν_{00-} at the boundaries of ionization, the current density from the ionized region may then be obtained from the familiar equation $i_+ = k_+ X_- e\nu_{00+}$.

(5)

It will be seen from the above that the calculation of the extent of ionic recombination under ordinary circumstances requires a considerable knowledge of various gas ion properties for the gas in question. In many cases these properties are either partially or entirely unknown. This suggests that for the most accurate measurements, the gas employed be one whose properties are known in sufficient detail, and whose purity has been assured by scrupulous care. It is obvious that the use of a gas in which negative ions are not formed will assure the minimum loss by recombination. Nevertheless, unless great care is taken in creating and maintaining gas purity, this advantage may be greatly lessened by small amounts of contamination. The resulting negative ion formation, though possibly small, is uncalculable, and hence the exact loss must remain unknown.

Finally it may be pointed out that in many actual instances certain of the detailed calculations outlined above will be unnecessary. Approximations, when the quantities involved are small will readily suggest themselves. Moreover if ordinary care is involved in the choice of gas and geometry, successive approximations to the true ion density from the measured density will not, in general be required.

Tension and Birefringence in a Vinylite Plastic*

H. W. Farwell
Columbia University, New York, New York
(Received October 16, 1939)

This paper describes experiments on the birefringence of a strip of plastic material, first when the stretched strip is maintained at constant length and second when it carries a constant load. The results indicate that in neither case is the birefringence proportional to the tension. The data are further examined, and the argument is presented to show that in the constant length experiment the ratio of tension T at any time after the initial tension, T_1, is established should be the same function of the time as is the expression $\left[1-2\mu \log_e \frac{L}{L_1}\right]$ for the constant load experiment. Finally it is shown that the tension ratio data can be represented by a curve of the type, $\frac{T'}{T_1}=Ae^{-at}+Be^{-bt}+Ce^{-ct}$.

THE type of plastic material used in experiments previously reported[1] as well as the method there employed seemed to permit a definite answer to some of the questions which have been asked about the relation between birefringence and strain, or birefringence and stress. There are positive assertions made that the birefringence is necessarily proportional to stress, and more cautious statements that in such materials as are generally classified as plastic the birefringence, or, in some references, the phase change per unit thickness, is given by a relation of the type $\alpha T+\beta S$, where α and β are constants, T the stress, and S the strain.

A simple modification of the apparatus used earlier made it possible to take simultaneous measurements of birefringence and stress for two different tests, one in which the stretched length was maintained constant during a considerable period of time, and the other in which the specimen was under constant load. The temperature regulation was improved, the water through the coil around the chamber being circulated by a motor-driven pump, and the supply tank being heated by a lamp in a thermostatically controlled circuit. The birefringence measurements were made as before, except that there was added to the optical system between the specimen and the polarizer a slide carrying four different thicknesses of mica, so that if at any time the black band produced by the specimen moved too far to either extreme of the spectrum, the introduction of a sheet of mica of suitable thickness would move the band to a more favorable position.

All of the strips used in the experiments were cut from the same sheet of Vinylite plastic (obtained through the courtesy of the Carbide and Carbon Chemicals Corporation), and were at the start 8 cm long, 1 cm wide and about 0.037 cm thick. The length of the strips was parallel to the direction of calendering. No strip was used twice and no strip was handled more than necessary. The temperature inside the chamber was 31.8°C.

For the first case the strip was inserted in the chamber as in the earlier experiments, but lowered until the lower clamp rested on the base of the chamber. Then the microscope at right angles to the transmitted beam of light was adjusted until its horizontal cross-hair was at the tip of a needle carried on the lower clamp. The clamp was then weighted to give a 300-g load. At the start of the experiment the nut at the top of the screw supporting the upper clamp was given one full turn, 1 mm, every 30 seconds until the movement of the needle tip showed that the full load was on the plastic strip.

At that moment the experiment proper began, with one observer regularly observing the position of the spectrum band, while another at the same intervals removed weights from the hanging load until the movement of the needle point indicated that the balancing weight had been reached. When the rate of change had become

* Publication assisted by the Ernest Kempton Adams Fund for Physical Research of Columbia University.
[1] H. W. Farwell, J. App. Phys. **10**, 109 (1939).

less rapid a single observer took two readings on band position before and after each load measurement.

The tension in the strip was proportional to the load, since there was no change in length, and the earlier observations on this material showed no volume change. The results are plotted in Fig. 1, where instead of time is given $\log_e t$; the tension, after the first few minutes, evidently relaxing here, as in numerous other plastics, so that $T=a-b \log t$. For comparison the relative birefringence is plotted on the same scale, the absolute values having been multiplied by a constant in order to represent the initial birefringence by the same number, 300, as the initial load.

It is clear that the birefringence is not proportional to the tension in this case. It may be of interest to note that the strips, which were stretched to nearly twice their original length and in which the tension had in 5 days relaxed to some $\frac{2}{3}$ of the initial value, began to shorten with the removal of the final load and in a few minutes were not more than 10 cm long, with a final distortion of about 10 percent.

For the other experiment, the load was added in the same manner as described, so that in both cases the initial conditions were the same. However, instead of decreasing the load, the length was allowed to increase, as was easily arranged by having the lower clamp at a suitable distance above the bottom of the chamber. The nut on the supporting screw at the top of the chamber permitted a simple means of measuring the change in length. As before, two observers were required at the start, one for the birefringence measurements at regular intervals, and the other at the same times to bring the needle point up to the cross-hair and record the length.

Here, of course, both stress and strain are changing, but since there is no change in volume in the material, the stress is always given by $T=W/A$, where W is the weight hanging from the strip and A is the cross-sectional area of the strip. V_0, the volume of the strip, $=A_0L_0=AL$. Hence $T=W/V_0 \cdot L=kL$, the tension is proportional to the length of the strip. If the strain is taken as $(L-L_0)/L_0$, and if $B=\alpha T+\beta S$, B plotted against L should give a straight line. The result of the experiment is shown in Fig. 2, which also includes the stretching in the preliminary period, during which time the length increased from 8.0 cm to 14.3 cm. Here again the birefringence is not proportional to the stress during the period of constant load, and it does not follow the strain.

The results of the two experiments can be shown together on a single diagram if we plot the relative tension against the relative birefringence. Naturally we take as reference state the situation when the 300-g load has just been fully accepted by the strip, the tension and birefringence at that moment will increase if the load is constant, and decrease if the length is constant. The two results appear in Fig. 3 in

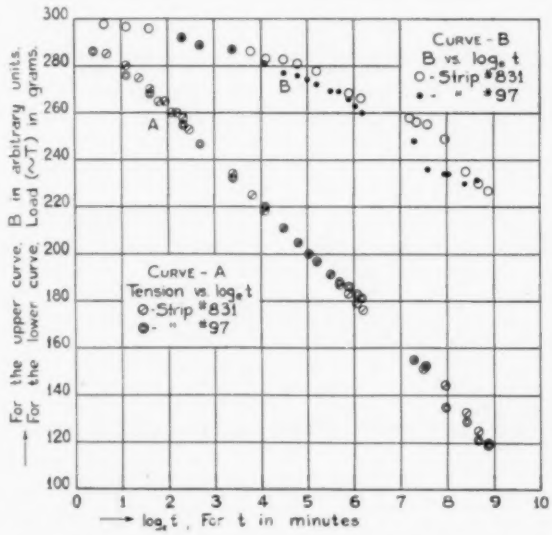

FIG. 1. Upper curve: Birefringence B (in arbitrary units) plotted against the logarithm, to the base e, of the time t during which a load acts on two given strips of Vinylite plastic of constant length. Lower curve: Load (proportional to stress) in grams plotted against $\log_e t$, for the same strips of plastic.

which it is quite evident that these are neither straight lines, nor branches of one and the same curve. While the values from different strips are not completely in agreement the general results are in accord. Considering the nature of the material it is perhaps unreasonable to expect that two strips cut side by side from the same sheet should give precisely the same results.

The real point seems to be that while in many cases the birefringence can be definitely related to the external stress, this is only because in

those cases that stress produces changes in the internal molecular or atomic fields which are of a single kind. We may term this a *stress* birefringence. However, in materials such as those with which these experiments are concerned, the external stress operates not only as it would in the hypothetical case of a substance with atoms having, say, symmetrical fields of force, but in addition it produces actual changes in the internal structure, developing a kind of crystalline property which is essentially different from that in the other case. So that here there is a *structure* birefringence as well as a stress birefringence. There appears to be no reason for assuming that a structure birefringence should follow directly an applied stress. It is doubtful if the two can be separated, although the *structure* birefringence is of the same general sort as the *stream* birefringence noted in numerous instances of long colloidal particles when the solution is set into motion.[2]

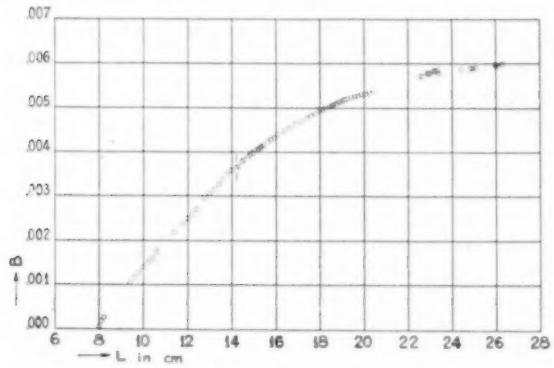

FIG. 2. The relation of birefringence to length of Vinylite plastic under constant load. The strip is being loaded during the interval from 8.0 to 14.3 cm. When the 14.3-cm length is reached, it has a constant load.

As a further attempt to make the data useful for the inquiry about the properties of plastics a study of the form of the length-time and tension-time curves was made, since it is probable that there is some relation between the two.

Let L_0 be the original unstretched length of the plastic, M_0 its width, D_0 its thickness, W_1 the initial load which makes the length L_1. The tension, T_1, as soon as the load is fully on the strip is equal to $W_1/A_1 = W_1/V_1 \cdot L_1$.

If now the length is kept constant, the tension will relax and the load supported must be decreased. The tension at any time, $T' = W/A_1$, as A_1 does not change. Since the tension depends, at least for identical strips, only on the original tension and on the time elapsed, T' may be expressed at $T_1 f(t)$. $dT'/dt = T_1 f'(t)$, where $f'(t)$ is a negative quantity, and since $T' = T_1$ when $t = 0$, $f(0) = 1$.

In the second case W is constant $= W_1$, but L is constantly increasing. The initial tension, T_1, is not maintained because the relaxation phenomenon is proceeding, and under the given conditions the area of cross section must decrease. At a time when the tension is T and the length is L the changes which take place in the succeeding interval Δt may be considered as taking place in two steps, each of length Δt, instead of simultaneously in a single interval. In the first interval consider the *length* constant, and in the second interval consider the *load* constant.

Then in the first interval the tension changes from T to

$$T + \Delta T = T + (\partial T/\partial t) \cdot \Delta t = T + T \cdot f'(t) \cdot \Delta t.$$

During the second interval the strip must therefore be extended, since there is now an additional tension

$$W_1/A - (T + T \cdot f'(t) \cdot \Delta t) = -T \cdot f'(t) \cdot \Delta t$$

(a positive quantity) resulting from the relaxa-

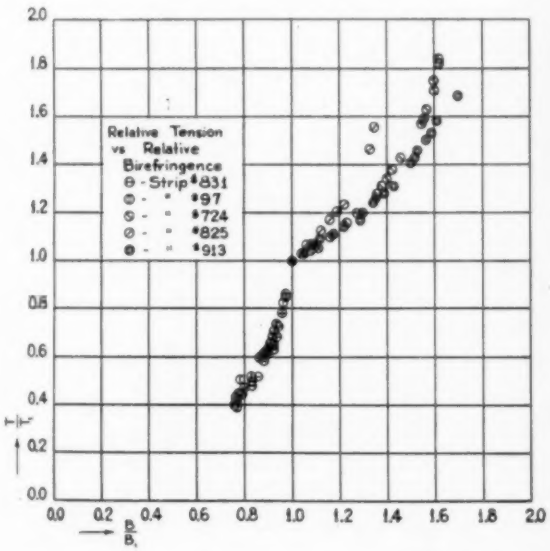

FIG. 3. Variation of relative tension with relative birefringence. B_1 and T_1 are measured when the 300-gram load has just been fully accepted by the strip of plastic.

[2] H. W. Farwell, J. App. Phys. **8**, 416 (1937).

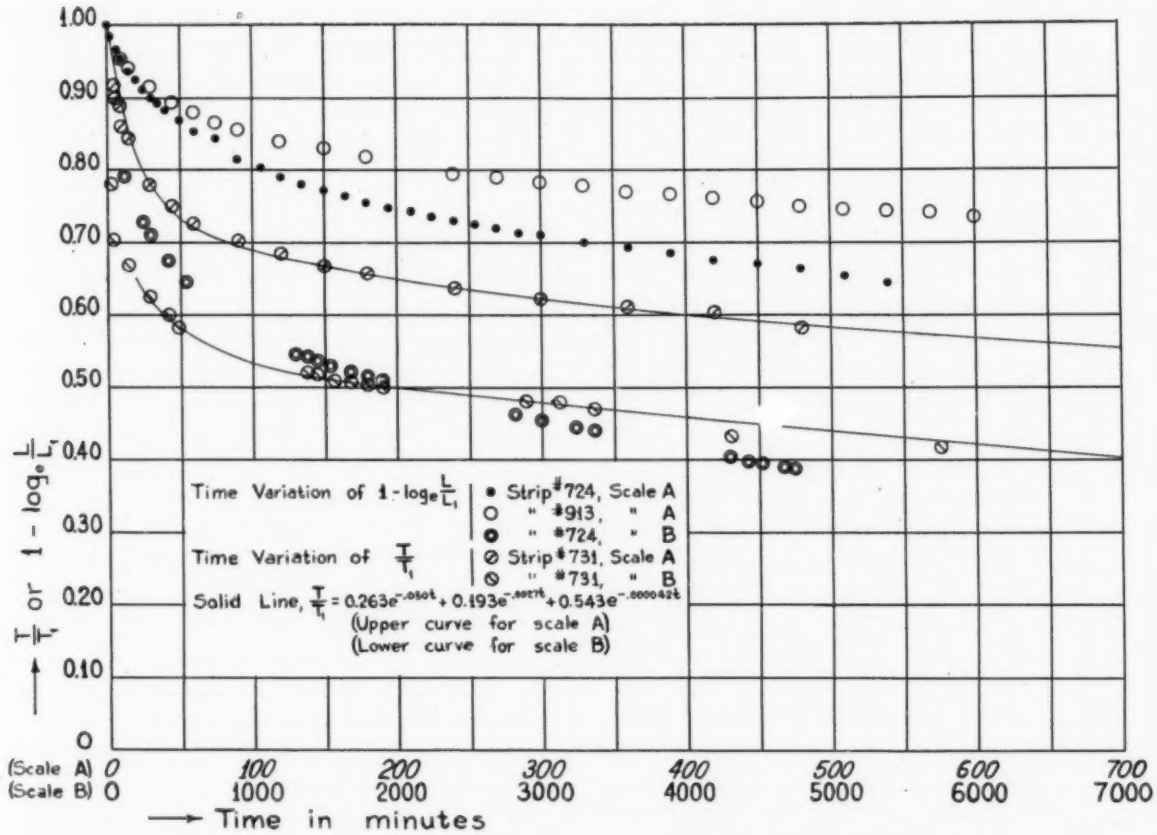

FIG. 4. Curve showing that in the constant length experiment the ratio of tension T at any time aftert he initial tension T_1 is established should be the same function of the time as is the expression $1-2\mu \log_e L/L_1$ for the constant load experiment.

tion in the first interval. This will produce an increase in length, ΔL, for which an expression can be found.

Since the strip is under constant load

$$T=\frac{W}{A}=\frac{W}{cD^2}, \text{ as width} = c\cdot\text{thickness}$$

$$\frac{dT}{dL}=-\frac{2W}{cD^3}\cdot\frac{dD}{dL}=-\frac{2T}{D}\cdot\frac{dD}{dL}=\frac{2T\mu}{L}$$

TABLE I. *Thickness in microscope divisions* (1 *div.* = 0.0175 *mm*).

20.0	20.7	20.7	21.0
20.1	20.1	20.8	21.5
20.0	20.4	20.4	21.3
20.1	20.4	20.6	20.9
20.2	20.2	21.2	21.0
20.1	20.5	20.3	
20.0	20.1	22.0	
20.2	20.5	21.5	
19.9	20.7	21.0	
20.0	21.0	20.8	

where μ is Poisson's ratio, usually defined as

$$-\frac{dD}{D}\Big/\frac{dL}{L}.$$

That is,

$$dT=2\mu\frac{T}{L}\cdot dL.$$

But from the case of constant length $dT=-dT'$ and $dT'=Tf'(t)dt$

$$\therefore\quad dL=\frac{L}{2\mu T}\cdot Tf'(t)dt \quad\text{or}\quad \frac{dL}{L}=-\frac{1}{2\mu}f'(t)dt.$$

Since at $t=0$, $L=L_1$ and $f(0)=1$, it follows that

$$1-2\mu\log_e\frac{L}{L_1}=f(t),$$

provided that μ is not a function of L. Or for a material for which $\mu=0.500$

$$1-\log_e\frac{L}{L_1}=f(t).$$

Therefore, in the constant length experiment T'/T_1 is the same function of the time as is $1-\log_e L/L_1$ in the constant load experiment. Although this says nothing about the form of $f(t)$, a comparison can be made by plotting T'/T_1 against time on the same diagram on which $1-\log_e L/L_1$ is plotted against time. This is shown in Fig. 4, in which it is seen that there is no complete proof of agreement. Actual differences between strips indicate that perhaps this is as far as one can go until there is some way to be certain of quite similar strips.

However, it may be noted that in Fig. 4 there is as much lack of accord between the values obtained for $1-\log_e L/L_1$ for different strips as between the T/T_1 and $1-\log L/L_1$ curves. While this may be due entirely to differences in the strips themselves, it may be caused in part by periodic temperature variation. It will be seen that the two tension curves agree rather well over a considerable range, and it might be expected that the other curves should be as self-consistent. Tests at the conclusion of one of the long runs indicate that the strip under constant load is quite sensitive to even small temperature variations, while a corresponding sensitiveness in tension change at constant length is not detectable by the method used. The material under constant load probably behaves as rubber has been shown to act, with a different coefficient for contraction than for expansion, and the conditions favorable for an alternate contraction and expansion actually may have been provided by the thermostatic control used in the experiment. A separate control experiment indicated that over a period of several hours the temperature variation within the chamber was less than 0.1°C, yet the method of control itself depended upon a temperature variation, when the temperature fell below the point set in the thermometer tube, the heater was brought into the circuit, to be cut out when the temperature had risen. The various tests ran for days, the longest for 10 days, and in that period there was considerable variation in the room temperature. Certainly any future measurements on change of length ought to be safeguarded by a very good temperature control.

It is evident that high precision in these measurements can hardly be expected, the material itself being what it is. Nevertheless in carrying out the experiments there has been in general a consistent set of results. The greatest source of error lies in the determination of the thickness of the strip. The strips are not of uniform thickness, as is shown in Table I by the set of measurements taken on the edge of one strip as it was moved along a slide under a measuring microscope.

Since only in the constant load experiment is the thickness changing and then the area over which the analyzing light spreads is always in the same general region of the strip, the error introduced in the results by calculating the thickness from the length measurement is certainly less than the variation indicated in the table above. In the tension measurements the observer at the time felt that the first few measurements were correct within 5 grams and the later ones within one gram. There is also a source of error in assuming the birefringence constant over the spectral range employed. This error, however, is completely masked by the larger uncertainty in the thickness.

As to the form of $f(t)$ much has been written. Phillips[3] found for rubber that $T=a-b\log t$ was in general agreement with his experimental results, and this seems to have been widely accepted, although it was remarked at the time that numerous other expressions could be found to agree well with the data. However, such a form does not fit well with $1-\log L/L_1$, and the data at hand permit other analyses. Professor J. R. Dunning remarked on the similarity of the tension-time curves and those of certain radioactive decay curves. By using the customary methods of analysis of these curves it is possible to fit the tension-time data with an expression of the form

$$T/T_1=Ae^{-at}+Be^{-bt}+Ce^{-ct},$$

where for the particular strips used the constants have these values, $A=0.263$; $B=0.193$; $C=0.543$; $a=0.050$; $b=0.0027$ and $c=0.000043$. The solid lines drawn on Fig. 4 are for this equation, and the agreement with the observed T/T_1 values is evident. The agreement with the values of $1-\log_e L/L_1$ is, of course, as indicated

[3] P. Phillips, Trans. Phys. Soc. London **29**, 491 (1905).

in the general result, Fig. 4, of the $f(t)$ comparison.

Under the circumstances it is probably unwise further to discuss implications, however tempting it may be to do so. More data should be made available to provide a satisfactory basis for better interpretation.

I wish to thank Mr. Geoffrey Keller for his assistance at those times when the changes were most rapid.

The Analysis of Symmetrical Vibrating Systems

Louis A. Pipes
Harvard University, Cambridge, Massachusetts
(Received December 4, 1939)

The Lagrangian equations of motion of a general mechanical system of n degrees of freedom that is executing small motions about a position of equilibrium are subjected to a Laplacian transformation. The transformed equations are then subjected to a similarity transformation. By means of this transformation, a separation of the transformed equations is effected provided the system has the special type of symmetry under consideration. The solution of the usual determinantal equation is avoided. The methods of the Laplacian transformation and matrix algebra as presented in (1) and (2) are assumed in the discussion.

I. The General Equations

THE Lagrangian equations of motion of a general mechanical system defined by n parameters $(x_1, x_2, \cdots x_n)$ that is executing small motions about a position of equilibrium may be written in the form:

$$\begin{aligned} &Z_{11}(x_1)+Z_{12}(x_2)+\cdots+Z_{1n}(x_n)=F_1(t),\\ &Z_{21}(x_1)+Z_{22}(x_2)+\cdots+Z_{2n}(x_n)=F_2(t),\\ &\cdots\cdots\cdots\cdots\cdots\cdots\\ &Z_{n1}(x_1)+Z_{n2}(x_2)+\cdots+Z_{nn}(x_n)=F_n(t), \end{aligned} \tag{1}$$

where the Z_{ij}'s are differential operators of the form:

$$Z_{ij}=A_{ij}d^2/dt^2+B_{ij}d/dt+C_{ij} \tag{2}$$

and the $F_i(t)$ quantities are forces impressed on the various component parts of the system and are supposed known functions of time. Let us introduce the notation:

$$(x)=(x_r), \quad r=1, 2, \cdots n, \tag{3}$$

the coordinate matrix,

$$[A]=[A_{rs}], \quad r=1\cdots n, \quad s=1\cdots n, \tag{4}$$

the inertia matrix, and two additional square matrices, similarly defined:

$$[B]=[B_{rs}], \text{ the damping matrix,} \tag{5}$$

$$[C]=[C_{rs}], \text{ the stiffness matrix.} \tag{6}$$

Let us also introduce a column matrix whose elements are the applied forces:

$$(F)=(F_r), \text{ the force matrix.} \tag{7}$$

In this notation, the set of equations (1) may be written in the form:

$$[A](\ddot{x})+[B](\dot{x})+[C](x)=(F), \tag{8}$$

where the dots indicate differentiation of the elements of the matrices with respect to time.

II. The Symmetrical System

The set of equations (1) specify the motion of a very general system. The solution of these equations subject to prescribed initial conditions has occupied the attention of mathematicians and physicists since the time of Lagrange. Many methods of great power have been evolved for the solution of these equations.[4] All of these methods in one form or another involve the solution of a high order algebraic equation called the "determinantal equation" of the system.

Certain systems of practical importance have the property of perfect symmetry. The elements of the inertia, damping, and stiffness matrices of such systems satisfy the equations:

$$A_{ii}=A_0, \tag{9}$$

$$A_{ij}=A \quad \text{for } i\neq j, \tag{10}$$

$$B_{ii}=B_0, \tag{11}$$

$$B_{ij}=B \quad \text{for } i\neq j, \tag{12}$$

$$C_{ii}=C_0, \tag{13}$$

$$C_{ij}=C \quad \text{for } i\neq j. \tag{14}$$

That is, the inertia, damping, and stiffness matrices have equal elements on their principal

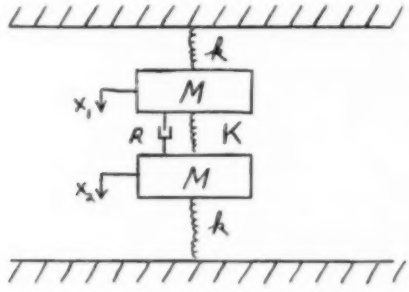

FIG. 1.

diagonals and other equal elements off their principal diagonals.

The analysis of systems exhibiting this type of symmetry will be discussed in this paper. It will be shown that for systems of this type it is unnecessary to solve the "determinantal equation" of the system. The method to be presented is similar to a transformation to normal coordinates by a similarity transformation.

III. The Laplacian Transformation of the General Equations

Following the method of (3) we will subject the general matrix Eq. (8) to a Laplacian transformation as follows: Let

$$y_i(p)\doteq x_i(t), \quad i=1, 2, \cdots n, \tag{15}$$

$$G_i(p)\doteq F_i(t), \quad i=1, 2, \cdots n. \tag{16}$$

That is, for each element of the coordinate matrix (x) and the force matrix (F) of (8) we introduce its Laplacian transform.

Let (x^0) be a column matrix whose elements give the initial displacements at $t=0$.

Let (x^1) be a column matrix whose elements are the initial velocities at $t=0$. Then let us define:

$$Z_{ij}(p)=p^2A_{ij}+pB_{ij}+C_{ij}=\begin{cases}Z_0 & \text{if } i=j,\\ Z & \text{if } i\neq j,\end{cases} \tag{17}$$

then the matrix Eq. (8) is transformed to

$$[Z(p)](y)=(G)+p^2[A](x^0)+p[B](x^0)+p[A](x^1). \tag{18}$$

IV. The Similarity Transformation

The matrix Eq. (18) will now be transformed in a manner analogous to that of the method of normal coordinates.

Consider a square matrix $[S]$ defined by:

$$[S]=[S_{rs}], \quad r=1, 2, \cdots n, \quad s=1, 2, \cdots n, \tag{19}$$

$$S_{rs}=a^{-(r-1)(s-1)}, \tag{20}$$

$$a=e^{2\pi i/n}, \quad i=(-1)^{\frac{1}{2}}. \tag{21}$$

The matrix $[S]$ has the properties:

$$[S]'=[S], \tag{22}$$

where $[S]'$ is the transpose of the matrix $[S]$.

$$[S]^{-1}=(1/n)[\bar{S}], \tag{23}$$

where $[S]^{-1}$ is the inverse of $[S]$ and $[\bar{S}]$ is the conjugate of $[S]$.

It will now be shown how a similarity transformation of (18) by means of the matrix $[S]$ results in a simplification provided that the matrices $[A]$, $[B]$ and $[C]$ have the symmetry discussed in Section II.

Let us multiply both sides of (18) by the matrix $[S]^{-1}$. We then obtain:

$$[S]^{-1}[Z][S][S]^{-1}(y)=[S]^{-1}(G)+p^2[S]^{-1}[A][S][S]^{-1}(x^0)+p[S]^{-1}[B][S][S]^{-1}(x^0)+p[S]^{-1}[A][S][S]^{-1}(x'). \tag{24}$$

Now let us introduce the notation:

$$(G)_s=[S]^{-1}(G)=(G_{rs}), \quad r=1, 2, \cdots n, \tag{25}$$

$$(y)_s=[S]^{-1}(y)=(y_{rs}), \tag{26}$$

$$(x^0)_s=[S]^{-1}(x^0)=(x_{rs}{}^0), \tag{27}$$

$$(x^1)_s=[S]^{-1}(x^1)=(x_{rs}{}^1), \tag{28}$$

$$[Z]_s=[S]^{-1}[Z][S], \tag{29}$$

$$[A]_s=[S]^{-1}[A][S], \tag{30}$$

$$[B]_s=[S]^{-1}[B][S]. \tag{31}$$

Then (24) may be written in the form:

$$[Z]_s(y)_s=(G)_s+p^2[A]_s(x^0)_s+p[B]_s(x^0)_s+p[A]_s(x^1)_s. \tag{32}$$

Now by a direct multiplication of (29) and in view of (17) we have:

$$[Z]_s=\begin{Vmatrix} [Z_0+(n-1)Z] & 0 & 0 & \cdots & 0 \\ 0 & (Z_0-Z) & 0 & \cdots & 0 \\ \cdot & \cdot & \cdot & \cdot & \cdot \\ 0 & 0 & 0 & \cdots & (Z_0-Z) \end{Vmatrix} \tag{33}$$

That is, the similarity transformation transforms the matrix $[Z]$ into the diagonal form (33).

The matrices $[A]$, $[B]$, and $[C]$ are diagonalized in a similar manner. In view of the diagonal form of the square matrices of Eq. (32), this equation separates into the n scalar equations:

$$[Z_0+(n-1)Z]y_{1s}=G_{1s}+p^2[A_0+(n-1)A]x_{1s}^0+p[B_0+(n-1)B]x_{1s}^0+p[A_0+(n-1)A]x_{1s}^1, \tag{34}$$

$$(Z_0-Z)y_{rs}=G_{rs}+p^2(A_0-A)x_{rs}^0+p(B_0-B)x_{rs}^0+p(A_0-A)x_{rs}^1, \quad r=2, 3, \cdots n. \tag{35}$$

We then have immediately

$$y_{1s}=G_{1s}/[Z_0+(n-1)Z]+p^2[A_0+(n-1)A]x_{1s}^0/[Z_0+(n-1)Z]$$

$$+p[B_0+(n-1)B]x_{1s}^0/[Z_0+(n-1)Z]+\frac{p[A_0+(n-1)A]x_{1s}^1}{[Z_0+(n-1)Z]}, \tag{36}$$

$$y_{rs}=G_{rs}/(Z_0-Z)+p^2(A_0-A)x_{rs}^0/[Z_0-Z]+p(B_0-B)x_{rs}^0/[Z_0-Z]+p(A_0-A)x_{rs}^1/(Z_0-Z), \tag{37}$$

$$r=2, 3, 4, \cdots n.$$

From Eqs. (36) and (37) it is easy to compute the inverse transforms of the y_{rs} quantities.

Let us write

$$x_{rs}(t)\doteqdot y_{rs}(p). \tag{38}$$

Or, in matrix form

$$(x)_s\doteqdot(y)_s. \tag{39}$$

If we premultiply (39) by $[S]$ we obtain:

$$[S](x)_s\doteqdot[S](y)_s. \tag{40}$$

In view of (26) this becomes

$$[S](x)_s\doteqdot(y) \tag{41}$$

and by (15) we have finally,

$$(x)=[S](x)_s. \tag{42}$$

We thus obtain the various coordinates explicitly.

V. Example

The general theory developed above will now be applied to determine the free oscillations of the symmetrical system of Fig. 1.

The two equal masses are arranged symmetrically as shown and the system is damped by means of the dashpot connected between the two masses. The three spring constants are marked on the figure.

Let the system be initially at rest at $t=0$ and let the initial displacement of the upper mass be x_1^0 and of the lower mass be x_2^0.

The equations of motion of the system are:

$$\begin{aligned} M\ddot{x}_1+kx_1+K(x_1-x_2)+R(\dot{x}_1-\dot{x}_2)&=0, \\ M\ddot{x}_2+kx_2+K(x_2-x_1)+R(\dot{x}_2-\dot{x}_1)&=0. \end{aligned} \tag{43}$$

Comparing these with the general Eq. (8) we see that:

$$[A]=\begin{Vmatrix} M & 0 \\ 0 & M \end{Vmatrix}, \tag{44}$$

$$[B]=\begin{Vmatrix} R & -R \\ -R & R \end{Vmatrix}, \tag{45}$$

$$[C]=\begin{Vmatrix} (K+k) & -K \\ -K & (K+k) \end{Vmatrix}. \tag{46}$$

The conditions of symmetry (9–14) are thus satisfied. In our general equations we now have $n=2$. By (27) we have:

$$\begin{Vmatrix} x_{1s}^0 \\ x_{2s}^0 \end{Vmatrix}=[S]^{-1}(x^0)=\tfrac{1}{2}\begin{Vmatrix} 1 & 1 \\ 1 & -1 \end{Vmatrix}\cdot\begin{Vmatrix} x_1^0 \\ x_2^0 \end{Vmatrix}, \tag{47}$$

Therefore,

$$x_{1s}^0=\tfrac{1}{2}(x_1^0+x_2^0), \tag{48}$$

$$x_{2s}^0=\tfrac{1}{2}(x_1^0-x_2^0). \tag{49}$$

In this case since we have no driving forces $(G)=(0)$, and since we have no initial velocities, $(x^1)=(0)$. Accordingly, substituting the above relations into (36) and (37) we obtain:

$$y_{1s}=p^2Mx_{1s}^0/(p^2M+k), \tag{50}$$

$$y_{2s}=p^2Mx_{2s}^0/[p^2M+2pR+(k+2K)] + 2pRx_{2s}^0/[p^2M+2pR+(k+2K)]. \tag{51}$$

Let us suppose that

$$(k+2K)>R/M. \tag{52}$$

Now, from a table of transforms (2, Part II) we have:

$$p^2/(p^2+w^2)\doteqdot\cos(wt), \tag{53}$$

$$p^2/(p^2+2ap+w_0^2)\doteqdot-(w_0/w)e^{-at}\sin(wt-b), \quad w_0>a, \tag{54}$$

where $w^2=w_0^2-a^2$ $\tan(b)=w/a$,

$$p/(p^2+2ap+w_0^2)\doteqdot e^{-at}\sin(wt)/w \quad \text{if } w_0>a. \tag{55}$$

Comparing these transforms with those of our problem we see that:

$$x_{1s}=x_{1s}^0\cos(w_1t), \tag{56}$$

where

$$w_1=(k/M)^{\frac{1}{2}}, \tag{57}$$

$$x_{2s}=-x_{2s}^0e^{-at}\sin(w_2t-b)/w_2 + 2ax_{2s}^0e^{-at}\sin(w_2t)/w_2, \tag{58}$$

where

$$w_0^2=(k+2K)/M, \tag{59}$$

$$a=R/M, \tag{60}$$

$$w_2^2=w_0^2-a^2, \tag{61}$$

$$b=\tan^{-1}(w/a). \tag{62}$$

Now to obtain the true coordinates from the transformed coordinates we make use of (42) and, in this case, we have:

$$\left\|\begin{matrix}x_1\\x_2\end{matrix}\right\|=[S](x)_s=\left\|\begin{matrix}1&1\\1&-1\end{matrix}\right\|\cdot\left\|\begin{matrix}x_{1s}\\x_{2s}\end{matrix}\right\|. \tag{63}$$

Therefore,

$$x_1=x_{1s}-x_{2s}, \tag{64}$$

$$x_2=x_{1s}-x_{2s}. \tag{65}$$

Hence, substituting from (56) and (58) we have:

$$x_1=(x_1^0+x_2^0)\cos(w_1t)/2 + (x_2^0-x_1^0)w_0e^{-at}\sin(w_2t-b)/2w_2 + a(x_1^0-x_2^0)e^{-at}\sin(w_2t)/w_2, \tag{66}$$

$$x_2=(x_1^0+x_2^0)\cos(w_1t)/2 + w_0(x_1^0-x_2^0)e^{-at}\sin(w_2t-b)/2w_2 + a(x_2^0-x_1^0)e^{-at}\sin(w_2t)/w_2. \tag{67}$$

We see that the ultimate effect of the dashpot is to cause the two masses to oscillate in unison. If the initial displacements x_1^0 and x_2^0 are equal, the solution reduces to the first term as we should expect from physical considerations.

The simplicity of the method presented may be noted in that the solution of the determinantal equation of the system has been avoided. In the simple case discussed above, the equation is one of the fourth order. If we had considered initial velocities and impressed driving forces, the procedure followed would be the same and a substitution into the general Eqs. (36) and (37) would have provided us with the required solution.

VI. Conclusion

It is evident from the general theory presented that the analysis of symmetrical dynamical systems is greatly facilitated by the use of an algebraic similarity transformation followed by a Laplacian transformation. The cases of free or forced oscillations with given initial displacements and velocities are easily treated.

By the use of this method the solution of the determinantal equation is avoided and hence the numerical work is enormously reduced. It must be realized, however, that the method is applicable only to systems having the type of symmetry described in Section II.

Bibliography

1. L. A. Pipes, "Matrices in Engineering," Elec. Eng. **56**, 1177–1190 (1937).
2. L. A. Pipes, "The Operational Calculus," Parts I, II, and III, J. App. Phys. **10**, 172–80, 258–264, 301–311 (1939).
3. L. A. Pipes, "Matrix-Operational Methods in Mechanical Vibrations," J. Frank. Inst. **225**, 343–349 (1938).
4. Duncan and Collar, "Matrices Applied to the Motion of Damped Systems," Phil. Mag. [7] **19**, 197–219 (1935).

The Solution of Torsion Problems by Numerical Integration of Poisson's Equation

R. WELLER* AND G. H. SHORTLEY, *Mendenhall Laboratory of Physics,*
AND
B. FRIED, *Engineering Experiment Station,*
Ohio State University, Columbus, Ohio

(Received October 18, 1939)

This paper considers numerical methods for the solution of Poisson's equation in an arbitrary two-dimensional region with given boundary values. The methods are similar to those discussed by Shortley and Weller for Laplace's equation. It is shown that the entire theory of networks may be applied to Poisson's equation without change. Formulas for the treatment of irregular points and for blocks of points are developed. In addition to the mathematical considerations, the application of the methods to the case of torsion in shafts of any cross section is described. Additional formulas are derived for the determination of the maximum shear at any point in a shaft as well as the torsional stiffness of such a shaft.

INTRODUCTION

POISSON'S equation appears in many important practical applications of physics: stress distributions in machine and structural parts subjected to torsion, electrostatic fields containing distributed charge, the flow of heat in a body which contains distributed sources of heat energy, and others. Recently[1] two of the authors considered the numerical solution of Laplace's equation in two dimensions. Here we give a similar treatment of Poisson's equation. Although, because of their considerable engineering interest, we discuss in particular problems of torsional stress, the methods which we develop are generally applicable.

It is shown in treatises on the theory of elasticity[2] that the stress distribution in the torsion of a shaft of uniform cross section is conveniently described by a function ψ obeying the equation.

$$\partial^2\psi/\partial x^2+\partial^2\psi/\partial y^2+2G\theta=0,$$

where θ and G are, respectively, the torsional strain and the modulus in shear of the shaft, which is taken to extend in the z direction. The function ψ, when plotted over the xy plane, gives a pillow-shaped surface, the boundary values of which may be taken as zero. The magnitude of the gradient of ψ at a point gives there the maximum shear, and twice the volume included between the ψ surface and the xy plane gives the torque applied to the shaft. We now consider numerical methods (applicable to boundaries of any shape) for determining the form of the ψ-surface, of calculating its slope at any point, and of finding the volume corresponding to the applied torque. Insofar as torsion is concerned, the following discussion is directly applicable only to solid shafts; the problem of hollow shafts involves special considerations to determine the boundary values of ψ on the interior surfaces.[2]

* Now at The State College of Washington, Pullman, Washington.

[1] G. H. Shortley and R. Weller, J. App. Phys. **9**, 344 (1938); J. App. Mech. **6**, A-71 (June, 1939).

[2] S. Timoshenko, *Theory of Elasticity* (McGraw-Hill).

SOLUTION OF POISSON'S EQUATION

The following discussion is somewhat skeletal, since the general ideas are the same as for Laplace's equation, for which see reference 1.

Basic procedure

In a two-dimensional region, we treat the differential equation

$$\Delta\psi+\alpha=0 \qquad (1)$$

by laying down a square net of interval h and employing, except for points adjacent to an irregular boundary, the corresponding difference equation

$$\frac{1}{h^2}[\psi(x, y+h)+\psi(x, y-h)+\psi(x+h, y)+\psi(x-h, y)-4\psi(x, y)]+\alpha(x, y)=0. \qquad (2)$$

The operations corresponding to the Liebmann

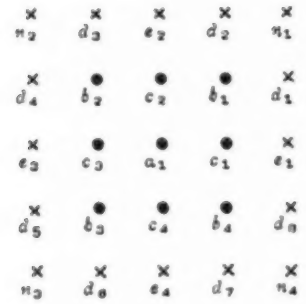

FIG. 1. A simple network. Crosses represent boundary points which remain constant. Circles represent points to be improved.

procedure for Laplace's equation involve first assigning arbitrary values to the function at the net-points, then traversing the net repeatedly, replacing the value at each point by the mean of its four nearest neighbors plus $\frac{1}{4}\alpha h^2$. That is, for a regular point surrounded by four others at distance h, the improvement formula derived from (2) is

$$\psi(x, y)=\tfrac{1}{4}[\psi(x, y+h)+\psi(x, y-h)+\psi(x+h, y)+\psi(x-h, y)+\alpha(x, y)h^2]. \quad (3)$$

Consider, for example, the simple net of Fig. 1. Let crosses represent boundary points where ψ is given, circles interior points where the trial ψ is to be improved. Then if, for simplicity, we designate the value of ψ at a point simply by the letter representing the point, and use primes to represent improved values, the improvement formulas are

$$b_2'=\tfrac{1}{4}[c_2+c_3+d_4+d_3+\alpha_{b_2}h^2],$$
$$c_2'=\tfrac{1}{4}[b_2'+a_1+b_1+e_2+\alpha_{c_2}h^2], \quad \text{etc.},$$

continuing over the net in any convenient order but always using improved values as soon as they are available. This improvement process is iterated until the values at all points become stationary, at which time the solution of (2) is complete for the net of the interval used and to the number of significant figures employed, except for rounding-off errors. These errors, will, in general, be of the order of $\frac{1}{10}$ the number of internal points in the net taken in the last significant figure.[1]

In general the error occasioned by using a difference equation in place of the differential equation is proportional to h^2 and approaches 0 rapidly with decrease of h.

It should be noted that, whereas in solving Laplace's equation one takes no account of the net interval h in the use of the improvement formulas, here the value of h enters explicitly into each formula.

Calculation of points with nonequidistant neighbors

In many cases a point near a boundary will not be surrounded by equidistant neighbors, or one may desire to make a change of net interval in a restricted region. Special formulas must be provided for such cases. These are obtained as in the case of Laplace's equation[1] by computing the value of $(\Delta\psi)_0$ at the point in question from a polynomial of as high an order as possible passed through this and the neighboring points.[3] The improvement formula is then obtained by solving for ψ_0 the equation $(\Delta\psi)_0+\alpha_0=0$.

For four points located at distances s_1h, s_2h, s_3h, s_4h from the origin, as in the figure, ψ_0 is to be improved by the formula

$$\left(\frac{2}{s_1s_2}+\frac{2}{s_3s_4}\right)\psi_0=\frac{2}{s_1(s_1+s_2)}\psi_1+\frac{2}{s_2(s_1+s_2)}\psi_2+\frac{2}{s_3(s_3+s_4)}\psi_3+\frac{2}{s_4(s_3+s_4)}\psi_4+\alpha_0h^2. \quad (4)$$

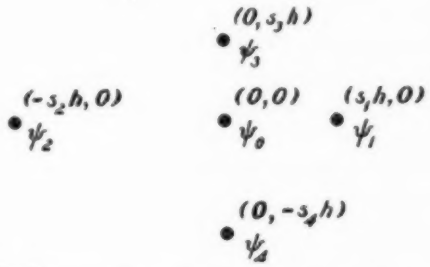

[3] If we express the value $(\Delta\psi)_0$ of the Laplacian at the origin in terms of the values ψ_0, ψ_1, ψ_2, $\cdots$ of ψ at (0,0), (x_1,y_1), (x_2,y_2), $\cdots$ by the equation

$$(\Delta\psi)_0=a\psi_0+\sum_{i=1}^{\cdots}b_i\psi_i,$$

we obtain the following equations for the determination of the coefficients a and b_i:

$$a+\Sigma b_i=0;$$
$$\Sigma b_ix_i=0, \qquad \Sigma b_iy_i=0;$$
$$\Sigma b_ix_i^2=2, \qquad \Sigma b_iy_i^2=2, \qquad \Sigma b_ix_iy_i=0;$$
$$\Sigma b_ix_i^ny_i^m=0, \text{ if } n+m>2.$$

As many as possible of these equations, in order, are to be satisfied.

In most cases for a point near the boundary, as least two of the s's equal unity and (4) becomet simpler in form; Table I gives the coefficients for this case.

If it is desirable to change from a net of size h in one region to a net spacing of $2h$ in another (Fig. 2), the formula (4), with some of the s's equal to 1 and some equal to 2, will take care of all points except those located in positions such as b, i, k. For these, the improvement formula is of the following type:

$$\psi_i = \tfrac{1}{16}[4\psi_c + 5\psi_g + 5\psi_j + \psi_m + \psi_n + 6\alpha_i h^2]. \quad (5)$$

If there is a line of symmetry, only the points lying on one side of it need be treated, the points lying on the axis being improved by merely considering the whole net and the ψ-function as reflected in the line of symmetry.

Formulas for blocks of points

As in the case of Laplace's equation, more rapid convergence may be obtained by improving a block of several points simultaneously. In the case of Poisson's equation the formulas are, for the nine-block (Fig. 1):

$$a_1' = \tfrac{1}{16}[\Sigma d + 2\Sigma e + (6\alpha_{a_1} + \Sigma\alpha_b + 2\Sigma\alpha_c)h^2];$$

$$b_1' = \tfrac{1}{4}[a_1' + e_1 + e_2 + n_1 + 2\alpha_{b_1}h^2], \quad \text{etc.};^4 \quad (6)$$

$$c_1' = \tfrac{1}{4}[a_1' + b_1' + b_4' + e_1 + \alpha_{c_1}h^2], \quad \text{etc.};$$

[4] If one of the corner points, n, happens to be missing because of the incidence of a boundary one can use the two d points instead, with a formula of the type

$$b_1' = \tfrac{1}{8}[2a_1' + e_1 + e_2 + 2d_1 + 2d_2 + 3\alpha_{b_1}h^2].$$

The same formula is available for the b point of the four-block (Fig. 3).

TABLE I. *Coefficients occurring in (4).*

s	$\frac{2}{s}$	$\frac{2}{1+s}$	$\frac{2}{s(1+s)}$	s	$\frac{2}{s}$	$\frac{2}{1+s}$	$\frac{2}{s(1+s)}$
0.01	200.0000	1.9802	198.0198	0.51	3.9216	1.3245	2.5971
.02	100.0000	1.9608	98.0392	.52	3.8461	1.3158	2.5304
.03	66.6667	1.9417	64.7249	.53	3.7736	1.3072	2.4664
.04	50.0000	1.9231	48.0769	.54	3.7037	1.2987	2.4050
.05	40.0000	1.9048	38.0952	.55	3.6364	1.2903	2.3460
.06	33.3333	1.8868	31.4465	.56	3.5714	1.2821	2.2894
.07	28.5714	1.8692	26.7023	.57	3.5088	1.2739	2.2349
.08	25.0000	1.8518	23.1481	.58	3.4483	1.2658	2.1825
.09	22.2222	1.8348	20.3874	.59	3.3898	1.2579	2.1320
.10	20.0000	1.8182	18.1818	.60	3.3333	1.2500	2.0833
.11	18.1818	1.8018	16.3800	.61	3.2787	1.2422	2.0365
.12	16.6667	1.7857	14.8809	.62	3.2258	1.2346	1.9912
.13	15.3846	1.7699	13.6147	.63	3.1746	1.2270	1.9476
.14	14.2857	1.7544	12.5313	.64	3.1250	1.2195	1.9055
.15	13.3334	1.7391	11.5942	.65	3.0769	1.2121	1.8648
.16	12.5000	1.7241	10.7759	.66	3.0303	1.2048	1.8255
.17	11.7647	1.7094	10.0553	.67	2.9850	1.1976	1.7875
.18	11.1112	1.6949	9.4162	.68	2.9412	1.1905	1.7507
.19	10.5263	1.6807	8.8456	.69	2.8985	1.1834	1.7151
.20	10.0000	1.6667	8.3333	.70	2.8571	1.1765	1.6807
.21	9.5238	1.6529	7.8709	.71	2.8169	1.1696	1.6473
.22	9.0909	1.6393	7.4516	.72	2.7778	1.1628	1.6150
.23	8.6956	1.6260	7.0696	.73	2.7397	1.1561	1.5837
.24	8.3334	1.6129	6.7204	.74	2.7027	1.1494	1.5533
.25	8.0000	1.6000	6.4000	.75	2.6667	1.1429	1.5238
.26	7.6923	1.5873	6.1050	.76	2.6316	1.1364	1.4952
.27	7.4074	1.5748	5.8326	.77	2.5974	1.1299	1.4675
.28	7.1429	1.5625	5.5803	.78	2.5641	1.1236	1.4405
.29	6.8966	1.5504	5.3462	.79	2.5316	1.1173	1.4143
.30	6.6667	1.5385	5.1282	.80	2.5000	1.1111	1.3889
.31	6.4516	1.5267	4.9249	.81	2.4691	1.1050	1.3642
.32	6.2500	1.5152	4.7348	.82	2.4390	1.0989	1.3401
.33	6.0606	1.5037	4.5568	.83	2.4096	1.0928	1.3167
.34	5.8824	1.4925	4.3898	.84	2.3809	1.0869	1.2940
.35	5.7143	1.4815	4.2328	.85	2.3529	1.0811	1.2719
.36	5.5556	1.4706	4.0849	.86	2.3256	1.0753	1.2503
.37	5.4054	1.4598	3.9455	.87	2.2988	1.0695	1.2293
.38	5.2631	1.4493	3.8139	.88	2.2727	1.0638	1.2089
.39	5.1282	1.4388	3.6893	.89	2.2472	1.0582	1.1891
.40	5.0000	1.4286	3.5714	.90	2.2222	1.0526	1.1696
.41	4.8780	1.4184	3.4596	.91	2.1978	1.0471	1.1507
.42	4.7619	1.4085	3.3534	.92	2.1739	1.0417	1.1323
.43	4.6512	1.3986	3.2526	.93	2.1505	1.0363	1.1143
.44	4.5455	1.3889	3.1566	.94	2.1276	1.0309	1.0967
.45	4.4444	1.3793	3.0651	.95	2.1053	1.0256	1.0796
.46	4.3478	1.3699	2.9780	.96	2.0833	1.0204	1.0629
.47	4.2553	1.3605	2.8948	.97	2.0618	1.0152	1.0466
.48	4.1667	1.3514	2.8153	.98	2.0408	1.0101	1.0307
.49	4.0816	1.3423	2.7393	.99	2.0202	1.0050	1.0152
.50	4.0000	1.3333	2.6667	1.00	2.0000	1.0000	1.0000

and for the four-block (Fig. 3):

$$a' = \tfrac{1}{24}[7\Sigma d + 2\Sigma e + 2\Sigma f + \Sigma g + (7\alpha_a + \alpha_b + 2\Sigma\alpha_c)h^2];$$
$$b' = \tfrac{1}{4}[a' + \Sigma f + i_3 + 2\alpha_b h^2]; \qquad (7)$$
$$c_1' = \tfrac{1}{4}[a' + b' + e_1 + f_1 + \alpha_{c_1} h^2]; \quad \text{etc.}$$

If, as in the case of torsion, α is a constant independent of position, the first equations of (6) and (7) become, respectively,

$$a_1' = \tfrac{1}{16}[\Sigma d + 2\Sigma e + 18\alpha h^2],$$
$$a' = \tfrac{1}{24}[7\Sigma d + 2\Sigma e + 2\Sigma f + \Sigma g + 12\alpha h^2].$$

The difference function and extrapolation

In the case of Laplace's equation, we found that the labor of improvement was materially reduced by obtaining the difference between the first improved function and the original function, and then applying the improvement formulas to this difference function. The difference function was easier to handle because it had in general only a few significant figures, because it had zero boundary values, and particularly because it was useful for extrapolation since it sank continuously to zero everywhere in a determinable fashion.

In the case of Poisson's equation we can work similarly with the difference function, with all the advantages noted above and one other: *to "improve" the difference function we use the simpler formulas which are obtained by omitting all the α's in those we have given previously.*[5]

When the α's are omitted, all the improvement formulas for Poisson's equation become identical with those for Laplace's equation. Hence the difference functions behave exactly the same in the two cases, and for the same error in guessing the trial function the rate of convergence to the final value is exactly the same in the two cases. Therefore *the whole of the detailed discussion of reference 1, concerning proof of convergence, rates of convergence, advantages of the different block and extrapolation procedures, etc., may be taken over bodily and need not be repeated here.*

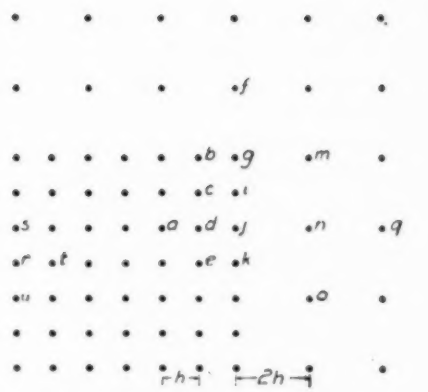

FIG. 2. Change of net constant.

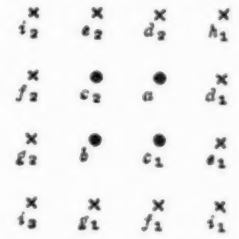

FIG. 3. The four-block.

The procedure for solving Poisson's equation by use of the difference function is the following: Having chosen the trial function, the improvement formula to be used for each point, and the order of traversing the net, *go over the trial function ψ once to obtain the function ψ'. Calculate the difference function $\delta = \psi' - \psi$.* This will have zero boundary values. *Improve the function δ repeatedly* in the same order as for ψ, *using the same improvement formulas but with all the α terms omitted*, to obtain successively δ', δ'', $\cdots$, $\delta^{(k)}$, $\cdots$. When this function has become fairly smooth, one-signed, and is falling fairly uniformly in a geometrical fashion, find the ratio $\delta^{(k)}/\delta^{(k-1)}$ at various points of the net. Using a mean value λ for this ratio, *add together ψ', δ', δ'', $\cdots$, $\delta^{(k-1)}$, $\delta^{(k)}/(1-\lambda)$ to obtain a new trial function*

[5] Let $\delta_i = \psi_i' - \psi_i$, $\delta_i' = \psi_i'' - \psi_i'$; etc. To demonstrate that δ' is derived from δ in the same way as ψ' from ψ but with the α's and the boundary values set equal to zero, we may proceed as follows: Let there be N interior points, improved in the order $1, 2, \cdots, N$. Then the formula for the improvement of the kth point may be written as

$$\psi_k' = \sum_{i=1}^{k-1} V_{ki}\psi_i' + \sum_{i=k+1}^{N} W_{ki}\psi_i + \sum_{\text{b.p.}} X_{k\beta}\psi_\beta + Y_{k\alpha}\alpha_k, \qquad (A)$$

where the V, W, X, Y, and α are constants independent of ψ; the ψ_β are the fixed values of ψ at the boundary points, and in general the coefficients of all but five or six terms vanish. Then

$$\psi_k'' = \sum_{i=1}^{k-1} V_{ki}\psi_i'' + \sum_{i=k+1}^{N} W_{ki}\psi_i' + \sum_{\text{b.p.}} X_{k\beta}\psi_\beta + Y_{k\alpha}\alpha_k;$$

$$(\psi_k'' - \psi_k') = \sum_{i=1}^{k-1} V_{ki}(\psi_i'' - \psi_i') + \sum_{i=k+1}^{N} W_{ki}(\psi_i' - \psi_i)$$

or
$$\delta_k' = \sum_{i=1}^{k-1} V_{ki}\delta_i' + \sum_{i=k+1}^{N} W_{ki}\delta_i. \qquad (B)$$

Comparison of (A) and (B) completes the demonstration.

$\bar{\psi}$. Apply the improvement process to $\bar{\psi}$ to obtain $\bar{\psi}'$, and if the difference between these functions indicates insufficiently complete convergence, obtain a new difference function and repeat the procedure.

To obtain good trial functions, it is best to solve the difference equations first for a net of very large spacing, then for one of half this spacing, and so on until the desired fineness is reached. In transferring values to a finer net, the interpolations may be made very accurately by the use of the difference equation itself, first diagonally to get the point at the center of each square, and then regularly to get the balance.[1]

Determination of Slopes

The maximum shear at any point in a torsional stress distribution is given by the maximum slope (i.e., the gradient) of the ψ-function.[6] It becomes necessary, therefore, to determine these slopes with some accuracy from the ψ-values of the converged network. At the boundary the *normal* slope is always the greatest (the tangential slope being zero). If a lattice line intersects the boundary at 90° the slope may be found conveniently by passing a parabola through the intersection with the boundary, where $\psi=0$, and the two nearest interior points along this line (Fig. 4). Let the distance between the boundary and the first point (ψ_1) be sh, where s is a fraction of the net interval. The magnitude of the slope at the boundary is then given by

$$\frac{\partial\psi}{\partial n}=-\frac{1}{h}\left(\frac{s+1}{s}\psi_1-\frac{s}{s+1}\psi_2\right). \tag{8}$$

If a lattice line intersects a boundary at 45° the normal slope may be similarly computed along a diagonal line of points.

The determination of the shearing stress from these slope values may be made only after a consideration of the volume enclosed between the ψ-surface and the xy plane. However, the ratio between two shears may be taken directly as the slope ratio at the points in question.

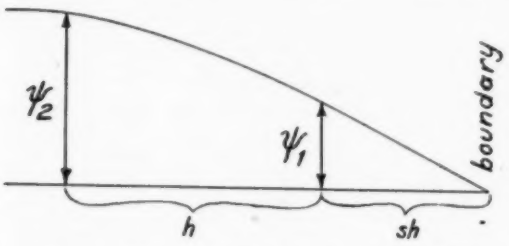

Fig. 4. Calculation of slope at the boundary.

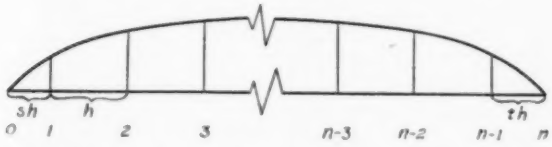

Fig. 5. First integration to obtain volume. A line of points across the surface is considered. This represents a cross section of the volume to be obtained.

Determination of Torque Volume

The torque producing shear in torsion is given by *twice* the volume included between the ψ-surface and the xy plane. To compute this volume, it is convenient to integrate along a complete set of parallel lines individually and then integrate the resulting sums once in the cross direction. Consider the row of points in Fig. 5. The formulas which we give below, and which seem to be as accurate as is justified by the difference equations we have used, were obtained by passing parabolas through all possible sets of three adjacent points and averaging the two areas so obtained for each section except those at the ends. If in Fig. 5, $s=t=1$, the area under the curve (ψ being zero at the ends) will be given by

$$A=[\tfrac{7}{6}\psi_1+2\tfrac{3}{4}\psi_2+\psi_3+\psi_4+\cdots+\psi_{n-3}+2\tfrac{3}{4}\psi_{n-2}+\tfrac{7}{6}\psi_{n-1}]h. \tag{9}$$

If the end intervals are not equal to h, but are sh and th, respectively, the area is given by

$$A=\left[\frac{1}{12}\left(2s^2+6s+5+\frac{1}{s}\right)\psi_1+\frac{1}{12}\left(-2s^2+2s+11+\frac{1}{s+1}\right)\psi_2+\psi_3+\psi_4+\cdots+\psi_{n-3}+\frac{1}{12}\left(-2t^2+2t+11+\frac{1}{t+1}\right)\psi_{n-2}+\frac{1}{12}\left(2t^2+6t+5+\frac{1}{t}\right)\psi_{n-1}\right]h. \tag{10}$$

[6] But note that the direction of the shearing force is perpendicular to the gradient of ψ. For an ordinary interior point (x, y), the two components of this gradient may be computed, to second-order accuracy, by the formulas

$$\text{grad}_x\,\psi(x,y)=[\psi(x+h,y)-\psi(x-h,y)]/2h,$$
$$\text{grad}_y\,\psi(x,y)=[\psi(x,y+h)-\psi(x,y-h)]/2h.$$

These are proportional to the components $(-\tau_{ys}, \tau_{xs})$ of the shearing stress; the maximum stress is the square root of the sum of the squares of these quantities.

The coefficients for use with this formula are given in Table II.

Now consider the net shown in Fig. 6 and assume that ψ is zero at all boundary points. To compute the volume between the ψ-surface and the xy plane proceed as follows. Apply Eq. (9) or (10) along lines B–B', C–C', D–D', etc., obtaining a certain sum for each. Now integrate from top to bottom using the sum along B–B' as ψ_1, the sum along C–C' as ψ_2, etc., in (9). The result will be the desired volume. Alternatively, the first integration could be made along the lines 1, 2, 3, $\cdots$ and then these values used as the $\psi_1, \psi_2, \cdots$ in (10) to obtain the total volume. In this case, s would be the distance from the leftmost point of the area to line 1, t the distance from line 7 to the rightmost point.

Stress Values

Now consider a shaft of any cross section to which a torque M_t is applied. Let it be desired to find the torsional stiffness and the shear at the boundaries of a section. The following procedure is indicated:

(1) Lay down on the cross section a network, taking for h a convenient number such as 1, 2, or 4. Call the ratio of any shaft dimension to the corresponding distance on the net the *scale-factor*. For example, if Fig. 6 represents the cross section of a shaft and the net points indicated are taken to have the separation $h=2$, the distance on the net between the two flat sides of the shaft is 12. If this distance is actually 2″, the scale-factor is $\frac{1}{6}$.

(2) Solve Poisson's equation in the form

Table II. *Coefficients for numerical integration.*

s	$\frac{1}{12}\left(-2s^2+2s+11+\frac{1}{s+1}\right)$	$\frac{1}{12}\left(2s^2+6s+5+\frac{1}{s}\right)$	s	$\frac{1}{12}\left(-2s^2+2s+11+\frac{1}{s+1}\right)$	$\frac{1}{12}\left(2s^2+6s+5+\frac{1}{s}\right)$
0.01	1.0009	8.7550	0.51	1.0135	0.8784
.02	1.0016	4.5934	.52	1.0131	.8820
.03	1.0024	3.2096	.53	1.0127	.8857
.04	1.0032	2.5203	.54	1.0122	.8896
.05	1.0039	2.1088	.55	1.0117	.8936
.06	1.0047	1.8362	.56	1.0112	.8977
.07	1.0054	1.6430	.57	1.0106	.9020
.08	1.0061	1.4994	.58	1.0100	.9064
.09	1.0068	1.3890	.59	1.0094	.9109
.10	1.0074	1.3017	.60	1.0088	.9156
.11	1.0081	1.2313	.61	1.0081	.9203
.12	1.0087	1.1735	.62	1.0074	.9251
.13	1.0093	1.1255	.63	1.0066	.9301
.14	1.0098	1.0852	.64	1.0059	.9351
.15	1.0104	1.0510	.65	1.0051	.9403
.16	1.0109	1.0218	.66	1.0043	.9455
.17	1.0114	0.9967	.67	1.0034	.9509
.18	1.0119	.9750	.68	1.0025	.9563
.19	1.0123	.9563	.69	1.0016	.9618
.20	1.0128	.9400	.70	1.0007	.9674
.21	1.0132	.9258	.71	0.9997	.9731
.22	1.0136	.9135	.72	.9987	.9788
.23	1.0139	.9028	.73	.9977	.9846
.24	1.0143	.8935	.74	.9966	.9905
.25	1.0146	.8854	.75	.9955	.9965
.26	1.0149	.8784	.76	.9944	1.0026
.27	1.0151	.8725	.77	.9933	1.0087
.28	1.0154	.8674	.78	.9921	1.0149
.29	1.0156	.8630	.79	.9909	1.0212
.30	1.0158	.8594	.80	.9896	1.0275
.31	1.0159	.8565	.81	.9884	1.0339
.32	1.0161	.8542	.82	.9871	1.0404
.33	1.0162	.8523	.83	.9857	1.0469
.34	1.0162	.8510	.84	.9844	1.0535
.35	1.0163	.8502	.85	.9830	1.0601
.36	1.0163	.8497	.86	.9815	1.0668
.37	1.0163	.8497	.87	.9801	1.0736
.38	1.0163	.8500	.88	.9786	1.0804
.39	1.0163	.8507	.89	.9771	1.0873
.40	1.0162	.8518	.90	.9755	1.0943
.41	1.0161	.8529	.91	.9739	1.1013
.42	1.0160	.8545	.92	.9723	1.1083
.43	1.0158	.8563	.93	.9707	1.1154
.44	1.0156	.8583	.94	.9690	1.1226
.45	1.0154	.8606	.95	.9673	1.1298
.46	1.0151	.8631	.96	.9656	1.1371
.47	1.0148	.8658	.97	.9638	1.1444
.48	1.0146	.8687	.98	.9620	1.1518
.49	1.0142	.8718	.99	.9602	1.1592
.50	1.0139	.8750	1.00	.9583	1.1667

$\Delta\psi+1=0$; i.e., set $\alpha=1$ in all improvement formulas.

(3) Compute slopes at points of interest by the use of Eq. (8).

(4) Compute the volume under the ψ-surface by (9) and (10) and *double* this to get the *torque volume* V.

(5) Divide the torque M_t by the torque volume V to obtain a constant called the *reduction-factor*.

(6) Multiply the slopes from step 3 by the reduction-factor and divide by the cube of the scale-factor to obtain the actual shears.

(7) The angular strain is given by the reduction-factor divided by twice the product of the modulus of rigidity and by the fourth power of the scale-factor.

The relations in steps 6 and 7 may be stated as formulas. The symbols, with the physical dimensions of each, are a, a given linear dimension in the cross section of the shaft (length); n, the distance on the net corresponding to the dimension a (dimensionless); M_t, the applied torque (force·length); G, the modulus in shear (force/area); V, the torque volume (dimensionless); M_t/V, the reduction-factor (force·length); a/n, the scale-factor (length). Then

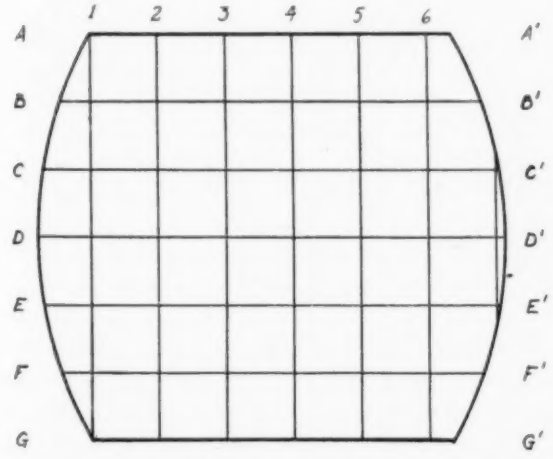

FIG. 6. Second integration to determine volume.

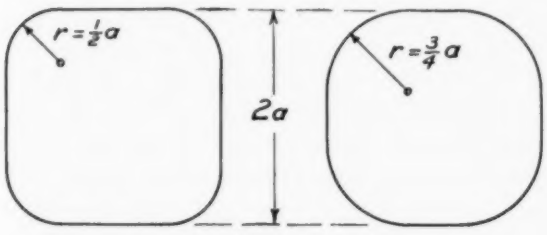

FIG. 7. Cross sections of shafts considered.

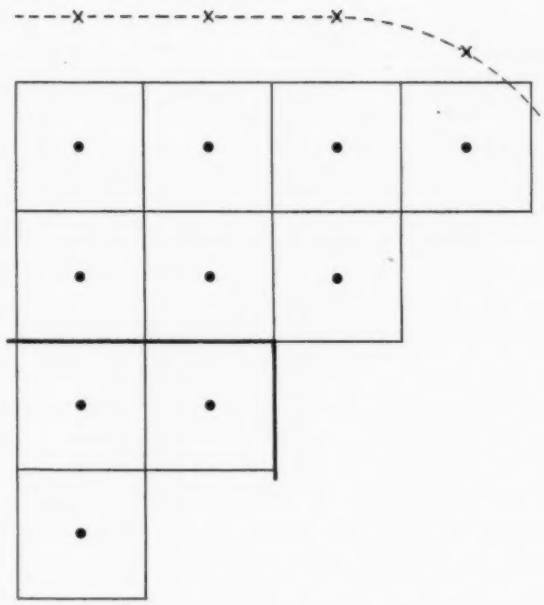

FIG. 8. The coarse network. Due to the fourfold symmetry only one-eighth of the net need be considered.

$$\text{Maximum shear} = \text{Slope}\cdot\frac{M_t}{V}\cdot\left(\frac{n}{a}\right)^3 = \tau_{\max} \quad \text{(force/area)}, \quad (11)$$

$$\text{Torsional strain} = \frac{1}{2G}\cdot\frac{M_t}{V}\cdot\left(\frac{n}{a}\right)^4 = \theta \quad \text{(radians/length)}. \quad (12)$$

ILLUSTRATIVE EXAMPLE

The authors have computed by the above methods the torsional characteristics of two shapes of shaft. Both of these are squares with rounded-off corners (Fig. 7). One has a corner radius of one-fourth of the width and the other a radius equal to three-eighths of the width. The former was done first since it appeared to be midway between a square shaft and the inscribed circular one. The latter was computed when it became evident that the first case was nearer to the square shaft in its torsional properties. In the former case a net having forty-nine interior points was first laid down on the cross section,

Fig. 8. Since this shape possesses four axes of symmetry it is sufficient to treat one-eighth of the total net. A nine-block was placed at the center and values satisfying the Poisson difference equation were obtained, carried to four significant figures. Reduction of the net interval was anticipated so the net interval was taken as $h=2$. Results from this net were transferred to a net of interval unity having about four times the number of interior points. This net (Fig. 9) included several nine-blocks. Results from this net were again transferred to a net having half the previous interval between points. These will be referred to as the coarse, the intermediate, and the fine nets, respectively. From each of these the slopes were computed at three points of interest, namely, in the *center* of the straight side, at the center of the rounded *corner*, and at the point where the straight side becomes *tangent* to the corner arc. The torque volume was also computed for each. Results are shown in Table III. It is evident that the intermediate net gives sufficient accuracy for engineering purposes, since it is in good agreement with the fine net which is probably accurate to three significant figures.

From the results on these two shapes, we may construct a table giving the properties of shafts of this form in which the corner radius r is a variable proportion of the side $2a$:

	$r=a$ (circle)	$r=0.75a$	$r=0.5a$	$r=0$ (square)
k	0.500	0.624	0.663	0.675
k_1	.0982	.1213	.1349	.1406
k_2	.196	.195	.204	.208
k'	.500	.470	.397	.000
k''	.500	.558	.496	.000

These k's are, in the notation of Timoshenko,[7] the factors to be employed in the following

TABLE III. *Slopes and torque volume for* $r=\frac{1}{2}a$.

	CENTER	TANGENT	CORNER	VOLUME
Coarse net	5.25	3.97	3.18	4412
Inter. net	5.28	3.97	3.17	4426
Fine net	5.305	3.972	3.177	4422

[7] Reference 2, p. 248.

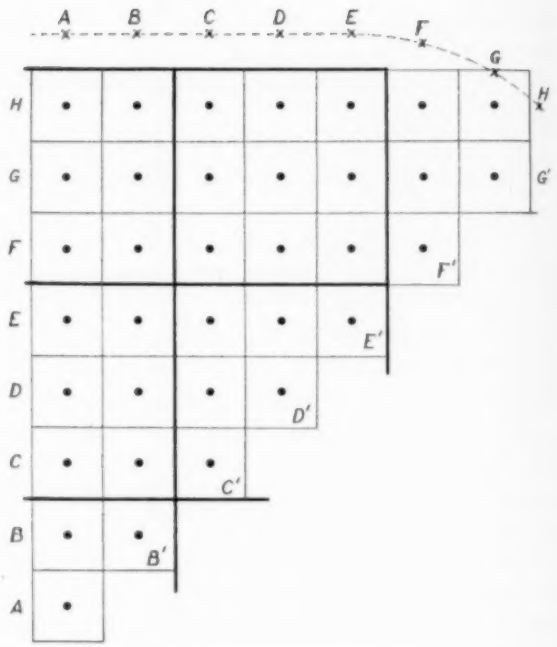

FIG. 9. The intermediate net.

equations for computing stresses and torques:

$$\begin{aligned} \tau_{\max} &= 2kG\theta a, \\ M_t &= k_1 G\theta (2a)^4, \\ \tau_{\max} &= M_t/k_2(2a)^3, \\ \tau_{\text{corner}} &= 2k'G\theta a, \\ \tau_{\tan} &= 2k''G\theta a. \end{aligned} \tag{13}$$

Values for $r=a$ and $r=0$ are available in texts on elasticity.

CONCLUSIONS

We have described a method by which the torsional characteristics of various shapes may be calculated easily and rapidly. The accuracy of the results may be made as great as desired by refinement of the nets. Irregular shapes which have previously been treated by much more troublesome methods introduce no special difficulty.

Other types of problems in torsion may be treated by similar numerical methods. We hope to consider the case of circular shafts of variable cross section at some time in the near future.

Polonium Alloy for Spark Plug Electrodes

J. H. Dillon
Physics Research Division, Firestone Tire and Rubber Company, Akron, Ohio
(Received January 16, 1940)

A method of improving the starting characteristics of spark plugs involving the use of polonium is described. Results of experiments concerned with the measurement of the apparent breakdown voltage under laboratory conditions and the starting characteristics of spark plugs in internal combustion motors at low temperatures are given. These results indicate that the use of polonium in commercially practical concentrations in standard electrode alloys definitely improves the starting performance of spark plugs. Large scale methods of extraction of polonium from residues of a radium refinery and the method of introducing polonium into the electrode alloy are to be discussed in a subsequent article.

Introduction

THE problem of improving the starting characteristics of spark plugs has assumed increasing importance in recent years with the development of higher compression motors and the trend toward more severe conditions of operation. The modern automobile is equipped not only with a starter motor and driving lights but also with any number of other electrical devices such as a heater motor, radio, defroster fan, fog lights, windshield wipers, and cigar lighters, all of which tend to discharge the same type of storage battery which has been used for automotive ignition since the internal combustion motor became practical for motive power. Hence, in spite of improvements in ignition systems, the modern automobile requires spark plugs which will start the motor with as few starter revolutions as possible so that the 100–200 amperes starter drain may take place in a minimum time.

The simplest method of improving spark plug starting qualities, that is, reducing the breakdown voltage, is to vary the geometry of the electrodes. The improvement thus obtainable is limited, unfortunately, for the rate of electrode wear is strongly dependent upon their size and shape. A sharply pointed electrode, for example, will rapidly burn to a blunt contour and an abnormally wide gap will soon result, if the electrodes are formed of the usual noncorrosive nickel-manganese alloy. Furthermore, pre-ignition difficulties develop with pointed electrodes even when made of metals of high heat conductivity.

A second method consists in introducing a small amount of a material into the electrode wire which lowers the thermionic work function of the electrode alloy. Some results have been published by Duffendack, Wolfe and Randolph[1] which show that the use of small amounts of barium in the electrode alloy reduces the thermionic work function and definitely lowers the apparent breakdown voltage,[2] particularly for old plugs which have had many miles of service. These results were explained by Loeb[3] on the basis of increased electron emission from the cathode under positive ion bombardment.

One other general method of improving the starting characteristics of a spark plug is accomplished by ionization of the gap. The effect of irradiating a spark gap with ultraviolet light is well known, the ionization resulting in a marked reduction in apparent breakdown voltage and also in a decrease in the scattering of the observations. The most practical method of introducing ions into the gap appears to be by the use of a radioactive material which emits alpha-

[1] O. S. Duffendack, R. A. Wolfe and D. W. Randolph, Preprint of paper, "The Development of an Electron Emitting Alloy," presented before The Electrochemical Society, April, 1931.

[2] Note: The "apparent breakdown voltage" is the minimum voltage at which a spark occurs under the actual conditions of spark plug operation or testing. It is a function of electrode geometry, the nature and pressure of the gas, the material of the electrodes, and the state of ionization of the gap. It should not be confused with the "true breakdown voltage" which is measured with a slowly varied d.c. voltage and irradiated gap. The latter is practically independent of the material of the electrodes at pressures above atmospheric.

[3] L. R. Loeb, Phys. Rev. **38**, 1891 (1931).

particles. Several patents[4] have been issued which cover the use of radium incorporated in a spark plug. The high cost of radium and the danger involved in handling it in a production unit probably explain why it has not come into general use in spark plugs.

When the list of naturally radioactive elements is examined, the only alpha-particle emitters, aside from radium, which can be considered as commercially available are uranium and thorium. Their activities are so low, however, that they offer little promise in spark plugs. Most of the other alpha-particle emitters are of extremely short life. Radiothorium and possibly ionium appear to have some possibilities but both are practically inseparable from thorium. Polonium appears to offer the best properties for use in spark plugs since it is over a thousand times more active than radium in equilibrium with its short life products and has a reasonably long half-life of about 136 days. Although polonium is used extensively in pure research, until recently it could hardly be considered as commercially available in large amounts. Nevertheless, it was selected for study by this laboratory and, when it was found to give the required effect in spark plugs, a commercial source was developed.

This paper will deal mainly with the effects of polonium in spark plugs. The large scale extraction of polonium from lead residues of a radium refinery, and the incorporation of polonium in spark plug electrodes will be discussed in a later article.

Types of Polonium Spark Plugs Tested

The first method of introducing polonium into spark plugs used in this work consisted in attaching a small length of polonium-plated electrode wire on the skirt of the plug in such a manner that some of the alpha-particles passed through the gap. These plugs were referred to as the polonium "teaser" type. It was found that the polonium coating on the teasers was stable at the extreme temperatures of spark plug operation and definite improvements in starting characteristics were observed with newly made plugs. However, in many cases a hard carbon coating formed in service on the polonium-plated "teaser" which reduced the range of the alpha-particles greatly. Hence, this type of plug was discarded.

A number of plugs were made with polonium plated directly on the electrode wires. In this type of plug, of course, the polonium was used very efficiently and large improvement in the starting characteristics was observed. The impracticability of this plug, however, was obvious since the polonium was lost very quickly as the electrodes wore away in service.

In the type of plug finally adopted as most practical, the electrode wires were made of an alloy of ordinary electrode metal and polonium. The method of producing this alloy will be described in a subsequent paper. Naturally, it was considered somewhat wasteful of polonium to distribute it throughout both the electrode wires. Nevertheless, when the geometries of the polonium alloy ground electrode type plug and the teaser type were compared, it was found that a much larger solid angle was subtended by the gap cross section at the emitting surface in the case of the polonium alloy ground electrode. In fact, the total amount of polonium required to produce a given number of ions in the gap was about the same in the two cases. In the case where polonium was dispersed in both the center and ground electrodes, a large fraction of the polonium is wasted but, at the present time, it is found that the cost of this additional polonium is more than offset by the relatively low cost of fabrication of the polonium alloy electrode type plug. The use of welded high concentration polonium alloy tips, which appears to offer great possibilities from the quality standpoint, is under consideration but entails the development of new production fabrication processes.

Selection of Experimental Conditions

Measurements of the apparent breakdown voltage (V_a),[2] of spark plugs are complicated by the extreme variability of that quantity, even with carefully controlled testing conditions. V_a has been found to vary in a single plug by as much as 100 percent within a period of a few minutes with no observable change in the external conditions. Thus, many measurements must be made with a large number of plugs in

[4] A. M. Hubbard, U. S. Patent 1,732,422 (1929); G. P. Capart, U. S. Patent 1,996,854 (1934); C. Michel, U. S. Patent 2,022,140 (1935).

order to arrive at a significant result. Another complicating factor is the sensitivity of V_a to the pre-treatment of the electrodes.

One example of this phenomenon was obtained with a single peak of the 60-cycle voltage of a transformer, impressed across a 0.5-mm gap 72 times/min. in air at atmospheric pressure. The gap was formed between the cylindrical and flat end surfaces, respectively, of two lengths of 1.8 mm diameter spark plug wire.[5] The electrodes were first cleaned with a fine abrasive paper. The initial value of V_a was 2000 r.m.s. volts. After sparking at 4000 r.m.s. volts for 2.3 hours at the rate of 72 peaks/min., V_a was found to have increased to 2800 r.m.s. volts. The electrodes were then polished again, and V_a was found to be 2100 r.m.s. volts. No change in appearance of the electrode surfaces was visible after the sparking treatment.

The type of variation of V_a with pre-treatment was very different for another set of conditions where spark plugs were mounted with 0.76-mm gaps in an air bomb at a pressure of 4.75 atmospheres. Tests were made with the voltage from an automobile ignition system impressed across pairs of plugs in parallel at the rate of 150 peaks/min. There were 8 tapped holes in the bomb so that 1 set of four plugs could be compared against another set. One set was given various extended sparking treatments while the control set was sparked only enough to make comparisons. Pairs of plugs of the 2 sets were connected successively in parallel in all the 16 possible combinations and the number of sparks passing in each during a 10-minute interval counted. The average ratio of counted sparks for the "treated set" to that for the control set was taken as the "relative sparking efficiency." This method was used in many of the evaluations because it proved more reliable than measurements of V_a made with a cathode-ray oscilloscope. It will be referred to as the "parallel efficiency test." Electrodes were smoothed and polished to remove burrs and then oxidized by heating to a bright red with a welding torch. This type of electrode treatment was the best discovered for obtaining uniform results from supposedly identical plugs.

[5] Composition: 95 percent Ni, 4 percent Mn, 1 percent other metals.

The results of one set of measurements are given in Table I. It is quite apparent from the results that, for these conditions of testing, relatively stable conditions can be obtained by sparking all plugs for a short period and then allowing them to rest. When the conditions of testing were varied, other types of pre-treatment were found necessary.

TABLE I. *Variation of relative sparking efficiency with pre-treatment. Voltage supplied by automobile ignition system; 150 voltage peaks/min. used in testing; pressure—4.75 atmospheres; gaps—0.76 mm.*

Period of Pre-treatment	Type of Additional Pre-treatment of "Treated" Plugs	Relative Sparking Efficiency
0	None*	1.00
5 min.	Sparking at 900 peaks/min.	1.40
55 min.	Resting	0.60
10 min.	Sparking at 900 peaks/min.	1.50
64 hr.	Resting	0.45
5 min.	Sparking at 900 peaks/min.	0.70
5 min.	Sparking at 900 peaks/min.	1.05
55 min.	Resting	0.45

* Electrodes of all plugs were polished and oxidized with torch before run was started.

For the sake of brevity, only the above two examples will be discussed here. A detailed theoretical explanation of these effects is hardly within the scope of this paper. Suffice it to say that the observed variations of V_a with pre-treatment appear to be involved with the formation of surface films of different work functions. Thus, in the case of the 60-cycle experiments at atmospheric pressure, it might be assumed that some sort of stable layer with a higher work function than that of the original electrode surface was formed by the spark. In the case of the experiments at elevated pressure, however, it would be necessary to postulate an activation of the electrode surfaces caused by the heavier high pressure spark. This activation might then disappear and leave the higher work function layer present to give a higher value of V_a after resting, in accord with the results of Table I. Whatever, the explanation of these phenomena may be, it appears that a further careful study along these lines should yield valuable information concerning the mechanism of the spark.

The following methods of evaluating polonium in spark plugs were used in the course of this work:

I. Isolated voltage peaks from a 60-cycle transformer impressed across the gap by means of an interrupter; V_a measured with an electrostatic voltmeter.

II. Plugs operated in a "Coöperative Fuel Research" single-cylinder motor under controlled speed, cylinder temperature, and power output; voltage across plug lowered until misfires occurred.

III. Plugs mounted in air bomb; voltage from an automobile ignition system impressed across individual gaps; V_a measured with a cathode-ray oscillograph.

IV. "Parallel Efficiency" method already described; "Relative sparking efficiency" (E) measured.

V. Plugs mounted in automobile motors; primary coil voltage necessary to start motor measured.

VI. Plugs mounted in automobile motors; number of crankshaft revolutions before starting measured.

Results

All these methods of test gave results indicating that plugs containing commercially practical amounts of polonium were definitely superior in starting characteristics to identical control plugs containing no polonium. Results obtained by Method I were found to give an extremely exaggerated picture of the action of alpha-particle bombardment of a spark gap. They will be discussed only in the light of academic interest. Methods IV and VI were found to give more significant and accurate results than the others and were used much more extensively. Hence, the results obtained by Methods IV and VI will be described in detail.

One set of experiments was made with the object of measuring the reduction in V_a caused by alpha-particle bombardment of spark gaps with an accurately controlled voltage peak. A convenient method for this purpose consisted in impressing across the gap individual peaks of the 60-cycle voltage furnished by a small transformer at a rate of 72 peaks per minute by means of a rotating interrupter. The interrupter consisted of a Bakelite disk with a 5-mm brass contact on its 90-cm circumference. This contact was connected to one of the electrodes by means of a brass ring and stationary carbon brush. A sharp brass wedge rubbed against the disk circumference in a bath of transformer oil. The wedge was connected to the high voltage terminal of a small transformer the other terminal of which was connected to ground and the other spark electrode. The disk was connected through a gear reducer to a synchronous motor so that it rotated at 72 r.p.m. The voltage of the transformer was measured with an electrostatic voltmeter. The apparatus was adjusted to give a symmetrical voltage peak by means of an oscilloscope.

The spark gap was mounted on a special micrometer device which permitted accurate gap setting. The gap could be enclosed in a small Bakelite pressure chamber with a fused quartz window. Various gap geometries were used such as cylinder-plane, plane-plane, cylinder-cylinder, point-cylinder, etc. The polonium was plated on a piece of 1.8 mm diameter nickel wire. This "polonium teaser" was mounted with its cylindrical surface at various distances from the gap axis. A geometrically identical "control teaser" without a polonium plating was used in the same position as that of the "polonium teaser" for comparison purposes.

The experiments consisted in counting the number of sparks passed per minute at various transformer voltages. The polonium teaser employed was plated with about 0.001 microgram of polonium distributed over 1 cm of its length. A typical set of curves for different gap settings (parallel cylinders) is given in Fig. 1. The surprisingly large effect of the polonium teaser as compared with the control teaser resulted from the selection of atmospheric pressure as a condition of test. The curves of Fig. 2 illustrate the decrease in the effect with increasing pressure. Unfortunately, the equipment was not suitable for pressures higher than 4 atmospheres. It is clear from comparison of the voltages necessary to give 50 sparks/min. (selected arbitrarily) that the effect of alpha-particle bombardment tends to decrease with decreasing gap for very small gaps.

The foregoing results are mainly of academic interest since spark plugs must fire at pressures of 7 atmospheres and higher and the voltage peak furnished by an automobile ignition system is much sharper than the 60-cycle peak used in these experiments. However, the sharpness of the

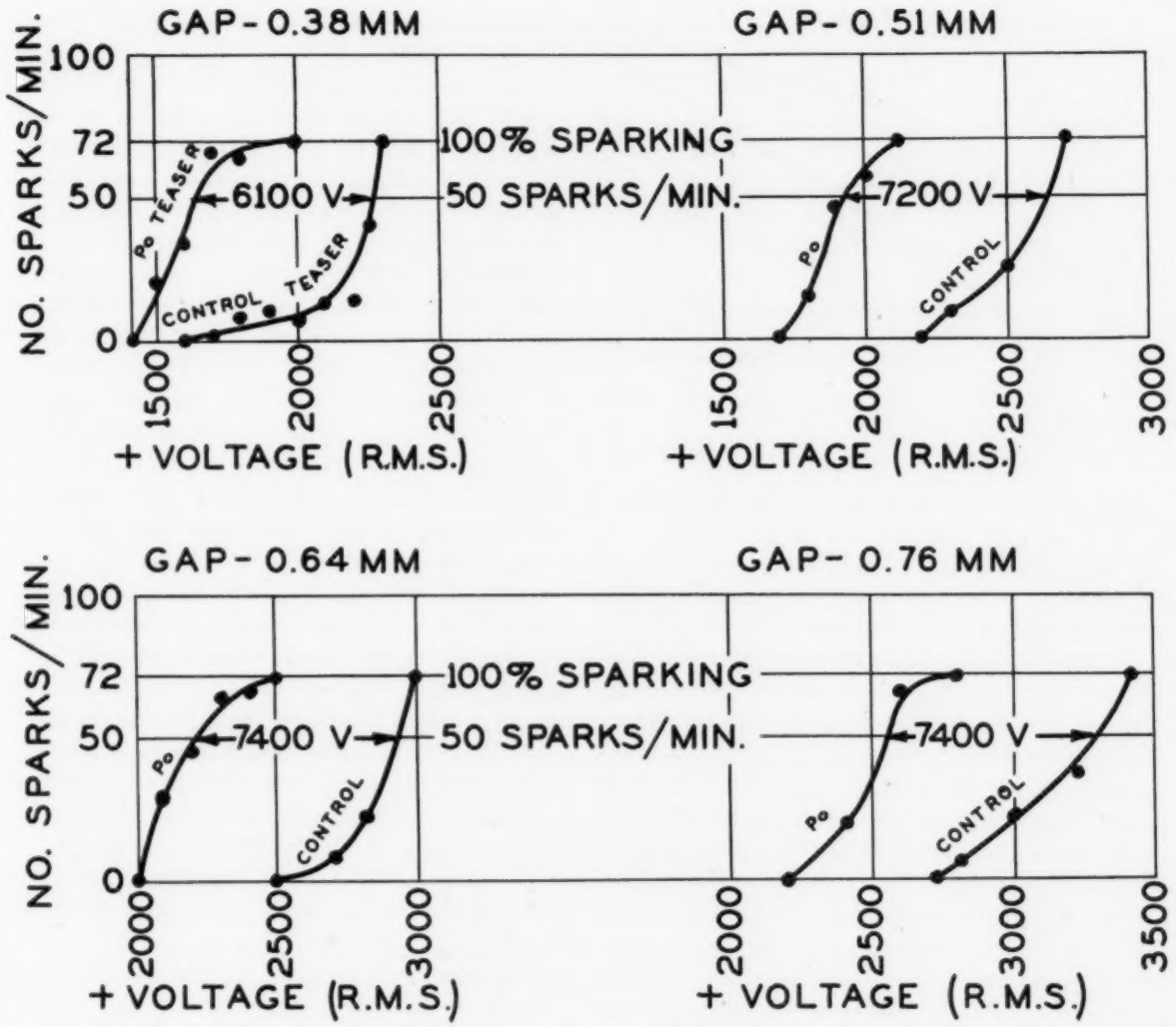

FIG. 1. Effect of polonium for various gaps. Parallel cylinders gap—1.8 mm diameter wire teasers 2.5 mm from gap axis.

ignition coil peak tends to introduce a condition where an ionizing agent can be applied with profit although the higher pressure in the cylinder tends to reduce the effect of that ionizing agent. Hence, the results of these experiments appeared to justify further work with polonium in spark plugs under actual firing conditions.

The results of one set of "parallel efficiency" tests are given in Table II. In accordance with conclusions reached from the results of Table I, all 8 plugs in the bomb (4 experimental and 4 control plugs) were pre-sparked for 2 minutes at 900 sparks/min. and then allowed to rest 30 minutes before each of the 16 comparisons constituting a single test. Most of the tests I–X were the averages of several such 16-comparison determinations. All plugs used in the tests were of a common passenger type (14 mm size) and had ground wires of 1.8 mm diameter. The ground wires of the plugs of groups 3 and 4 were shortened 1.5-mm and then 1.6-mm polonium alloy wire tips were spot-welded to them. The "swells" at the welds were carefully filed and polished down so that no traces of the welds were visible. Every effort was made to have the ground wires of the polonium alloy plugs geometrically identical with those of the controls. The gaps were set to 0.76 mm as accurately as possible. The secondary coil voltage was maintained constant by means of a potentiometer in

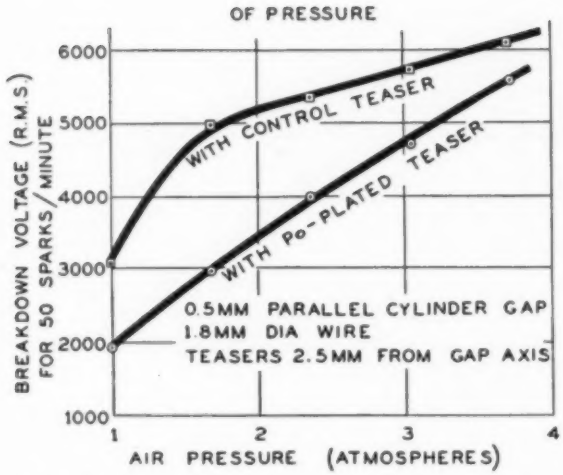

FIG. 2. Effect of polonium as a function of pressure.

the primary battery circuit and a cathode-ray oscilloscope connected across the secondary by means of a high resistance voltage divider.

The values of the "relative sparking efficiency" (E) of experimental plugs *versus* controls are given in the last column of the table. The values of E determined in Tests I–IV show a definite superiority on the part of the polonium alloy electrodes. It should also be noted that increases in the total polonium for a given type of ground wire resulted in negligible increases in E. Concentration of all the polonium in the immediate vicinity of the gap, however, resulted in a definite increase in E.

All the plugs of Test IV were subjected to severe service obtained by running with the electrodes just below the pre-ignition temperature in an outboard motor for 2.5 hours at 4500 r.p.m. Plugs were run 1.25 hours in each of the 2 cylinders in order to obtain uniform treatment. The results of Tests V and VI, after this service, show a marked increase in E. A fairly reasonable explanation of this effect appears to be that a diffusion of polonium toward the electrode surfaces, caused by the high electrode temperatures, took place thus increasing the effective alpha-particle ionization in the gap. The argument might be advanced that certain impurities which tend to lower the work function might have been evaporated in the high temperature service. Thus, it might be argued that the normal (no polonium present) value of V_a was increased so that alpha-particle ionization would have a greater effect. The results of test X, however, where a set of plugs (N) with electrodes which had received no thermal treatment whatsoever were found to be very inferior with respect to the controls (A), which had been flamed and run in the motor, refute this latter explanation.

The effect of the sharp burrs and machined ends on the electrodes of new plugs is clearly

TABLE II. *"Parallel efficiency" tests. Gaps—0.76 mm; voltage—automobile ignition system.*

	Experimental Plugs					Control Plugs				
Test No.	Group No.	Total Po ($\mu\mu$g)	Location of Po Alloy	Initial Electrode Treatment	Subsequent Service	Group No.	Initial Electrode Treatment	Subsequent Service	Air Press. (Atmos.)	E
I	1	130	Entire side wire	Polished and flamed	None	A	Polished and flamed	None	4.75	1.4
II	2	50	" "	" "	"	A	" "	"	"	1.6
III	3	32	1.6-mm tips welded on ends of side wires	" "	"	A	" "	"	"	2.6
IV	4	12	" "	" "	"	"	" "	"	"	2.6
V	4	12	" "	" "	2.5 hr. in outboard motor*	"	" "	2.5 hr. in outboard motor*	"	5.2
VI	4	12	" "	" "	" "	"	" "	"	5.75	5.7
VII	4	12	" "	" "	" "	B	None (burrs on electrodes)	None	4.75	1.0
VIII	4	12	" "	" "	" "	B	" "	"	1.0	∞
IX	B	0	None	None (burrs on electrodes)	None	A	Polished and flamed	2.5 hr. in outboard motor	4.75	2.7
X	N	0	"	Polished only	"	A	" "	"	4.75	0.02

* The outboard motor used was of a common 2-cylinder racing type and was operated at 4500 r.p.m. in a fixed position with propeller under water in a tank.

TABLE III. *Cold starting measurements. 0.65-mm gaps; standard 18-mm Firestone shells and insulators; temperature −26°C; coil primary voltage 3.75 volts.*

PLUG GROUP	LOCATION OF POLONIUM	TOTAL POLONIUM PER PLUG (μμg)	POLONIUM AGE BASED ON STANDARD NEW PLUGS (MOS.)	SERVICE OF PLUGS	SUBSEQUENT ELECTRODE TREATMENT	RATIO OF MOTOR REVOLUTIONS BEFORE STARTING, PO PLUGS *vs.* CONTROLS
A.	Entire side wire	18.5	3.2	None	Polished	1.5
B.	1.6-mm welded tips on side wires	10.1	8.5	8000 miles of fast service in Ford V-8 Motor	None	3.2
B.	" "	"	"	" "	Sand blasted	1.3
C.	1.6-mm welded tips on side wires	3.7	16	8000 miles of fast service in Ford V-8 Motor	None	2.0
C.	" "	"	"	" "	Sand blasted	1.3

shown in Tests VII and IX. The fact that the polonium alloy electrodes were found very superior to the new unpolished electrodes when tested at atmospheric pressure (Test VIII) is consistent with the data of Fig. 2.

The tests described thus far were directed at measuring V_a or some related quantity. The following experiments were concerned with the starting behavior of spark plugs in motors. Three Studebaker motors were set up on blocks in a refrigerated room which was maintained at −26°C within 1°C. The motors may be briefly described as follows:

Motor No. 1—1936, 6 cylinders, aluminum pistons;
Motor No. 2—1936, 8 cylinders, aluminum pistons;
Motor No. 3—1937, "Truck," 6 cylinders, cast iron pistons.

The exhausts were attached to a suction line which reduced the pressure by 20 cm of water. Drains were attached to the manifolds. Separate batteries were used for the ignition and starter motors. Thus, the ignition primary voltage could be controlled with a potentiometer. The batteries used for the starter motors were changed as frequently as was necessary to keep the cranking speed constant to within 5 percent. All freshly charged batteries were slowly cooled to the temperature of the room before use. Throttles were set at "high idle setting" and the timing was set as specified for normal service. "Regular" gasoline and 10 W. oil were used. Oil dilution was checked at regular intervals. A cathode-ray oscilloscope with a linear sweep circuit was connected across the secondary of the ignition coil through a high resistance voltage divider. Examination of the cathode-ray pattern permitted knowledge of whether or not the plugs were firing. By counting the number of deflections of the cathode-ray trace, the speed of rotation of the crankshaft could be computed.

A single measurement was accomplished as follows: The primary coil voltage was first set at a value well below the "firing value." The number of oscilloscope deflections occurring in 15 seconds was then counted and the cranking speed calculated. The primary voltage was next raised to a value (3.75 v) well above the firing value. The motor was then turned over at full choke and high idle throttle setting and the number of oscilloscope deflections before the motor fired was counted and recorded as the "starting index." In no case was a motor allowed to run more than 5 seconds after starting. Two or three consecutive repeat tests were made in this manner. The experimental plugs were then removed and replaced with the appropriate control plugs. The motor was then allowed to cool for 45 minutes before the next test was made.

During this 45-minute period, similar runs were made on the other 2 motors and results calculated. The ratio of the starting index of a set of polonium alloy plugs to that of the appropriate control plugs, averaged over several runs on each of the 3 motors, was taken to represent the improvement in starting produced by the polonium alpha-particle bombardment.

Typical data obtained in these experiments are

given in Table III. In all cases, the control plugs were subjected to exactly the same treatment as the polonium alloy plugs. Only the average figure for each set of plugs is given for the sake of brevity. It should be remarked that very few reversals (values of the starting ratio less than unity) were observed and, almost invariably, it was found that these reversals could be explained by variation in cranking speed, motor flooding, etc. The average ratio for all polonium alloy plugs *versus* controls (8 sets of plugs) was 1.66.

It is interesting to note in the results of Table III that the plugs of Groups *B* and *C*, after running for 8000 miles in a Ford V-8 test car, yielded larger values of the starting ratio than the new plugs of Group *A*, even though the latter contained more polonium. This fact is consistent with the results of Table II but may result from the more effective location of the polonium near the gap in Groups *B* and *C*. The reduction of the starting ratio after sand blasting is very definite, however, indicating diffusion of polonium to the electrode surfaces under the high temperature service conditions or possibly the formation of a porous layer of oxide of lower stopping power than that of the electrode metal itself.

The figure given in the 4th column of Table III represents the effective age of the polonium in the plugs based on an initial figure of 54 $\mu\mu$g polonium per ground wire. This figure was selected as the initial amount of polonium in a new plug on mainly economic grounds. It is clear from the results with the plugs of Group *C* that this initial amount is satisfactory to show a definite improvement in starting characteristics 16 months after manufacture. Since the time of these experiments, it was decided to use the same concentration of polonium in both electrodes as formerly used in only the ground wires. Hence, present production plugs of this type should show an advantage in starting for a period considerably longer than 16 months.

The stability of polonium at electrode temperatures has been established by the results of Table III. Early in the course of the development, polonium-plated nickel foils were maintained at an average temperature of 500°C for 24 hours and then at 700°C for 6 hours in a muffle furnace with no measurable evaporation of polonium. Furthermore, not over 10 percent of the polonium is lost in the alloying process which involves temperatures of 1500°C and higher.

Discussion

Because of the extremely complex character of the spark phenomenon, particularly under the conditions of automotive spark plug performance, it is very difficult to predict what effect a given number of alpha-particles projected across the gap will have on the sparking voltage. Suffice it to say that electrodes containing 200 $\mu\mu$g polonium/gram electrode alloy will produce about 40,000 ions/sec. in the gap (correcting for loss of ionizing power of alpha-particles after striking the opposite electrode) when the plug is 1 year old. Estimates of spontaneous ionization in air at atmospheric pressure due to radioactive materials naturally present, cosmic rays, etc. have ranged from 1 to 7 ions/sec./cm^3. Since the volume of a typical gap is about 0.002 cm^3, this would amount to a maximum of only 0.014 ion/sec. produced naturally in the gap. Thus it would seem safe to guess that an increase from 0.014 to 40,000 ions/sec. produced in the gap at the beginning of the compression stroke should materially aid in the process of ionization by collision and positive ion bombardment of the cathode which precede spark breakdown.

It is of interest to note that about 3 grams of thorium, occupying 0.25 cm^3, or 0.5 gram uranium, occupying 0.27 cm^3 are equivalent in alpha-particle emission to the 40 $\mu\mu$g of polonium present initially in the ground wire of a 14-mm plug. The volume of the ground wire is about 0.021 cm^3.

In conclusion, it should be remarked that the alpha-particles may produce a small chemical effect in the fuel mixture within a small volume enclosing the gap. Based on known chemical effects of alpha-particles on hydrocarbons, it seems possible that minute amounts of less-saturated hydrocarbons might be produced within this small volume, defined by the range of the alpha-particles at full compression. The existence of this slightly more combustive mixture in the immediate vicinity of the gap might conceivably constitute part of the observed improvement in starting characteristics as well as the reduction in V_a. Until this possibility is

established by experiment, however, it seems safe to conclude that the major part of the effect results from reduction in V_a.

ACKNOWLEDGMENT

The author wishes to express his appreciation to Mr. J. E. D. McCarty, spark plug engineer, for his excellent cooperation in this development. Sincere thanks are due Dr. J. N. Street, whose active interest and many helpful suggestions made completion of the work possible. The author also wishes to thank Mr. F. S. Grover for his able assistance in construction of apparatus and making the many tedious experiments.

Wave Propagation in Shearing Quartz Oscillators of High Frequency

EDWARD W. SANDERS*
Federal Communications Commission, Engineering Department, Fort McHenry, Baltimore, Maryland
(Received December 18, 1939)

Experimental verification of a theory of edge grinding is given by demonstrating the presence of elastic waves along the X axis of a low frequency-temperature coefficient quartz plate.

THE researcher in piezoelectric materials, and particularly in natural quartz crystal, recognizes two fundamental types of oscillation; *viz.*, longitudinal and shearing. The first type is characteristic of the X-cut crystal, in which the thickness or critical dimension lies along the piezoelectric (X) axis. The second, or shearing mode of oscillation, is peculiar to the Y-cut crystal plate and of almost all other oscillating plates having very low frequency-temperature coefficients. It is also characteristic of the harmonic oscillator plate. The Y-cut crystal has its critical dimension along the Y axis; the various low coefficient cuts (AT, V, and R) are in essence Y cuts so orientated as to have the critical dimension along an axis displaced from the Z, or optical axis. Data on the most favorable orientations have been given in the literature.[1]

The frequency of oscillation of a shearing type of oscillating plate may be expressed by the following relation:

$$f=\frac{1}{2}\left(\frac{m^2}{a^2}+\frac{n^2}{b^2}\right)^{\frac{1}{2}}\left(\frac{c_{ii}}{\varphi}\right)^{\frac{1}{2}}, \qquad (1)$$

where f = the frequency of oscillation in cycles per second
a,b = the dimensions of the shearing plane in centimeters
m,n = any positive integers
c_{ii} = the elastic modulus in the shearing plane in dynes/cm²
φ = the density of quartz = 2.65 grams/cm³.

An examination of Eq. (1) shows that the frequency of oscillation is dependent upon the magnitude of both a and b. This may be experimentally demonstrated by shortening the b dimension of a typical shearing oscillator. In every case the frequency of oscillation is increased. In a shearing oscillator b will be parallel to the X axis and a parallel to the Y' axis. The third dimension will be displaced from the optical axis for the low frequency-temperature coefficient plates.

If the oscillation frequency lies between 2500 and 4000 kc. the a dimension may be only 2.5 percent as large as the b dimension. As the frequency is increased the ratio of a to b becomes progressively smaller. For a plate of very high frequency, then, we may assume the term n^2/b^2 of Eq. (1) to be negligible when compared to m^2/a^2. If we consider b to increase without limit then,

$$f=\frac{1}{2a}\left(\frac{c_{ii}}{\varphi}\right)^{\frac{1}{2}}. \qquad (2)$$

* Radio Inspector, Field Division, Engineering Department, Federal Communications Commission, Fort McHenry, Baltimore, Maryland. Paper approved for publication by Chief of the Field Section, F.C.C., Washington, D. C.

[1] F. R. Lack, G. W. Willard, and I. E. Fair, "Some Improvements in Quartz Crystal Circuit Elements," Bell Sys. Tech. J. **13**, 453 (1934). Issac Koga, "Notes on Piezoelectric Quartz Crystals," Proc. I.R.E. **24**, 510 (1936).

From Eq. (2) it is possible to derive an empirical formula useful to the practical crystal grinder. This same Eq. (2) also gives the oscillation frequency of an X-cut plate when the longitudinal modulus c_{11} is substituted therein. It should be noted here, however, that the equation as applied to the X-cut plate may be differently derived. It is not necessary to assume b as being an infinite plane. The equation shows that the oscillation frequency of an X-cut plate depends only on the magnitude of the a dimension. This also is easily verified by simple experimentation. Shortening the b dimension in no way affects the frequency except in coupling regions. If b is greatly reduced there may be a slight change in frequency as a result of reduced dielectric length between the crystal electrodes.

When a shearing plate is oscillating at high frequency we may assume a wave to be propagated across the plate in the direction of the b (or X) axis. If the b dimension is equal to an odd integral number of half-waves the plate will be quite active. If an odd integral number of half-waves are not present, however, the activity of the plate will be very low or possibly zero. In this latter case it will be necessary to shorten the b dimension until an odd whole number of half-waves is propagated across the plate. The crystal grinder calls this shortening process "edge-grinding." During some studies in crystal fractures the writer was fortunate enough to obtain positive evidence of the existence of wave propagation along the b dimension.[2]

Let us assume a wave to be propagated through the crystal along b and further assume b to be equal in length to an odd integral number of half-waves. The propagated wave will, of course, be reflected on reaching the opposite edge of the plate. The combination of propagated wave and reflected wave sets up a standing wave pattern on the crystal surfaces. Under these conditions there will be loops and nodes of voltage at various points on the surface of the oscillating plate. The crystals used in the experimental work[2] were mounted between plates which provided an air-gap of approximately 0.002 inch between the crystal and the electrode surfaces. If the crystal plate be highly excited by slowly increasing the vacuum tube anode potential a radiofrequency voltage will finally be attained across the crystal of sufficient magnitude to break down the air gap between crystal and electrodes. The breakdown points are highly localized because of the standing waves on the crystal and if a suitable electrode material is used it may be caused to oxidize at the points of breakdown. When these electrodes are examined they reveal a series of straight lines parallel to each other and to the Z axis. They are, of course, perpendicular to the X axis. No optical instruments are necessary to view these lines. They may be made quite heavy by allowing the plate to "burn" for five minutes or longer. As was pointed out in the previously-mentioned paper[2] there is no danger of fracturing the oscillating plate so long as the anode voltage to the vacuum tube is raised slowly. Any sudden change in circuit parameters, however, is most certain to fracture the quartz plate.

The distance between these lines in ten specimens was measured[3] and found to be approximately equal to the a dimension. It is believed that positive evidence of wave propagation in high frequency shearing oscillators has been given and that the theory of edge-grinding has been conclusively substantiated.

[2] Edward W. Sanders, "Modes of Fracture in Piezo-Electric Crystals," QST **21**, 17 (1937).

[3] Optical Laboratory, Frankford Arsenal, War Department, Philadelphia, Pennsylvania.

EASTMAN SPECTRUM ANALYSIS PLATES

IN MANY metallurgical operations *Eastman Spectrum Analysis Plates* have been found useful because of their suitability for extremely rapid processing. This property, coupled with their low background density and high contrast, makes these plates particularly valuable for routine spectrographic analysis of metals.

Data sheets giving the sensitometric characteristics and other properties of *Eastman Spectrum Analysis Plates* will be forwarded promptly upon request.

EASTMAN KODAK COMPANY
Research Laboratories **ROCHESTER, N. Y.**

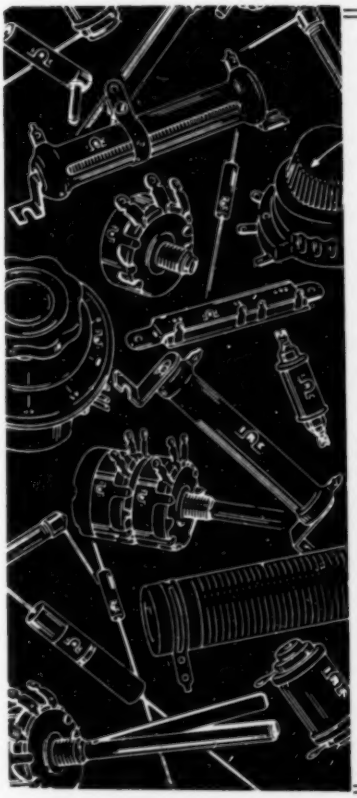

RESISTANCE ENGINEERING DATA BULLETINS

These IRC Resistance Engineering Data Bulletins contain the results of many years of specialized experience in the production of more resistance types for more applications than any other manufacturer in the world. They have been classified and prepared to bring exact needed engineering information to assure selection of the *right* resistor for *any* job. Please ask for them by number.

1. Metallized and Wire Wound Volume Controls and Potentiometers up to 2 watts and 20 meg. resistance.

2. Metallized Type Resistors: Insulated 1/2, 1 and 2 watts; high frequency; high range; high frequency power resistors; high voltage power resistors.

3. Insulated Wire Wound Resistors: Type BW from 1/2 to 1 and 2 watts; Type MW 5 to 20 watts.

4. Power and Precision Wire Wound Resistors: Power types from 10 to 200 watts, fixed and adjustable types, in wide variety o shapes, mountings, etc. Inductive and non-inductive. 14 Precision types to as close as 1/10 of 1% accuracy.

5. Attenuators: Unique new IRC molded motor commutator type 20-step attenuator; also, conventional type 30-step units. Ladder, Potentiometer or Bridge T.

6. Power Rheostats: Quick heat-dissipating all-metal (aluminum) 25 and 50 watt types.

IRC

INTERNATIONAL RESISTANCE CO.
419 N. BROAD ST., PHILADELPHIA, PA.

New books

Mechanics of Liquids

By RALPH W. POWELL

All the essential concepts of hydraulics and fluid mechanics are explained here clearly and concisely. All notable recent advances in the field, such as those made by Reynolds, Prandtl, von Karman, Nikuradse and Cross, are adequately covered. Designed for the one-semester course, the book gives an excellent groundwork in the fundamental theory and applications needed by the hydraulic engineer. $3.50.

Household Physics Laboratory Manual

By MADALYN AVERY

This set of laboratory exercises emphasizes those principles and applications of elementary physics most useful to the home economist. They are eminently practical and teachably presented. Ready in April. $1.75 (prob.).

The Photismi de Lumine *of Maurolycus*

Translated with Introduction
By HENRY CREW

This translation makes available for the first time in English one of the most interesting historical works on optics. $3.00.

Macmillan New York

EPPLEY THERMOPILES *for* RADIANT ENERGY MEASUREMENTS

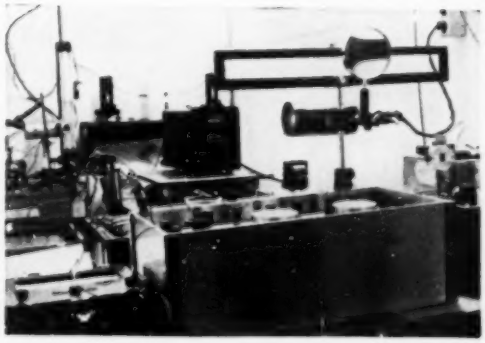

A view of some of the apparatus used for calibrating thermopiles at the Eppley Laboratory, Inc.

Adequate manufacturing, testing and calibrating equipment in the hands of our skilled and experienced technicians insures satisfaction to the users of Eppley Thermopiles.

We are prepared to furnish thermopiles of either bismuth-silver or copper-constantan, mounted in vacuum or air type cases. We also furnish thermopiles and mountings especially designed to meet individual needs. A card will bring you our Bulletin R–3 which contains illustrations, sample curves, complete descriptive matter, prices, references, etc., with regard to Eppley Thermopiles.

EPLAB

THE EPPLEY LABORATORY, INC.
SCIENTIFIC INSTRUMENTS
NEWPORT, R.I.
U.S.A.

TWO IMPORTANT NEW BOOKS

PRINCIPLES OF TELEVISION ENGINEERING

By DONALD G. FINK, Managing Editor, *Electronics*. 528 pages, 6 x 9. $5.00

The author of this book presents a thorough, comprehensive treatment of modern cathode-ray television. Covering the television system from camera in the studio to viewing screen at the receiver, the book not only discusses fundamental processes of television reception and transmission, but also supplies design data and descriptions of modern equipment. The appendix contains transmission standards, recommended practices, and definitions and names of controls.

TELEVISION BROADCASTING. Production, Economics, Technique

By Major LENOX R. LOHR, President, National Broadcasting Company. 272 pages, 6 x 9. $3.00

This book presents descriptions of operating techniques, of equipment, and discussions of fundamental television program considerations. A feature of the book is the wealth of pictures, diagrams, etc., which greatly clarify the textual matter. An actual working television program script is included.

Send for copies on approval

McGRAW-HILL BOOK COMPANY, INC.

330 West 42nd Street New York, N. Y.

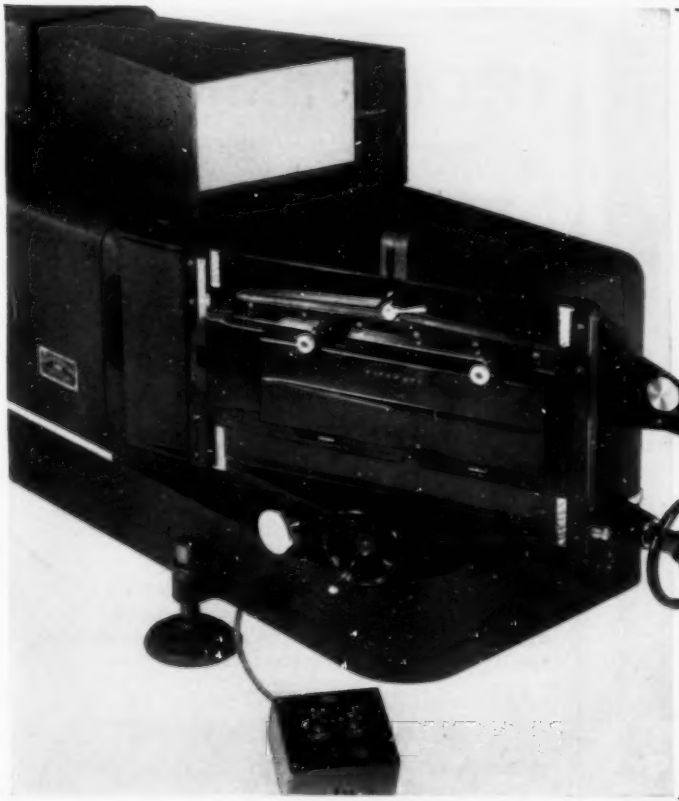

New! TWO LENS QUARTZ

SPECTROGRAPH

Range 1850Å to 12000Å

One Plate covers the region 2100Å-3300Å most used in analytical work.

One Control sets wave range, focuses, and tilts plate holder, *automatically*.

Any Spectrum Line can be brought to center of plate.

Projection of wavelength setting, and of range covered, on large translucent screen. Numbers 1 inch high, always visible.

Littrow Weaknesses Avoided. No stray light. No tilting of lenses necessary. No right angle reflecting prisms. Illuminating bench aligned with slit.

The GAERTNER SCIENTIFIC CORPORATION

1212 Wrightwood Ave. • Chicago • U. S. A.

Linde

RARE GASES
AND MIXTURES

NEON
ARGON
HELIUM
KRYPTON
XENON
MIXTURES

. . . highest purity
. . . for scientific purposes

Linde rare gases are of consistently high purity. They are used in the study of electrical discharges, in rectifying and stroboscopic devices, and in inert atmospheres where heat conduction must be reduced.

Linde rare gases are shipped in spherical glass bulbs, designed to facilitate removal without contamination. Special mixtures for experimental purposes can be supplied upon request.

The Linde Air Products Company
Unit of Union Carbide and Carbon Corporation
30 East 42nd Street UCC New York, N. Y.
Offices in Principal Cities

The word "Linde" is a trade-mark.

FINE WIRES
TAYLOR PROCESS

THE TAYLOR PROCESS is a method for making wires from substances which lack ductility. The elements or alloys, because the drawing is done in glass or quartz, are in a very pure state. Lengths of more than a few feet cannot be obtained. The wires may be had with or without the glass insulation. We make Taylor Process wire of Pt, Rh, Au, Ag, Cu, Fe, Zn, Cd, Pb, Sb, Bi, Sn, Se, Te, Tl, Ga, and In, Constantan, Bi-Sn, Cd-Sb (used where large E.M.F. is desired) and many other alloys. Our wires are packed in containers holding one foot and, with few exceptions, the sizes are from one *mm* to one micron. We manufacture, too, fine wire by the Wollaston Method, by extrusion and by bare drawing.

WE ARE SPECIALISTS IN PLATINUM AND CAN SUPPLY IT IN WHATEVER FORM YOU REQUIRE

BAKER & CO., INC.
113 Astor Street, Newark, New Jersey

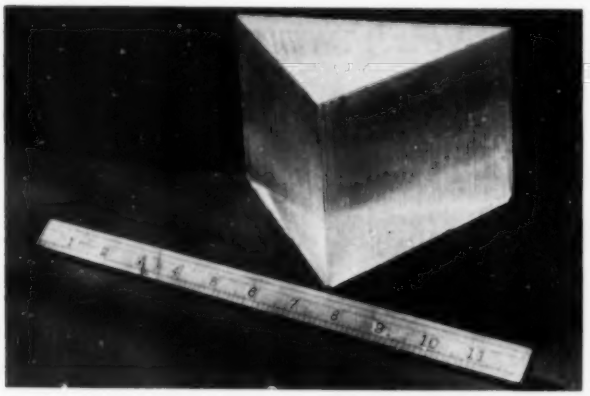

An eight pound rock salt prism blank cut from a twenty-five pound single crystal

SYNTHETIC CRYSTAL OPTICS

For infrared and ultraviolet spectroscopy and for polarizing optics. . . . Single crystals of Lithium Fluoride, Sodium Chloride, Sodium Nitrate, and Potassium Bromide. . . . Write for information.

THE HARSHAW CHEMICAL CO.
SPECIAL PRODUCTS DIVISION CLEVELAND, OHIO

TYPE B POTENTIOMETER

A high-grade, general-purpose laboratory potentiometer with 3 ranges: 1.6, .16 and .016 volts. Extremely accurate and convenient. Used in leading standardizing laboratories.

Described in Bulletin No. 270 which also lists Rubicon portable potentiometers.

Other products: standards of resistance, inductance and capacitance, Wheatstone and Kelvin bridges, resistance boxes, galvanometers, electrometers, permeameters, colorimeters.

RUBICON COMPANY
29 North 6th Street Philadelphia, Penna.

"APIEZON"

OILS, GREASES and WAXES

for high vacuum work have vapor pressures as low as 10^{-6} mm. of Hg, and even unmeasurable at room temperature.

THE Apiezon products which we now carry in our Philadelphia stock, include special oils for oil-diffusion vacuum pumps, and a variety of oils, greases and waxes for sealing joints and stop-cocks in high vacuum systems. Bulletin 1565-R listing physical characteristics and prices will be forwarded upon request.

JAMES G. BIDDLE CO.

ELECTRICAL AND SCIENTIFIC INSTRUMENTS

1211-13 ARCH STREET. PHILADELPHIA, PA.

SEND FOR *this* ***Useful Handbook***

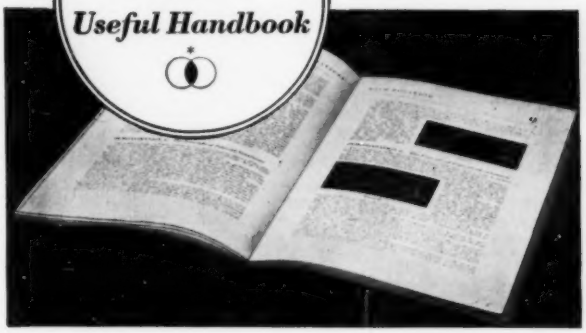

of Important Interesting Experiments with Polarized Light

"Suggestions for the Use of Polaroid* Light Controls" is a 20-page handbook, giving full instructions for performing twenty-one experiments with Polaroid filters in the classroom or laboratory. It includes the brilliant classical experiments of Malus, Arago, Biot and Brewster—together with dramatic demonstrations of the applications of Polaroid light control now occurring in sunglasses, glare-free illumination, 3-dimensional pictures, photography, machine design, et cetera.

Write Division 4 . . . for the Handbook and a Survey of this new field of applied science.

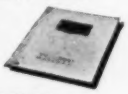

POLAROID CORPORATION

721 Main Street, Cambridge, Mass.

*T. M. REG. U. S. PAT. OFF.

THE SOCIETY OF EXPLORATION GEOPHYSICISTS

Articles Published in *GEOPHYSICS*, Volume IV, Number 3 (July, 1939)

The Relation of Geophysics to Geology — *F. M. Kannenstine*

On the Strategy and Tactics of Exploration for Petroleum, III — *E. E. Rosaire*

A Problem in Seismic Depth Calculation — *Roland F. Beers*

Determination of Density for Reduction of Gravimeter Observations — *L. L. Nettleton*

Terrain Corrections for Gravimeter Stations — *Sigmund Hammer*

Concentrations of Hydrocarbons in the Earth — *Eugene McDermott*

On Geochemical Prospecting — *Leo Horvitz*

The subscription rate is $6.00 yearly in the United States, $6.50 elsewhere. Back numbers are obtainable at $3.00 in the United States, $3.20 elsewhere. The following back numbers are available:

1935—Vol. VI, No. 1, *Journal of the Society of Petroleum Geophysicists* (supply limited)

1936—Vol. I, Nos. 2 and 3, *Geophysics* (No. 1 out of print)

1937—Vol. II, Nos. 1, 2, 3 and 4, *Geophysics*

1938—Vol. III, Nos. 1, 2, 3 and 4, *Geophysics*

Orders should be addressed to

THE SOCIETY OF EXPLORATION GEOPHYSICISTS

P. O. Box 777, Austin, Texas

HYDRON

THERMAL UNITS *to meet highly specialized requirements*

Metallic Bellows

HYDRON Metallic Bellows are used as control elements in temperature-and-pressure-control devices, and for liquid or gas seals of compressors and pumps. We are specialists in the design and production of complete thermostatic and pressure units for temperature and pressure controls. We are, therefore, prepared to extend the fullest co-operation to engineering departments of control manufacturers in the solution of design and engineering problems.

CLIFFORD MANUFACTURING CO.

564 E. FIRST STREET, BOSTON

BOSTON CHICAGO DETROIT LOS ANGELES

PRODUCERS OF BELLOWS EXCLUSIVELY

SERVING AUTOMATIC CONTROL MANUFACTURERS

INDEX TO ADVERTISERS

Name	Page
BAKER & COMPANY, INC. — Platinum crucibles, dishes, triangles, filter cones, anodes, cathodes, electrodes, platinum tipped crucible tongs, fine wires and bismuth foil.	viii
JAMES G. BIDDLE COMPANY — "Jagabi" Rheostats; Adam Hilger and Kipp & Zonen Optical Instruments; "Pointolite" Lamps; Electrical Testing and Speed-measuring Instruments.	ix
CAMBRIDGE UNIVERSITY PRESS	vi
CENTRAL SCIENTIFIC COMPANY — Manufacturers of Cenco Physical Apparatus and Instruments to meet all requirements of University, College and High School Physics Laboratories. Specializing in high vacuum pumps and development of instruments and apparatus for various sciences.	Cover 4
CLIFFORD MFG. COMPANY — Hydron metallic bellows for temperature and pressure control devices. Data for engineers.	ix
EASTMAN KODAK COMPANY — Purified Organic Chemicals for research purposes; Plates for Photography, Photomicrography, Spectroscopy, Photometry, Astronomy; Wratten Light Filters; Cameras and Films.	v
THE EPPLEY LABORATORY, INC. — Standard Cells, thermopiles, pyrheliometers and temperature bridges.	vi
GAERTNER SCIENTIFIC CORPORATION — Spectroscopes, Spectrometers, Spectrographs, Spectrophotometers, Heliostats, Measuring Microscopes, Comparators, Cathetometers, Reading Telescopes, Interferometers, Chronographs, Dividing Machines, etc.	vii
GENERAL RADIO COMPANY — Manufacturers of electronic measuring instruments; vacuum-tube voltmeters, amplifiers and oscillators; wave analyzers, noise meters and analyzers, stroboscopes; laboratory standards of capacitance, inductance and frequency; impedance bridges, decade resistors and condensers; air condensers and variable inductors; rheostats, Variacs, transformers; other laboratory accessories.	Cover 3
HARSHAW CHEMICAL COMPANY — Optical Lithium Fluoride grown in single crystal to predetermined size. Industrial Chemicals.	viii
INTERNATIONAL RESISTANCE COMPANY — Manufacturers of metallized and wirewound fixed and variable Resistors including high voltage and high frequency types.	v
LEEDS & NORTHRUP COMPANY — Manufacturers of Galvanometers, Resistors, Bridges, Condensers, Inductances, Potentiometers, Testing Sets; Temperature Measuring, Recording and Controlling Apparatus; Instruments for Measuring and Controlling Conductivity of Electrolytes and Hydrogen Ion Concentrations.	i
THE LINDE AIR PRODUCTS COMPANY — Oxygen, Argon, Helium, Krypton, Neon, Xenon, Rare Gas Mixtures, Nitrogen, Hydrogen, Calcium Carbide, Acetylene, equipment for Oxy-Acetylene welding and cutting.	viii
MACMILLAN COMPANY	vi
MCGRAW-HILL BOOK COMPANY, INC.	vii
OHMITE MANUFACTURING COMPANY — Manufacturers of close control rheostats, fixed and adjustable power resistors, precision and non-inductive resistors, attenuators, tapswitches and R.F. chokes.	x
POLAROID CORPORATION — Polaroid experimental kit for demonstrating Polarized light. Hand book.	ix
REINHOLD PUBLISHING CORPORATION	ii
RUBICON COMPANY — Galvanometers, electrometers, potentiometers, Wheatstone and Kelvin bridges, resistance boxes, hydrogen ion and conductivity apparatus.	viii
THE SOCIETY OF EXPLORATION GEOPHYSICISTS	ix
WESTINGHOUSE ELECTRIC & MANUFACTURING COMPANY	iii
JOHN WILEY & SONS, INC.	iv

INDEX—*Continued*

Situations Open

PHYSICIST wanted familiar with the technique of nuclear physics for research work. Will be connected with the petroleum industry in the southwest. Must have training equivalent to a Doctor's degree in Physics. Address Box E3-11. Rm. 1502, 175 Fifth Ave., New York, N. Y.

GEOLOGIST wanted familiar with problems of radioactivity and geological time. Will be connected with the petroleum industry in the southwest. Must have training equivalent to a Doctor's degree. Address Box F3-12. Rm. 1502, 175 Fifth Ave., New York, N. Y.

OHMITE RESISTORS AND RHEOSTATS

STOCK OR SPECIAL UNITS TO MEET THE EXACT NEED

★ You can often find a quick, dependable, economical solution to your control problem in the wide range of Ohmite stock types, sizes and ratings—the largest, most complete stock of close-control Rheostats, wire-wound Resistors, and high-current Tap Switches available today. Or, special units can be designed and produced promptly to meet your specific need.

Write Today for Catalog 17

OHMITE MANUFACTURING COMPANY
4890 Flournoy Street ★ Chicago, U. S. A.

Be Right with OHMITE
RHEOSTATS • RESISTORS • TAP SWITCHES

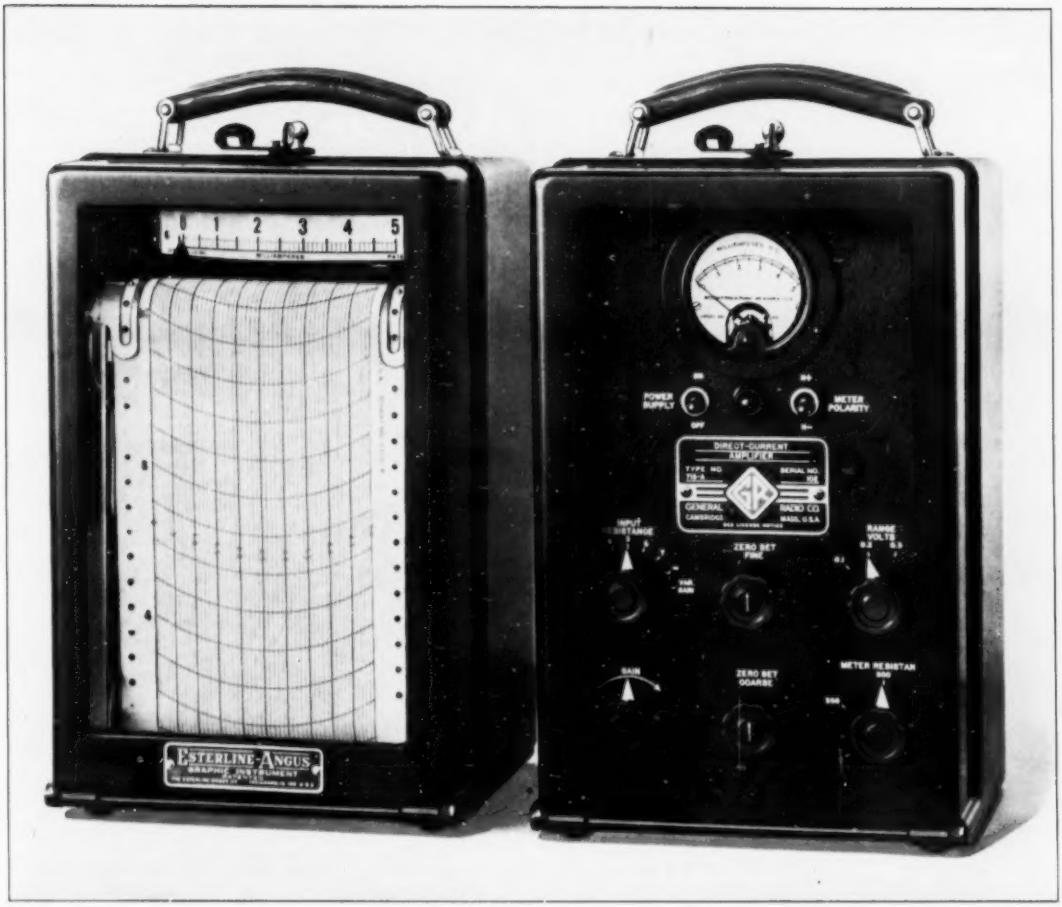

FOR CONTINUOUS RECORDING OF SMALL VOLTAGES AND CURRENTS

THE General Radio Type 715-A Amplifier, with an appropriate recorder, constitutes a calibrated recording voltmeter. With suitable input resistances the combination is also a recording milliammeter or microammeter.

Its industrial applications are many and include such as continuous recording of light intensity, frequency, sound and radio meteorograph observations.

The amplifier, in addition, can be used in automatic control circuits where the amplifier output operates relays to control the device which drives the amplifier.

This amplifier has high gain, operates from an a-c power source, is very simple to use, requires practically no attention and can be run for long periods for continuous recording, is exceptionally stable with freedom from effects of line voltage variations and has a wide range of built-in input voltage and resistance combinations.

Full-scale output of the amplifier has been made 5 milliamperes to operate a 5-milliampere Esterline-Angus Graphic Recorder. This full-scale output can be obtained on calibrated ranges from input voltages of 0.1, 0.2, 0.5, and 1.0 volt. Higher voltages can be recorded on an uncalibrated range up to 50 volts or more.

The input resistance can be varied between 100 ohms and 10 megohms in powers of 10, by means of a panel switch. In addition an input potentiometer is provided for a variable gain at an input resistance of 150,000 ohms.

PRICES: Type 715-AE Amplifier (Cast Metal Case, Illustrated) . $250.00
Type 715-AM Amplifier (Walnut Cabinet) $225.00

• ***Write for Bulletin 570 for Complete Information***

GENERAL RADIO COMPANY

Cambridge, Massachusetts

BRANCHES: NEW YORK AND LOS ANGELES

MANUFACTURERS of PRECISION ELECTRICAL LABORATORY APPARATUS

Cenco Roto Ranger

A Combination Electric Measuring Instrument For All Ordinary Laboratory Measurements

No confusion in reading the pointer indications on this meter. Each of the 12 scales are independent. They are engraved on a cylinder which rotates with the turning of the selector switch. Only one scale is visible in the window beneath the pointer at a time. Simultaneous with rotation of the scale cylinder, the selector switch selects the corresponding multiplier, shunt or resistance bridge circuit for the scale exposed.

Direct Current Scales:

(1) 0 to 1 ma (2) 0 to 10 ma (3) 0 to 1000 ma
(4) 0 to 3 amp. (5) 0 to 2 volts (6) 0 to 10 volts
(7) 0 to 150 volts (8) 0 to 1000 volts

Resistance Scales:

(9) 0 to 100 ohms (10) 0 to 50,000 ohms (11) 0 to 3 megohms

Alternating Current Scales:

(12) 0 to 250 volts

82466 . . . . . $38.50

CENTRAL SCIENTIFIC COMPANY

SCIENTIFIC INSTRUMENTS & LABORATORY APPARATUS

CHICAGO
1700 Irving Park Blvd.,
Lakeview Station

TRADE MARK CENCO REG. U.S. PAT. OFF.

BOSTON
79 Amherst St.,
Cambridge A Station

LANCASTER PRESS, INC., LANCASTER, PA.